Goldberg, Martin Jeffry

TOTALLY EMPIRICAL WAVEFUNCTIONS FROM X-RAY DIFFRACTION DATA

City University of New York PH.D. 1984

TOTALLY EMPIRICAL WAVEFUNCTIONS FROM X-RAY DIFFRACTION DATA

by

Martin Jeffry Goldberg

A dissertation submitted to the Graduate Faculty in Chemistry in partial fulfillment of the requirements for the degree of Doctor of Philosophy, The City University of New York.

1984

This manuscript has been read and accepted for the Graduate Faculty in Chemistry in satisfaction of the dissertation requirement for the degree of Doctor of Philosophy.

4.27.84
date

Chairman of Examining Committee

5/2/84
date

Executive Officer

Supervisory Committee

The City University of New York

Abstract

TOTALLY EMPIRICAL WAVEFUNCTIONS

FROM X-RAY DIFFRACTION

by

Martin Jeffry Goldberg

Advisor: Professor Louis J. Massa

The interpretation of coherent x-ray diffraction experiments by a quantum model is described. Adjusting the coefficients of an LCAO expansion to best fit measured Bragg intensities results in a totally empirical quantum wavefunction. The quantum model is compared to a multipole expansion. The constraints imposed by quantum mechanics are examined, and several methods of satisfying these constraints while best fitting a wavefunction to measured Bragg intensities are detailed. Application is made to beryllium metal, with a resultant fit R_1=.00249. Similar applications to graphite and diamond are outlined. The formalism is extended to explicitly include solid-state effects, and this extension is applied to a model problem of an infinite line of hydrogen atoms. Neglect of solid-state effects can lead to errors of as much as 1% per electron. A more realistic treatment of crystal vibrations using a TLS model for external motions and 3N-6 spectroscopic-like local modes for internal motions is suggested. Related numerical algorithms are displayed. Directions for future work are suggested.

to N

Acknowledgements

I would like to express my gratitude to the following people. Thanks to Dick Marsh, who taught me the importance of looking inside "black boxes" instead of using them incorrectly; to Bill Goddard III, who showed me when not to use approximations; to Aron Kuppermann, who taught me how molecular motions really work; to Bob Richman, who taught me that three-page derivations of formulas can be fun; to Lou Massa, who allowed me the freedom to develop as an independent scientist; to Angelo Santoro and John Lombardi, for advice and encouragement; to Sam LaPlaca, Rick Boehme, and Carol Frishberg, for help with calculations; to Cathy Abrams and T. Vasu, for moral support; to Sal d'Ambra, for showing me how programs should be written; and to Nina d'Ambra, for encouragement, aid, and general wonderfulness.

TABLE OF CONTENTS

LIST OF TABLES

LIST OF FIGURES

Chapter I. Introduction

When a beam of x-rays shines on a crystal, some of the x-rays bounce off in various directions and form a pattern of spots of varying brightness called a "diffraction pattern." The positions of the spots, and their intensities, are related to the electron distribution in the crystals. This thesis will detail a method for interpreting the x-ray diffraction patterns which is more valid than the theoretically unsound method currently used.

Since most of the information published in the literature of chemistry, physics, geology, and biology about bond lengths and angles of nearly all elements and compounds comes from x-ray diffraction patterns, it is crucial to interpret the data as accurately as possible. Simple interpretation methods have an error of about five percent, yet experimental errors in the most recent data have been far less than one half of one percent. Thus the highly accurate data now available deserves a highly accurate interpretation.

Quantum mechanics is a set of rules which explain most accurately the behavior of matter on the scale of electrons, which is the size that crystallography is concerned with. Interpretation of recent crystallographic data must use quantum mechanics to be as accurate as the data itself.

Quantum mechanics puts restrictions on the number of electrons that can travel in the same path. One electron completely fills a particular "spinorbital" path. Negative numbers of electrons are physically meaningless for a real object. Spinorbitals are like parking spaces. One car fills the space completely; fewer than zero cars is meaningless. The "single-determinant" approximation, which will be used for this thesis, neglects the possibility of "double-parking."

The paths will have either zero or one electron in them. This is done by a mathematical property called "idempotency." Idempotency is based on the fact that the only numbers equal to themselves squared are zero and one. If the matrix representing the spinorbitals equals itself squared, the matrix is called idempotent; spinorbitals so represented will be either empty (0 electrons) or full(1 electron).

Since the Bragg experiment measures the electron distribution within a crystal(1), the interpretation of this experiment should be consistent with crystal symmetry and with the behavior of electrons. Crystals are periodic, and this periodicity should be accounted for. Electrons obey the laws of quantum mechanics, and should not be treating as electrostatic charge clouds. Dame Kathleen Lonsdale described the ultimate goal of a crystallographer nearly a quarter century ago(2). She said,

> "A proper determination would include exact mean positions of all atoms, including hydrogen; a study of the electron distribution of the atoms in a state of rest; a knowledge of the zero-point motions and of the thermal vibrations of all atoms, analyzed with respect

> to translations and oscillations of the molecules as a whole and of the atoms relatively to each other within the molecule; the distribution of these with respect to amplitude and frequency, at various temperatures; a study of imperfections, unavoidable or deliberately introduced; and of surface modification of structure."

The reason for doing basic chemical research is to learn about the behavior of matter - about chemistry. The proper positioning of atoms gives an excellent fit to x-ray data, and the bonding patterns can be inferred from the bond lengths, to some degree of approximation. However, the chemistry - the redistribution of electrons due to atoms bonding to each other - is obtainable directly from the data. Even though it is a small effect, this slight redistribution of electron density is all that prevents the crystal from flying apart into a mixture of monatomic gases. Thus, it is of interest to collect crystal data of high enough quality to see the chemistry, and to interpret the data in a way that makes chemical sense.

There are now over a dozen systems with "chemistry quality" data ($R_{internal}$ < 1% or so), and synchrotron sources, such as the recently-completed National Synchrotron Light Source at Brookhaven National Laboratory, make collection of this sort of data in the future a certainty.

A more sophisticated method of analyzing these data is called for, since the limiting factor of the experiment is no longer poor data resolution. The electrons of the crystal must be described quantum mechanically, since electrons are archetype quantum objects. Our formalism accomplishes this by using an idempotent N-electron

single-determinant reduced density matrix to describe the nuclei in an orbital basis (LCAO), called the P matrix(3). This is corrected to account for the non-orthogonality of the basis orbitals, and the overlap of orbitals from adjacent unit cells of the crystal, by the overlap matrix S. This description is related to the diffraction experiment by an orbital product scattering factor matrix f(K). The S matrix, if it includes overlaps between all unit cells, leads to a P matrix which refers to Wannier orbitals. This quantum-mechanical wavefunction description of x-ray diffraction is of an identical form to ab initio and semiempirical wavefunctions. However the method of arriving at this wavefunction is quite different. Unlike ab initio non-empirical wavefunctions there are no energy evaluations and no Hamiltonian operator. In addition, unlike semiempirical wavefunctions, the basis functions are explicitly defined, and no integrals are approximated or parametrized. The only variational parameter that this wavefunction minimizes is the quality of fit to the data. This is a totally empirical wavefunction. It will fit the data better than an ab initio Hartree-Fock wavefunction in the same basis, but the energy calculated from a totally empirical wavefunction will not be as low, and may not satisfy the virial theorem(4).

An extreme advantage of a totally empirical wavefunction model over a non-wavefunction fit to data is that, once you have a wavefunction, a prediction can be made for any ground-state static electronic property. In addition, data from any experiment which measures this

sort of property can be simultaneously fit by the wavefunction. This is a natural way of putting together data from several kinds of experiment. Table 1 lists the properties which can be predicted by a totally empirical Bragg-scattering wavefunction model, and the experiments whose results can either be predicted by, or used as input data to determine, this wavefunction. Excluded are experiments such as IR/Raman spectroscopy, which involve transitions from one state to another - the model in this thesis describes the ground electronic state only, with a thermally-averaged and time-averaged occupation of vibrational states. The properties in Table 1 are of four types: classical one-electron moments, quantum one-electron expectation values, classical two-electron properties (of which none exist), and quantum two-electron expectation values. Since our single-determinant approximation neglects electron correlation, the values predicted for this last type of property will probably not fit experiment very well.

The idea of a simultaneous fit to another experiment and Bragg scattering is not new. Examples in the literature include x-ray plus neutron scattering ("X+N") (5), and x-ray plus nuclear quadrupole resonance(6,7,8). A quantum example also exists - X-ray scattering plus directional Compton profile(9).

How can one be sure that an experimentally measured density can be modeled at all by a wavefunction? This is the question of N-representability - whether a density can be represented by an N-electron quantum wavefunction. The theorem of Hohenberg and Kohn(10)

shows that the ground-state wavefunction of a many-particle system, if non-degenerate, is a unique functional of the particle density. Of course, this functional is not yet known, but it does exist. Gilbert's theorem(11) shows that any non-negative density normalized to N electrons can be modeled exactly by at least one N-electron single-determinant wavefunction, using this construction. You arbitrarily carve up the density into N/2 "regions", and each orbital is a phase factor times the square root of one region, as shown in Figure 1.

The x-ray coherent diffraction experiment, called Bragg scattering, is a measure of density. Therefore by Gilbert's theorem, it can be modeled by a single-determinant wavefunction.

Harriman(12) has shown that these "regions" need not have sharp boundaries, and "that for any given density an arbitrary number of functions, which are continuous, smooth, orthonormal, and extend over all space, exist" which exactly fit the density.

Using a limited basis set of atomic orbitals, and limited information about the density, one can approximate the exact Harriman's-construction wavefunction in a least-squares sense. This approximate wavefunction will fit the data well, using only a few parameters.

The result is directly comparable to an ab initio wavefunction if you use the same basis.

Figure 1

Gilbert's Theorem

from Reference(11)

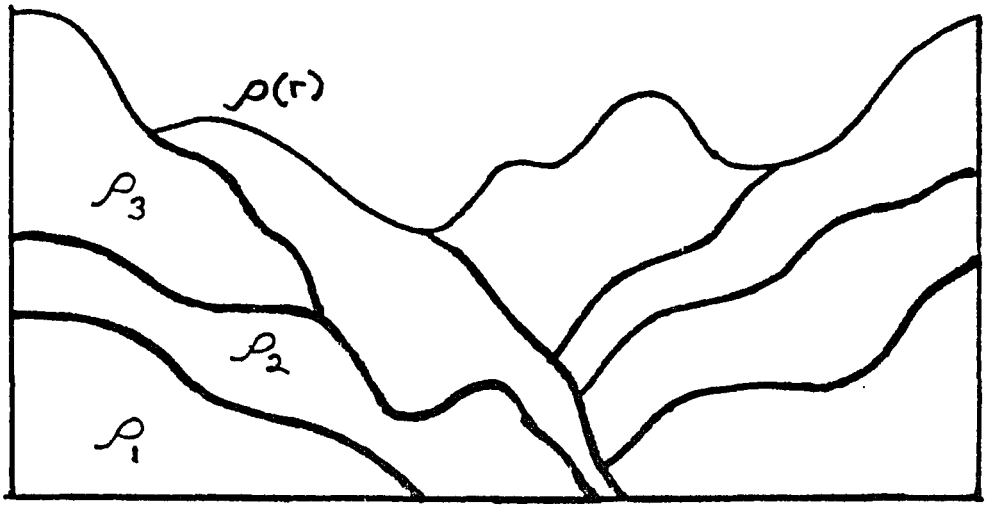

Non-magnetic case

If $\int \rho(r)\, dr = N,$

then divide the density arbitrarily into N/2 equal regions ρ_i,

and define $\psi_i \equiv \sqrt{\tfrac{1}{2}\rho_i(r)} \cdot e^{i\omega_i}$

such that $\langle \psi_i \mid \psi_j \rangle = \delta_{ij},$

and you have a quantum-mechanical single-determinant wavefunction.

Not much work has been done with totally empirical wavefunctions. Table 2 is a nearly complete list. The starting point for most determinations of such wavefunctions has been the iterative algorithm of Clinton et al.(13) This algorithm is

$$P' = 3P^2 - 2P^3 + \sum_i \lambda_i O_i \tag{1}$$

where the expectation values $\langle O_i \rangle$ are being least-squares fit by an idempotent density matrix P in an orthonormal basis g, using Lagrange multipliers λ determined by solving the system

$$\langle O_j \rangle = 2 \text{ Tr } (3P^2 - 2P^3 + \sum_i \lambda_i O_i) O_j \tag{2}$$

The expectation values are given by

$$\langle O_i \rangle = \text{Tr } PO_i \tag{3}$$

For Bragg data, the $\langle O_i \rangle$ are called F(K), and the O matrix in the basis g(r) is composed of elements

$$f_{ij}(K) = \langle g_i(r) | e^{ik \cdot r} | g_j(r) \rangle \tag{4}$$

so that the observed values $F_{obs}(K)$ are being fit by

Table 1

Electronic Properties
Connected with Totally Empirical Wavefunctions

Model Predicting	One-Electron Property	Two-Electron Property
	X-Ray Structure Factors $F_{cal}(K)$	
NON-QUANTUM OR QUANTUM MODEL	From References(14,15) Outer Moments $\langle r^n \rangle$ dipole moment $\langle r \rangle$ quadrupole moment $\langle r^2 \rangle$ ... Inner Moments $\langle r^{-n} \rangle$ electrostatic potential φ Hellmann-Feynman force $\mathcal{F}$ electric field gradient $\nabla\mathcal{E}$ charge density $\rho(r)$ Fermi contact term $\rho(0)$	NONE
	From Reference(16) Vibrational Force Constants $\mathcal{K}$	
QUANTUM MODEL ONLY	From Reference(17) Momentum density $\rho(k)$ Compton profile $\vec{\rho}(k)$	From Reference(20) Thermal Diffuse Scattering TDS
	Kinetic energy $\langle T \rangle$	Potential Energy $\langle V \rangle$ Total Energy $\langle H \rangle$
	From References(18,19) NMR Chemical Shifts δ Bond orders B.O. Diamagnetic susceptibility $\vec{\vec{\mu}}$ Polarizability tensor $\vec{\vec{\alpha}}$	From Reference(21) NMR spin-spin splittings J
QUALITY OF FIT	GOOD	FAIR TO POOR

Table 2

Totally Empirical Wavefunctions

	System	Experiment	Authors
	H atom	Bragg Scattering	Clinton, Massa(26)
	H atom	Bragg Scattering	Frishberg, Massa(26)
*+	$HCOOLi \cdot D_2O$	Bragg Scattering(22)	Ozerov group(22,23,24)
	Li atom	Bragg Scattering	Frishberg, Massa(25)
	Be atom	Bragg Scattering	Frishberg, Massa(25)
	H_2 molecule	Bragg Scattering	Frishberg, Massa(27)
	H_∞ crystal	Bragg Scattering	Goldberg, Massa(28)
		Positron Annihilation	Pecora(17)
*	Be metal	Bragg Scattering(56)	Goldberg et al.(29)

* denotes that the study used actual experimental data

+ denotes that the study approximated certain parameters unrelated both to experiment and to the functional form of the wavefunction.

$$F_{calculated}(K) = Tr\ P\ f(K) \tag{5}$$

Most ab initio studies use a non-relativistic Hamiltonian, and neglect both spin-orbit coupling and retardation-type effects. The totally empirical wavefunction uses no Hamiltonian, so it implicitly includes every effect not explicitly approximated out. The wavefunctions and P matrices of this thesis are generally spinless, since it deals mainly with Bragg scattering of x-rays, a process that is insensitive to spin. A P matrix in the closed-shell spin-paired approximation is normalized to half the number of electrons, and multiplied by two. This is equivalent,in the spin-paired case,to the full P matrix

$$P = \begin{matrix} P_{\alpha\alpha} & P_{\alpha\beta} \\ P_{\alpha\beta}^{+} & P_{\beta\beta} \end{matrix} \tag{6}$$

plus the approximations

$$P_{\alpha\alpha} = P_{\beta\beta} \qquad \text{and} \qquad P_{\alpha\beta} = 0 \tag{7}$$

since it is rigorously true that for x-rays

$$f_{\alpha} = f_{\beta} \tag{8}$$

Including spin-orbit coupling means that $P_{\alpha\beta}$ is non-zero. This may be necessary for modeling magnetic neutron scattering, which is a measure of unpaired spin

$$F^{K}_{\text{magnetic neutron scattering}}(K) = \int e^{ik\cdot r}(\rho_{\alpha}(r)-\rho_{\beta}(r))dr \tag{9}$$

For most cases, it will probably be sufficient to change (7) to

$$P_{\alpha\beta} = 0 \quad \text{but} \quad P_{\alpha\alpha} \neq P_{\beta\beta} \tag{10}$$

The simplest possible model for the electron density of a crystal is the ρ^3 model(30,31). Since the electron density is "clumpy," that is, concentrated near certain points and tenuous far from these points, one calculates that phase for each reflection which maximizes the average value of some odd power of ρ, usually ρ^3. Note that the ρ^3 model uses F_{obs} as its F_{cal}.

The next improvement is to treat these clumps of density as atoms. This approximation, referred to as the "free atoms" or "promolecule" refinement, calculates the scattering power of a model spherically symmetric atom or ion, using atomic HF or CI or some other(32) theoretical atomic calculation. The model then moves these atoms around to best fit the observed intensities, and as a side benefit predicts phases of each reflection.

An early improvement over the free atom treatment is to treat eaach atom as having some non-spherical shape, where the scattering in some directions differs from that in others(33,34). This sort of sophistication, assigning atoms aspherical electronic or vibrational properties, was debated in the literature in a series of articles in 1957(35,36,37), with the consensus being that, if the internal consistency of the data were better than about 10%, such treatment was justified.

A better treatment is to expand the density in an LCAO sense, and fit the data using a population matrix P, with each pair of orbitals in the basis having a scattering power $f_{ij}(K)$.

In a basis of m functions, it is found that there are

$$\text{Dimension}(f) = m(m+1)/2 \qquad (11)$$

distinct scattering powers, and a P matrix this size has been tried(38,39,40) without much success. The problem seems overparametrized. This has been referred to as the P_{NI} method(41).

The most popular method used is some form of multipole expansion of the electron density, with each nuclear position being used as an expansion center. There are several variants of this technique, including the Hirshfeld deformation(42), Coppens' $\mathcal{K}$ -refinement(43), and the multipole methods of Kurki-Suonio(44,45) and of Stewart(46).

There are several problems with the multipole techniques. The most

severe is positivity. In order for an electron density to be physically meaningful, it must be positive everywhere.

$$\rho(r) > 0 \quad \forall \; r \tag{12}$$

A negative density, or "positron density", corresponds to no physically possible crystal. Since the density is, quantum mechanically speaking, the square of the orbitals, one can guarantee positivity if the density is modeled as the square of some function. Figure 2 illustrates the danger of "positron regions" if one models the density as a sum of squares of basis orbitals rather than the square of an LCAO sum of basis orbitals.

Non-quantum models can have some positron regions, and positivity "must be taken as an extra condition restricting the possible values of the parameters."(47)

A multipole expansion of the density is not an interpretation of the data. It assigns no physical meaning to the multipoles - the model merely filters the data. It is not surprising, then, that one cannot connect a multipole model of x-ray diffraction with other experiments on the same crystal, such as Compton scattering(48) or NMR.

Further, the multipole model experiences difficulty separating out

Figure 2

Positron Regions

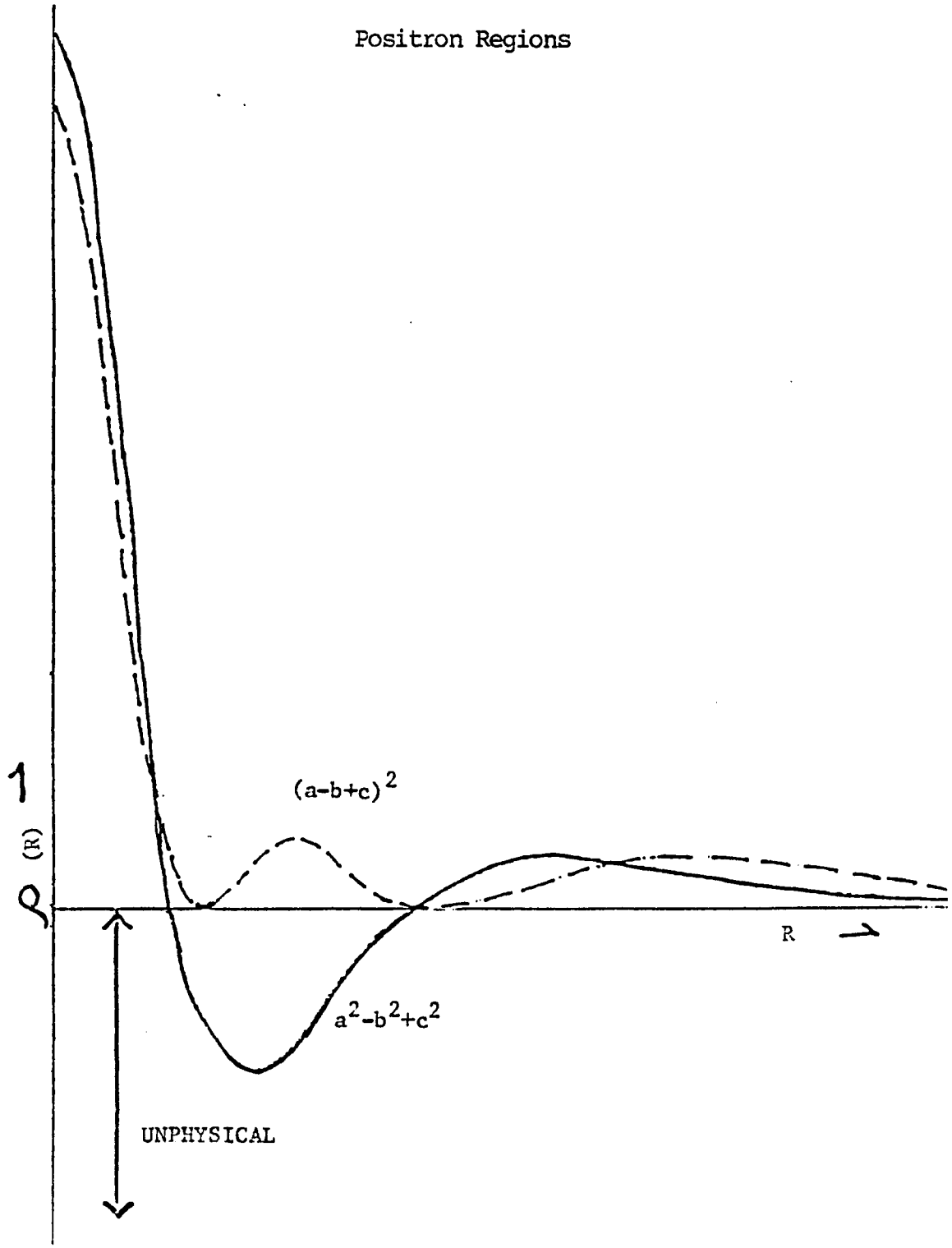

the effects of non-spherical vibration from those of a non-spherical charge vibrating spherically. This correlation of vibrational and electronic parameters is not as severe in a quantum model, as shall be seen in Chapter 3 below.

The multipole model assigns electrons to one atom or another, but not both simultaneously. It partitions the density in some way(49,50). This inability to describe charge sharing, or covalency, has severe effects. Since all interactions must be modeled as electrostatic, that is to say, ionic, atomic charges are likely to be exaggerated. Covalent bonding is inherently not explained by a multipole model. Since, especially in polar bonds, nuclei are not always found at the centroid of their electronic charge(51), the nuclei are not positioned at the right places by a multipole model. This Hellmann-Feynman shift of the density into the bonding and lone-pair regions means that either nuclear positions in a multipole model are wrong (unless fixed by a neutron-scattering experiment) or indeterminate. (By adding a dipole scatterer, one moves the effective nuclear position without moving the expansion center. Thus, in a large enough multipole expansion, one can put each nucleus anywhere, and have the density associated with it centered anywhere else. Assigning any physical meaning to such an expansion is obviously incorrect(52).) An example is that virtually all x-ray-only studies of molecules with hydrogen atoms have bond lengths to the H atoms about .1 Å too short(53), since the covalency shifts the centroid of the H electron about .1 Å into the bonding region.

Finally it is found that certain properties that a multipole expansion can predict are almost always in error. In particular, the electric field gradient at the nucleus, as measured by NQR, must be added in as a constraint to the x-ray refinement to come out fitting reality at all well(8). I can find no attempt anywhere in the literature even to try comparing the Fermi contact term $\rho(0)$ from an x-ray refinement with that of a Mossbauer experiment, although both make a prediction of its value. It is commonly claimed that model errors pile up at nuclear positions(54), and that maybe the atomic 1s cores are expanding or contracting, and these prevent obtaining a good value of $\rho(0)$. In a quantum model, such claims can be quantitatively examined, and a percent 1s core expansion calculated.

The quantum description of a covalent bond involves cross-terms; a bond between atoms μ and ν is written as a bonding electronic orbital with basis functions g on both centers

$$\psi_{bond} = c_\mu g_\mu + c_\nu g_\nu \tag{13}$$

leading to a P matrix

$$P_{bond} = \begin{matrix} c_\mu^2 & c_\mu c_\nu \\ c_\nu c_\mu & c_\nu^2 \end{matrix} \tag{14}$$

These cross-terms $C_\mu C_\nu$ are the bond, in a Mulliken sense. The larger $C_\mu C_\nu$ is, the stronger a bond. Antibonding orbitals are describable as

$$\psi_{\text{antibond}} = C_\mu g_\mu - C_\nu g_\nu \tag{15}$$

and the cross-term will be less than zero. An electrostatic description has all cross-terms between centers zero, thus non-bonding. This is also called a one-center description, if one allows each center to hybridize, leading to cross-terms between basis functions on the same center. A covalent, many-center description is desirable.

A common variant of the multipole formalism uses the Varghese-Mason(55) constraint. The multipoles M_j have the form

$$M_j = x^{2A}y^{2B}z^{2C}e^{-2ar^2} \quad \text{or} \quad x^{2A}y^{2B}z^{2C}e^{-2ar} \tag{16}$$

and are considered to be uniquely related to Gaussians or Slaters

$$g_j = x^{A}y^{B}z^{C}e^{-ar^2} \quad \text{or} \quad x^{A}y^{B}z^{C}e^{-ar} \tag{17}$$

by the simple equation

$$M_j = g_j^2 \tag{18}$$

Cross-terms $f_{\mu\nu}$ and $P_{\mu\nu}$ for $\mu \neq \nu$ are defined as zero, since(55) "The remaining multipoles which are not identically zero for symmetry reasons must be shown to be small since they will otherwise represent two-centre overlap terms being projected onto the single centre."

This V-M formalism has been referred to(41) simply as a multipole expansion. It is an extreme generalization of the one-center constraint. Where a one-center formalism disallows P matrix cross-terms between basis functions on different centers, the V-M formalism disallows all cross-terms of any sort in P, requiring elements $P_{\mu\nu}$ to satisfy the V-M constraint

$$P_{\mu\nu} = W_{\mu} \delta_{\mu\nu} \tag{19}$$

and reducing the equation

$$F_{cal}(K) = \mathrm{Tr}\, Pgg^{+} = \sum_{i} \sum_{j} P_{ij} \langle g_j | e^{ik\cdot r} | g_i \rangle \tag{20}$$

to

$$F_{cal}(K) = \sum_{j} W_j \int M_j(r)\,dr = \sum_{j} P_{jj} \langle g_j | e^{ik\cdot r} | g_j \rangle \tag{21}$$

The distinction is illustrated graphically in Figure 3.

Figure 3

Comparison of Idempotent, Non-idempotent,

and Multipole P Matrices

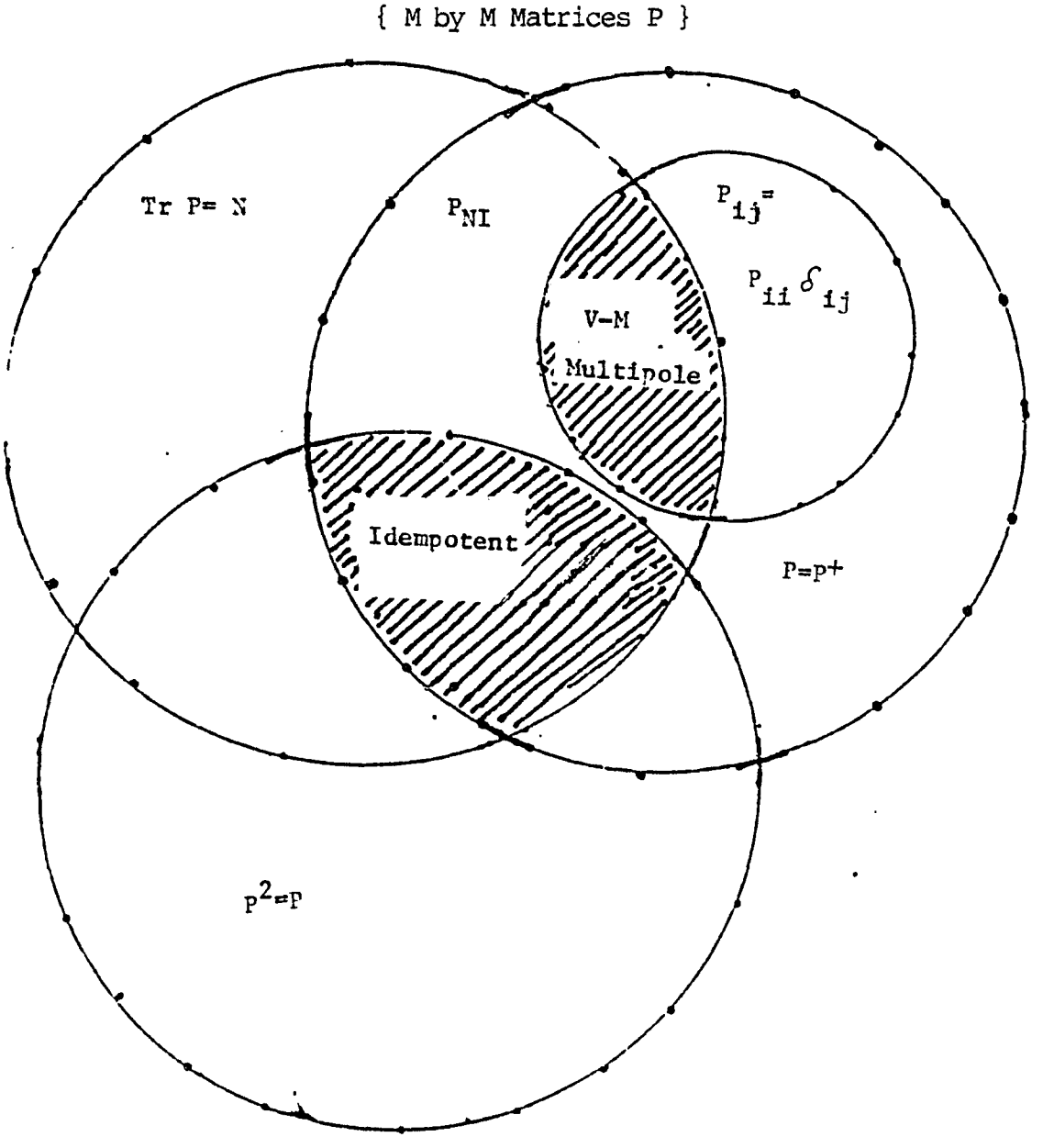

Whereas a non-idempotent P has

$$m(m+1)/2 - 1 \tag{22}$$

independent elements, and an idempotent P has

$$N(m - N) \tag{23}$$

a V-M matrix has only

$$(m - 1) \tag{24}$$

independent elements. Note that in the V-M procedure, some W are allowed to go negative, and hopefully will not go so negative that a positron region appears. Figure 2 shows positron regions. Quantum mechanics enforces positivity by requiring all self-terms $P_{\mu\mu}$ to be positive. If one requires

$$0 \leq W_j \leq 1 \tag{25}$$

in the V-M method, it is N-representable; each of the W_j is an eigenvalue, and each basis function is an eigenfunction.

The normal quantum refinement technique can generate V-M-type P

matrices, or more generally, block-diagonal P matrices, by going to several configurations. For example, defining

$$\psi_1 = C_1 g_1 + C_2 g_2 + C_3 g_3 \tag{26}$$

$$\psi_2 = C_1 g_1 + C_2 g_2 - C_3 g_3 \tag{27}$$

$$\psi_3 = C_1 g_1 - C_2 g_2 + C_3 g_3 \tag{28}$$

$$\psi_4 = C_1 g_1 - C_2 g_2 - C_3 g_3 \tag{29}$$

then

$$P_1 = \begin{matrix} C_1^2 & C_1C_2 & C_1C_3 \\ C_2C_1 & C_2^2 & C_2C_3 \\ C_3C_1 & C_3C_2 & C_3^2 \end{matrix} \qquad P_2 = \begin{matrix} C_1^2 & C_1C_2 & -C_1C_3 \\ C_2C_1 & C_2^2 & -C_2C_3 \\ -C_3C_1 & -C_3C_2 & C_3^2 \end{matrix} \tag{30}$$

and

$$P_3 = \begin{matrix} C_1^2 & -C_1C_2 & C_1C_3 \\ -C_2C_1 & C_2^2 & -C_2C_3 \\ C_3C_1 & -C_3C_2 & C_3^2 \end{matrix} \qquad P_4 = \begin{matrix} C_1^2 & -C_1C_2 & -C_1C_3 \\ -C_2C_1 & C_2^2 & C_2C_3 \\ -C_3C_1 & C_3C_2 & C_3^2 \end{matrix} \tag{31}$$

simplifying,

$$1/4\ (P_1+P_2+P_3+P_4)=P_{VM}= \begin{bmatrix} C_1^2 & 0 & 0 \\ 0 & C_2^2 & 0 \\ 0 & 0 & C_3^2 \end{bmatrix} \quad (32)$$

In general, for m basis functions, one needs 2^{m-1} configurations to block-diagonalize. Note that the diagonal elements of all four P above are identical from one model to the next, yet in ψ_1, all 3 basis functions are bonded, ψ_2 has g_2 antibonding, ψ_3 has g_3 antibonding, and ψ_4 has g_1 antibonding. Figures 4,5,and 6 show all 5 densities in an STO-3G basis for hydrogen, $\rho(+++)$ from ψ_1, $\rho(+-+)$ from ψ_2, $\rho(++-)$ from ψ_3, $\rho(+--)$ from ψ_4, and ρ(V-M); and the scattering curves associated with these ρ.

A quantum model of x-ray diffraction has previously been applied to some model systems(3,25,26,27,28). For all these, some theoretical structure calculation of the density of an isolated gas-phase atom or H_2 molecule was Fourier-transformed to give "observed" structure factors F_{obs}, and these were fit by equation (1) in an orbital basis, or a spinorbital basis(25). This was extended(28) to a model H_∞ system. Ozerov(22,23,24) has used a similar model, and fit real data with a quantum model. Chapter 3 of this thesis fits the beryllium metal scattering data of Larsen(56) to a quantum model.

Figure 4

The "Phase Problem" with P Matrices

WAVEFUNCTIONS

$$\Psi = \pm a\,\psi_1 \pm b\,\psi_2 \pm c\,\psi_3$$

$$+++ = a\,\psi_1 + b\,\psi_2 + c\,\psi_3$$

$$-++ = -a\,\psi_1 + b\,\psi_2 + c\,\psi_3$$

$$+-+ = a\,\psi_1 - b\,\psi_2 \pm c\,\psi_3$$

$$++- = a\,\psi_1 + b\,\psi_2 - c\,\psi_3$$

P-MATRICES

$+++$

$$\begin{pmatrix} aa & ab & ac \\ ba & bb & bc \\ ca & cb & cc \end{pmatrix}$$

$-++$

$$\begin{pmatrix} aa & -ab & -ac \\ -ba & bb & bc \\ -ca & cb & cc \end{pmatrix}$$

MULTIPOLE

$$\begin{pmatrix} aa & 0 & 0 \\ 0 & bb & 0 \\ 0 & 0 & cc \end{pmatrix}$$

$+-+$

$$\begin{pmatrix} aa & -ab & ac \\ -ab & bb & -bc \\ ca & -cb & cc \end{pmatrix}$$

$++-$

$$\begin{pmatrix} aa & ab & -ac \\ ba & bb & -bc \\ -ca & -cb & cc \end{pmatrix}$$

Figure 5

Densities from the Wavefunctions of Figure 4

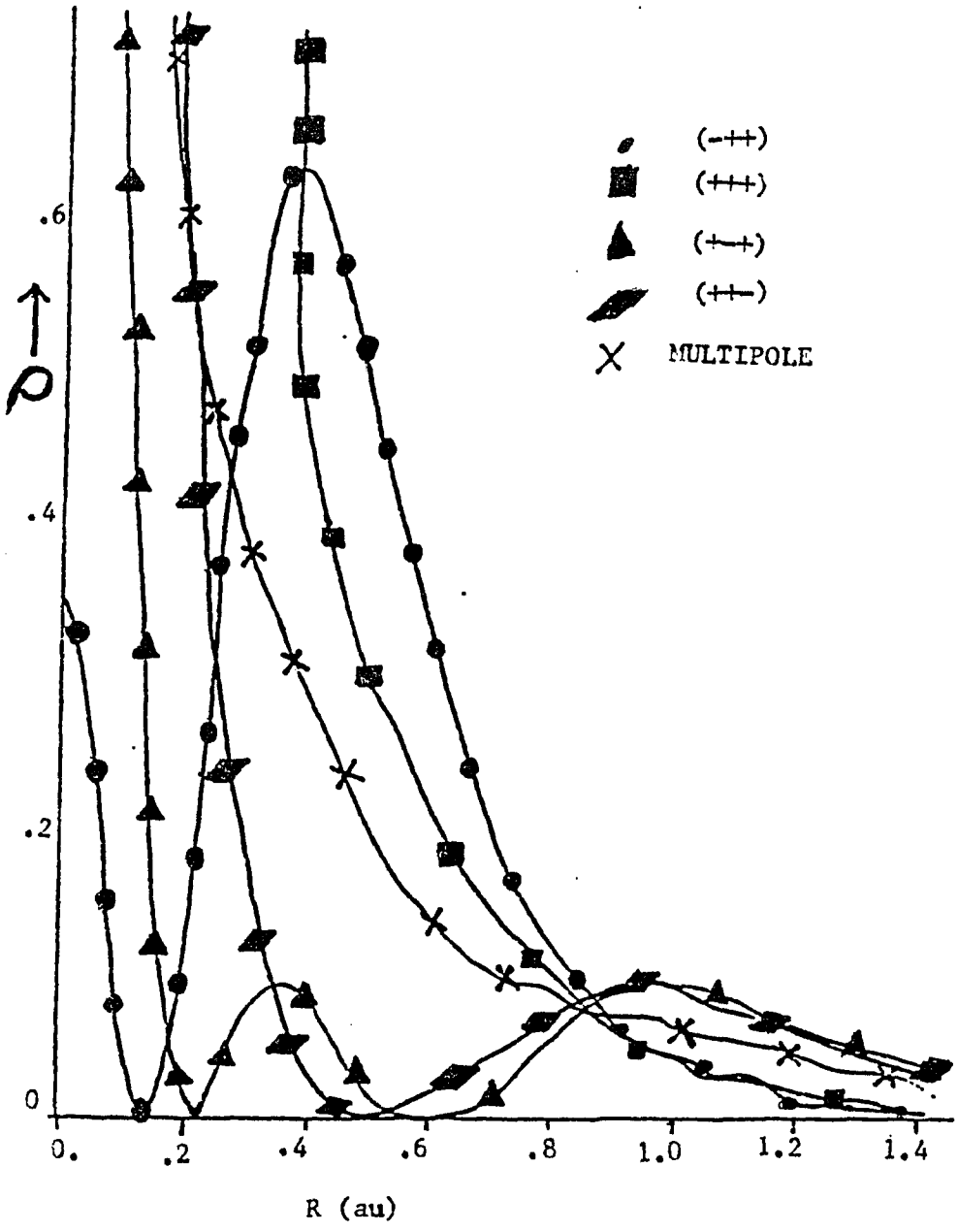

Figure 6

Scattering from the Wavefunctions of Figure 4

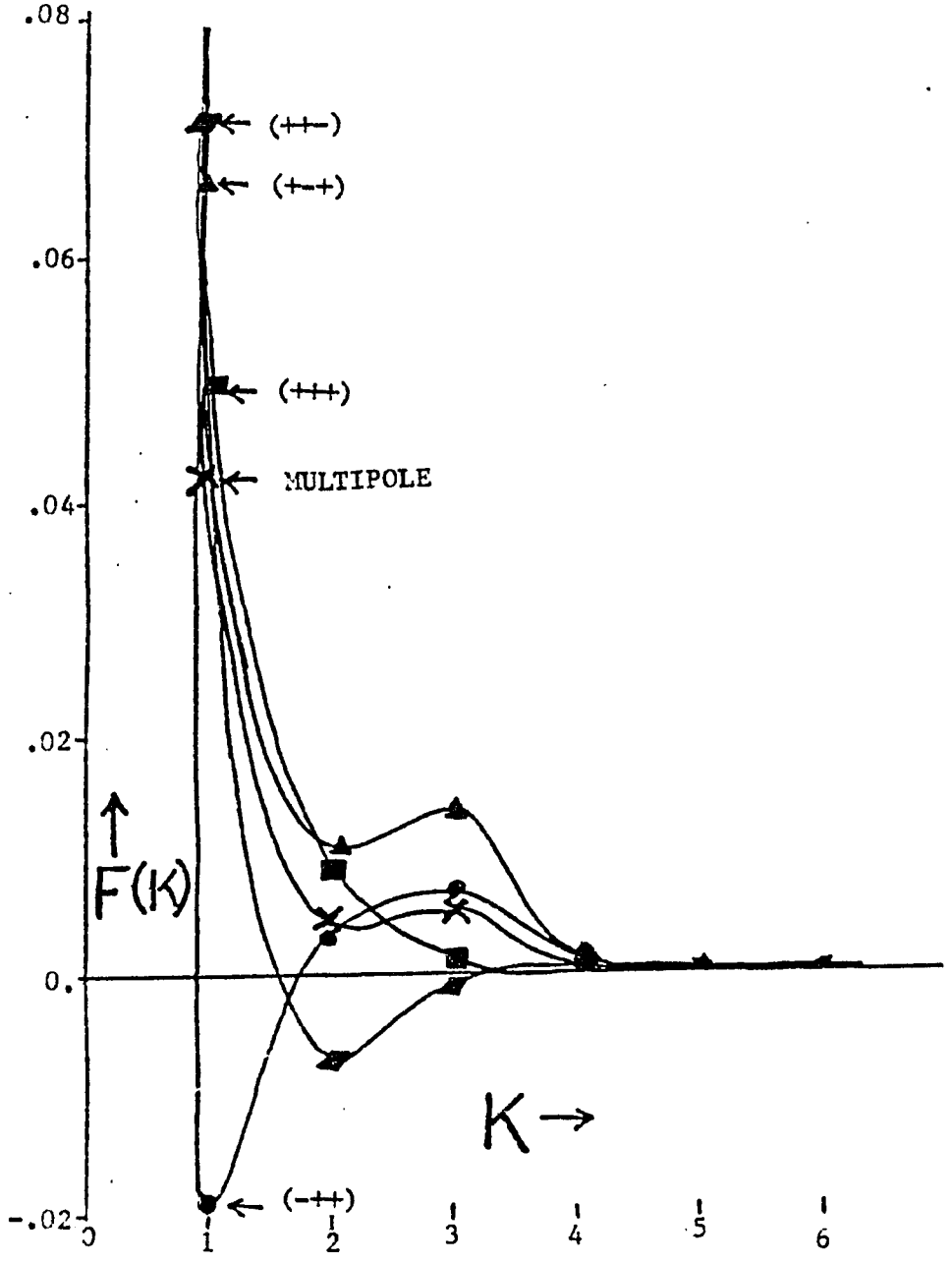

Chapter II. Mathematical Considerations

Usually, the basic element of quantum chemistry is the N-body wavefunction,

$$\Psi = \sum_{\text{determinants}} \chi_i \mathcal{A}(\psi_1(1)\psi_2(2)\psi_3(3)\ldots\psi_N(N)) \tag{33}$$

where χ_i is the occupation number of each determinant i, $\mathcal{A}$ is the antisymmetrizer, and the ψ_j are N (spin-) orbitals

$$\psi_j = \sum_{z=1}^{m} C_{jz} g_z \tag{34}$$

built up as linear combinations (LCAO) of the m basis functions g, and normalized to 1.

The N-body wavefunction contains far more information than will ever be needed to calculate any observed property. Since the full Hamiltonian, which governs the electronic motion, and hence all physically observable effects, contains no three-body terms large enough to affect anything(57), reduction from an N-electron to a 2-electron description loses no information. This 2-electron description is called the 2-electron reduced density matrix $\rho_2(1,2;1',2')$. An acceptable model for $\rho_2(1,2;1',2')$ enables one to simultaneously predict all electronic properties of that state. (Notice, however, that 2-state properties, such as photon

absorption/emission, require a model for both states involved, and this more complicated problem is beyond the scope of this thesis.) The most general matrix $\mu(1,2;1',2')$ is not acceptable. There are quantum constraints on it. Unfortunately, the forms of some of these constraints are unknown. A less general model, which is guaranteed to satisfy many quantum constraints, and is computationally simpler (although certain other constraints, such as the electron-electron cusp condition(58) are violated) is the Independent Particle Model, or IPM. This is known in various applications as the single-determinant approximation, Self-Consistent Field (SCF) model, Hartree-Fock method (HF), and the one-body approximation.

The IPM approximates the electron-electron correlation as the zero function. That is, the probability that an electron is within a certain region of space is independent of where the other electrons are. Since the neglected correlation is a rather weak function, this approximation is not too severe - ab initio calculations(59) indicate that ~99% of the energy can usually be modeled by a single determinant. The one-electron density matrix is written $\rho_1(1;1')$, and in the single-determinant approximation,

$$\rho_2(1,2;1',2') = \begin{pmatrix} \rho_1(1;1') & \rho_1(1;2') \\ \rho_1(2;1') & \rho_1(2;2') \end{pmatrix} \qquad (35)$$

In the general case, all the quantum constraints on the form of $\rho_1(1;1')$ are known. These constraints are collectively known as N-representability; which one- and two-body reduced density matrices can represent an N-body fermion wavefunction.

The density of electrons $\rho(r)$ is related(60) to $\rho_1(1;1')$ by

$$\mathrm{Tr}\ (\rho_1(1;1')) = \rho_1(1;1) = \Gamma(1) \tag{36}$$

$$\mathrm{Tr}\ (\Gamma(1)\ ) = \rho(r) \tag{37}$$

The density matrix $\Gamma(1)$ is the diagonal element of $\rho_1(1;1')$. The off-diagonal elements are connected with electron correlation. In an orthonormal basis of atomic orbitals g

$$\Gamma(1) = Pgg^{+} \tag{38}$$

The matrix of numbers P is properly called "the matrix representative in the basis g of the one-body reduced density matrix $\Gamma(1)$. Since P is a square matrix, it has off-diagonal elements P_{ij} for i not equal to j. These are not connected with electron correlation, as is $\rho_1(1;1')$ for 1 not equal to 1'. DO NOT CONFUSE OFF-DIAGONAL ELEMENTS WITH OFF-DIAGONAL ELEMENTS. P_{ij} is not $\rho_1(1;1')$. DO NOT CONFUSE THE DENSITY MATRIX (P) WITH THE DENSITY MATRIX ($\rho_1(1;1')$). From now on, the only density matrix referred to will be P. Also, to avoid confusion, P_{ij} with i not equal to j will be called cross-terms.

The quantum mechanical constraints on the density matrix P are:

1) The eigenvalues of P must all lie between 0 and 1.

2) P must be Hermitian, $P = P^{+}$ (39)

3) $Tr(P) = N$, the number of electrons (40)

Another constraint on the density, which will not be satisfied, is the electron-nuclear cusp condition(61):

$$\lim_{r \xrightarrow{\text{left}} r_{\text{nucleus}}} \left(\frac{\partial \rho(r)}{\partial r}\right) - \lim_{r \xrightarrow{\text{right}} r_{\text{nucleus}}} \left(\frac{\partial \rho(r)}{\partial r}\right) = -Z \qquad (41)$$

The change in density as one approaches the nucleus must be discontinuous, with the change in slope equal to minus the nuclear charge. (The electron-electron cusp condition dictates a change in slope of +1/2(58).)

In the Independent Particle Model, the eigenvalues of P are exactly zero or one. This condition on the eigenvalues is equivalent to the matrix condition

1') $P^2 = P$ (42)

The three conditions 1'), 2), and 3) are referred to as idempotency, Hermitivity, and N-normalization, respectively. Condition 3) is the easiest to satisfy. Any idempotent matrix must have an integer norm, since its eigenvalues 0 and 1 are both integer. One must

ensure only that the trace equals the correct integer, and not N-1 or N+1. Condition 2) is satisfied simply by constructing the lower left half of the matrix as the Hermitian adjoint of the upper right triangle. This makes all the self-terms (diagonal elements) real.

Condition 1') is the most difficult to satisfy. There are two methods in the literature of "purifying" a matrix to idempotency. McWeeny's method(62) is

$$P' = 3P^2 - 2P^3 \tag{43}$$

until

$$\mathrm{Tr}\ ((P^2 - P)^2) < \text{threshhold} \tag{44}$$

where the threshhold is roughly the square of the largest acceptable error. (A P matrix idempotent to 6 places has a threshhold of $\sim 10^{-12}$.)

Mestechkin's method(63) is

$$Y = 2P - 1 \tag{45}$$

and

$$Y' = Y + 1/2\ (1 + Y^2\ )Y \tag{46}$$

until

$$\mathrm{Tr}\ ((Y^2\ - 1)^{\ 2}\ ) < \text{threshhold} \tag{47}$$

and thus

$$P' = (Y' + 1)/2 \quad \text{and} \quad \mathrm{Tr}\ Y = N - m \tag{48}$$

Mathematically, P is called idempotent with

$$P^2\ = P \tag{49}$$

and Y is called involutional, with

$$Y^2\ = 1 \tag{50}$$

The elements of P are, in general, complex. Under what circumstances will constraining P to be real result in a worse fit to data? Suppose

$$\psi = \begin{pmatrix} C_1 & C_2 + iC_3 \end{pmatrix} \begin{pmatrix} g_1 \\ g_2 \end{pmatrix} \tag{51}$$

Then

$$F(K)= \mathrm{Tr}\begin{pmatrix} C_1C_1 & C_1C_2+iC_1C_3 \\ C_1C_2-iC_1C_3 & C_2C_2+C_3C_3 \end{pmatrix}\begin{pmatrix} f_{11} & f_{12} \\ f_{21} & f_{22} \end{pmatrix} \tag{52}$$

if

$$f_{11} = x_1+ix_2,\ f_{12} = x_3+ix_4,\ f_{22} = x_5+ix_6 \tag{53}$$

then

$$\begin{aligned} F(K) &= C_1^2(x_1+ix_2) + (C_1C_2+iC_1C_3)(x_3-ix_4) \\ &\quad +(C_1C_2-iC_1C_3)(x_3+ix_4) \\ &\quad +(C_2^2+C_3^2)(x_5+ix_6) \\ &= C_1^2x_1 + iC_1^2x_2 + 2C_1C_2x_3+2C_1C_3x_4 \\ &\qquad +(C_2^2+C_3^2)(x_5+ix_6) \end{aligned} \tag{54}$$

If

$$P_{real} = \begin{pmatrix} C_1^2 & C_1C_4 \\ C_4C_1 & C_4^2 \end{pmatrix} \tag{55}$$

then

$$F(K) = C_1^2(x_1+ix_2)+2C_1C_4x_3+C_4^2(x_5+ix_6) \tag{56}$$

and if

$$C_4^2 = C_2^2 + C_3^2 \tag{57}$$

then

$$F_{complex} - F_{real} = 2C_1(C_2x_3 + C_3x_4 - C_4x_3) \tag{58}$$

which is zero if and only if the scattering cross-term f_{12} is real. Reality of all cross-terms $f_{ij}(K)$ is equivalent to the crystal being centrosymmetric. Thus, one should constrain P to reality only for centrosymmetric crystals.

The iterative equations for fitting P to data, as developed by Clinton et al.(13) and extended by Henderson and Zimmerman(64) to constrained variational calculations, is based on the error measure

$$\epsilon_1 = \sum_K \left| |F_{obs}(K)| - |F_{cal}(K)| \right| \tag{59}$$

Other error measures used in crystallography are

$$\epsilon_n = \sum_K \epsilon_n^K = \sum_K (w_K)^{0,1,2} \left(\left(|F_{obs}(K)| \right)^{1 \text{ or } 2} - \left(|F_{cal}(K)| \right)^{1 \text{ or } 2} \right)^{1 \text{ or } 2} \tag{60}$$

and the robust-resistant functional(65) of Nicholson et al.,

$$\epsilon_{LL} = \sum_K \begin{cases} \left(\frac{z_K}{2}\right)\left(1 - \left(\frac{z_K}{a}\right)^2 + \left(\frac{1}{3}\right)\left(\frac{z_K}{a}\right)^4\right) & \text{if } |z_K| \le a \\ z_K^2/6 & \text{if } |z_K| > a \end{cases} \qquad 35 \quad (61)$$

where

$$z_K = \sqrt{w_K}\,(|F_{obs}(K)| - |F_{cal}(K)|)/GoF \qquad (62)$$

These error measures, their R-factors, and the iterative equations associated with each, are listed in Table 3. The least-absolute-value functionals seem far slower to converge, but their precision is higher(66).

Figure 7 shows the behavior, in a fixed basis, of some of the error functionals as a function of P, where

$$P_{exact} = \begin{pmatrix} 1/3 & \sqrt{2}/3 \\ \sqrt{2}/3 & 2/3 \end{pmatrix} \qquad (63)$$

and

$$P_{calc} = \begin{pmatrix} x & \sqrt{x(1-x)} \\ \sqrt{x(1-x)} & (1-x) \end{pmatrix} \qquad (64)$$

Figure 8 shows the behavior of $\partial\epsilon/\partial x$ for these functionals.

Table 3

Error Measures and Related Quantities

RAW ERROR (A)	TREFOIL # (B)	R-FACTOR(67)	$D^K = \left(\frac{\partial \epsilon}{\partial \rho}\right)_K$	G	$\sigma(p_\mu)(c)$	GoF	NOTES
$\epsilon_1 = \Sigma \lvert \lvert F_o \rvert - \lvert F_c \rvert \rvert$	2	$R_1 = \epsilon_1 / (\Sigma \lvert F_o \rvert)$	$-\mathrm{sgn}(\lvert F_o \rvert - \lvert F_c \rvert)\,\mathrm{sgn}(F_c) f^{Kt}$	$-\Sigma D^K$	$\lvert \epsilon_1 (E^{-1})_{\mu\mu} / \sqrt{\Sigma} \rvert$	$\epsilon_1 / \sqrt{\Sigma}$	(D)
$\epsilon_1' = \Sigma w_K \lvert \lvert F_o \rvert - \lvert F_c \rvert \rvert$	1	$wR_1 = \epsilon_1' / (\Sigma w_K \lvert F_o \rvert)$	$-\mathrm{sgn}(\lvert F_o \rvert - \lvert F_c \rvert)\,\mathrm{sgn}(F_c) f^{Kt}$	$-\Sigma w_K D^K$	$\lvert \epsilon_1' (E^{-1})_{\mu\mu} / \sqrt{\Sigma} \rvert$	$\epsilon_1' / \sqrt{\Sigma}$	
$\epsilon_2 = \Sigma \lvert I_o - I_c \rvert$	6	$R_2 = \sqrt{\epsilon_2 / (\Sigma I_o)}$	$-2\,\mathrm{sgn}(I_o - I_c) F_c f^{Kt}$	$-\Sigma D^K$	$\sqrt{\epsilon_2 (E^{-1})_{\mu\mu}} / \sqrt{\Sigma}$	$\sqrt{\epsilon_2} / \sqrt{\Sigma}$	
$\epsilon_2' = \Sigma w_K' \lvert I_o - I_c \rvert$	5	$wR_2 = \sqrt{\epsilon_2' / (\Sigma w_K' I_o)}$	$-2\,\mathrm{sgn}(I_o - I_c) F_c f^{Kt}$	$-\Sigma w_K' D^K$	$\sqrt{\epsilon_2' (E^{-1})_{\mu\mu}} / \sqrt{\Sigma}$	$\sqrt{\epsilon_2'} / \sqrt{\Sigma}$	
$\epsilon_3 = \Sigma (\lvert F_o \rvert - \lvert F_c \rvert)^2$	4	$R_3 = \sqrt{\epsilon_3 / (\Sigma \lvert F_o \rvert^2)}$	$-2(\lvert F_o \rvert - \lvert F_c \rvert)\,\mathrm{sgn}(F_c) f^{Kt}$	$-\Sigma D^K$	$\sqrt{\epsilon_3 (E^{-1})_{\mu\mu}} / \sqrt{\Sigma}$	$\sqrt{\epsilon_3} / \sqrt{\Sigma}$	
$\epsilon_3' = \Sigma w_K (\lvert F_o \rvert - \lvert F_c \rvert)^2$	3	$wR_3 = \sqrt{\epsilon_3' / (\Sigma w_K \lvert F_o \rvert^2)}$	$-2(\lvert F_o \rvert - \lvert F_c \rvert)\,\mathrm{sgn}(F_c) f^{Kt}$	$-\Sigma w_K D^K$	$\sqrt{\epsilon_3' (E^{-1})_{\mu\mu}} / \sqrt{\Sigma}$	$\sqrt{\epsilon_3'} / \sqrt{\Sigma}$	(E)
$\epsilon_4 = \Sigma (I_o - I_c)^2$	8	$R_4 = \sqrt[4]{\epsilon_4 / (\Sigma I_o^2)}$	$-4(I_o - I_c) F_c f^{Kt}$	$-\Sigma D^K$	$\sqrt[4]{\epsilon_4 (E^{-1})_{\mu\mu}} / \sqrt{\Sigma}$	$\sqrt[4]{\epsilon_4} / \sqrt{\Sigma}$	(F)
$\epsilon_4' = \Sigma w_K' (I_o - I_c)^2$	7	$wR_4 = \sqrt[4]{\epsilon_4' / (\Sigma w_K' I_o^2)}$	$-4(I_o - I_c) F_c f^{Kt}$	$-\Sigma w_K' D^K$	$\sqrt[4]{\epsilon_4' (E^{-1})_{\mu\mu}} / \sqrt{\Sigma}$	$\sqrt[4]{\epsilon_4'} / \sqrt{\Sigma}$	(G)

Notes

(A) F_o is the observed F(K), I_o is the observed F^2(K), F_c and I_c are the calculated values.

Sums are over all observed reflections, each with weight w_K.

(B) The TREFOIL number is the value of EPSWAY in Appendix B.

(C) Φ is defined in equation (268).

(D) 'Conventional' R-factor(1).

(E) 'Conventional' GoF, best electron density(67), used for Hamilton's test(68)

(F) Unbiased fit to experiment(69).

(G) Best Patterson map(67).

Figure 7

Error Measures for the Same P Compared

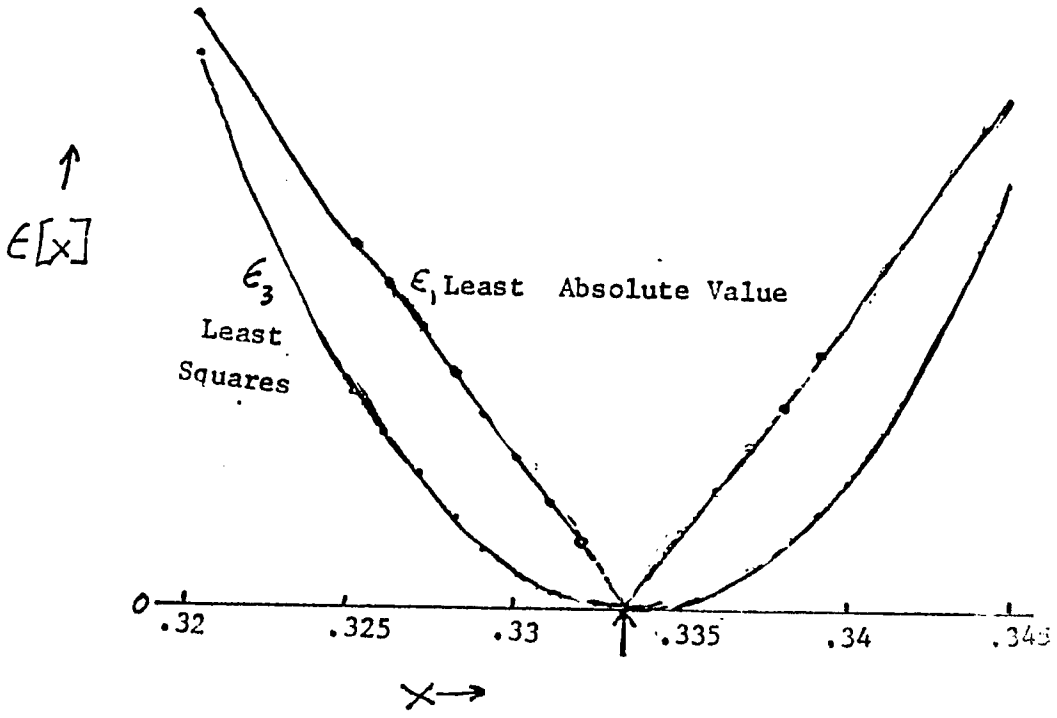

Figure 8

Gradients of the Error Measures of Figure 7

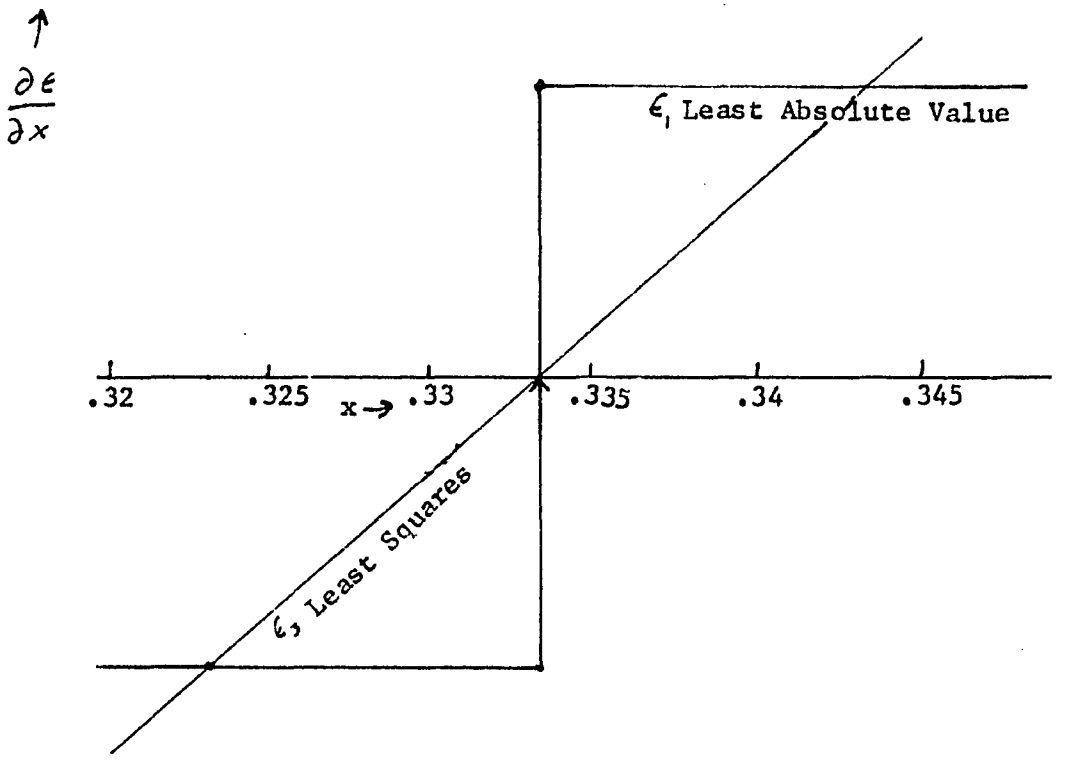

Noting that

$$\frac{\partial |x|}{\partial x} = \text{sgn}(x) = -1, 0, \text{ or } 1 \tag{65}$$

$$\frac{\partial}{\partial P_{\mu\nu}} \text{Tr}\, P f^K = \frac{\partial}{\partial P_{\mu\nu}} \left(\sum_{\mu=1}^{m} \sum_{\nu=1}^{m} P_{\mu\nu} f^K_{\nu\mu} \right) = f^K_{\nu\mu} \tag{66}$$

and that the iterative equations can be represented as

$$P' = 3P^2 - 2P^3 + \lambda_1 1 + \lambda_2 G \tag{67}$$

where

$$G = \sum_K w_K \frac{\partial \epsilon^K}{\partial P} \tag{68}$$

and

$$\begin{pmatrix} \lambda_1 \\ \lambda_2 \end{pmatrix} = \begin{pmatrix} N & -\text{Tr } P \\ \epsilon_{\text{goal}} & -\epsilon \end{pmatrix} \begin{pmatrix} \text{Tr } 11 & \text{Tr } 1G \\ \text{Tr } G1 & \text{Tr } GG \end{pmatrix}^{-1} \tag{69}$$

For various error measures ϵ_n, Table 3 can be derived.

ϵ_{goal} is a number which is lowered in a super-iterative procedure. Because the P-equations (22) are so slowly convergent, one cannot try to lower ϵ too precipitously. The starting value of should be a fairly large fraction T (1/2 to 3/4) of ϵ (P_{initial}) and

when (22) has converged to ϵ_{goal}, lower it by some amount. Computational experience has shown that, using

$$\epsilon_{goal'} = T\,\epsilon_{goal} = .75\,\epsilon_{goal} \tag{70}$$

is a reasonable choice, and anything less than T = 1/2 often leads to a failure to converge.

The idea behind the iterative equations is to solve for an idempotent matrix, and meanwhile, using Lagrange multipliers, to perturb in the conditions of N-normalization and fitting the data. Why does one use such an indirect method? Why not minimize the error measure ϵ while perturbing in normalization and idempotency? The reason lies in the nature of the constraint.

For the normalization constraint

$$N - \mathrm{Tr}\ P = 0 \tag{71}$$

the derivative is

$$\frac{\partial (N - \mathrm{Tr}\, P)}{\partial P_{\mu\nu}} = \frac{\partial N}{\partial P_{\mu\nu}} - \frac{\partial}{\partial P_{\mu\nu}} \sum_j P_{jj} = 0 - \delta_{\mu\nu} \tag{72}$$

and thus

$$\lambda_1 \quad 1 \tag{73}$$

For the idempotency constraint

$$\mathrm{Tr}\left((P^2 - P)^2\right) = 0 \tag{74}$$

the derivative is

$$\frac{\partial}{\partial P_{\mu\nu}}\left(\mathrm{Tr}\left((P^2-P)^2\right)\right) = \frac{\partial}{\partial P_{\mu\nu}}\left(\mathrm{Tr}\left(P^4-2P^3+P^2\right)\right)$$

$$= \frac{\partial}{\partial P_{\mu\nu}}\left(\sum_{ABCD}' P_{AB}P_{BC}P_{CD}P_{DA} - 2P_{AB}P_{BC}P_{CA} + P_{AB}P_{BA}\right) \tag{75}$$

$$= \sum_{ABCD}' \left(\begin{array}{l} \frac{\partial P_{AB}}{\partial P_{\mu\nu}}\left(P_{BC}P_{CD}P_{DA} - 2P_{BC}P_{CA} + P_{BA}\right) \\ + P_{AB}\frac{\partial P_{BC}}{\partial P_{\mu\nu}}P_{CD}P_{DA} - 2P_{AB}\frac{\partial P_{BC}}{\partial P_{\mu\nu}}P_{CA} \\ + P_{AB}P_{BC}\frac{\partial P_{CD}}{\partial P_{\mu\nu}}P_{DA} \\ + P_{AB}P_{BC}P_{CD}\frac{\partial P_{DA}}{\partial P_{\mu\nu}} \\ - 2P_{AB}P_{BC}\frac{\partial P_{CA}}{\partial P_{\mu\nu}} + P_{AB}\frac{\partial P_{BA}}{\partial P_{\mu\nu}} \end{array} \right)$$

By noting that

$$\frac{\partial P_{ij}}{\partial P_{\mu\nu}} = \delta_{ij}\delta_{\mu\nu} \tag{76}$$

equation (75) can be reduced to

$$\left(\begin{array}{l} P_{\nu C} P_{CD} P_{D\mu} - 2 P_{\nu C} P_{C\mu} + P_{\nu\mu} + P_{A\mu} P_{\nu D} P_{DA} - 2 P_{A\mu} P_{\nu A} \\ + P_{AB} P_{B\mu} P_{\nu A} + P_{\nu B} P_{BC} P_{C\mu} - 2 P_{\nu B} P_{B\mu} + P_{\nu\nu} \end{array} \right) \tag{77}$$

and remembering that A,B,C,D are dummy variables, it reduces to

$$\sum_{AB<} \left(\begin{array}{l} P_{\nu A} P_{AB} P_{B\mu} - 2 P_{\nu A} P_{A\mu} + P_{\nu\mu} + P_{B\mu} P_{\nu A} P_{AB} \\ - 2 P_{A\mu} P_{\nu A} + P_{AB} P_{B\mu} P_{\nu A} + P_{\nu A} P_{AB} P_{B\mu} - 2 P_{\nu A} P_{AM} + P_{\nu\mu} \end{array} \right) \tag{78}$$

Collecting terms, and noting that terms commute,

$$\begin{aligned} &\sum_{AB} (P_{\nu A} (P_{AB} P_{B\mu} - 2P_{A\mu} - 2P_{A\mu} + 2P_{AB} P_{B\mu} + P_{AB} P_{B\mu} - 2P_{A\mu}) + 2P_{\nu\mu} \\ &= \sum_{AB} 4P_{\nu A} P_{AB} P_{B\mu} - 6 P_{\nu A} P_{A\mu} + 2 P_{\nu\mu} \end{aligned} \tag{79}$$

Then the constraint would be

$$\text{Idem}\left(\; 4(P^{+})^3 - 6(P^{+})^2 + 2(P^{+}) \; \right) \tag{80}$$

Unfortunately, if the P matrix is nearly idempotent,

$$(P^+)^3 \sim (P^+)^2 \sim (P^+) \tag{81}$$

and

$$4(P^+)^3 - 6(P^+)^2 - 2(P^+) \sim 0 \tag{82}$$

which makes the constraint almost null, and thus the procedure will not work. In other words(70), "the distance λ moved along the generated directions tends to zero, causing jamming at a non-optimal point."

For the same reason, many other constrained minimization methods, which depend on the derivative of the constraint, such as the methods of Zoutendijk(70) and Rosen(71) (see Appendix E), are inapplicable.

The P-equations (122) have no obvious extension to including the optimization of parameters other than the P-matrix, such as atomic positions, basis function exponents, or vibration amplitudes U_{ij}.

The severest disadvantage of the P-equations is that their convergence is quite slow, although some error measures converge faster than others. In a relative timing test, for the same model problem, the relative convergence times, on an IBM 3033, are shown in Table 4.

Table 4

Convergence Times for the Iterative Equations
for Case 3, Model 2 of Chapter V,
Using Equation (67) for Various Error Measures

Error Measure	Convergence Time (Minutes CPU Time on an IBM 3033)
Least-Absolute-Value	
	50.498 (this is the ϵ used in Chapter V)
	60.756
Least-Squares	
	3.218
	4.187

The dramatic difference between the least-squares methods (ϵ_3 and ϵ_4) using the P-equations and the least-absolute-value methods(ϵ_1 and ϵ_2) can be rationalized as follows. Figures 7 and 8 show $\epsilon_1(P)$ to be a linear functional discontinuous at the solution, with a piecewise constant gradient. Convergence is at best linear. In contrast, $\epsilon_3(P)$ is a quadratic functional with a gradient that goes smoothly to zero at solution. Convergence is at best second-order, and apparently better than with a least-absolute-value criterion.

An alternative to the P-equations seems desirable, preferably one which can be extended to simultaneous optimization of any and all desired parameters, and which lends itself to being able to calculate error bars and covariance matrices for the final values of all parameters. The method outlined below fulfills all these specifications.

An idempotent P matrix has N(m-N) independent parameters. Suppose that one wants to also optimize some number of other variables v not in the P-matrix, such as atomic positions, vibrational amplitudes, etc.

Define a parameter vector p as

$$p = (N(m-N) \text{ independent } P_{\mu\nu}) \oplus (v = \text{other variables}) \qquad (83)$$

of dimension

$$\text{Dim}\ (p) = N\ (m - N\ ) + \text{Dim}\ (v) \tag{84}$$

In these terms, define a set of calculated x-ray scattering factors $F_{cal}(p)$ with an associated error functional $\epsilon_n[p]$ defined as, e.g.

$$\epsilon_1[\rho] = \sum_K \left| |F_{obs}(K)| - |F_{cal}(K,\rho)| \right| \tag{85}$$

and a gradient vector G with elements

$$G_j = \frac{\partial \epsilon}{\partial P_j} \tag{86}$$

The idempotency, normalization, and Hermitivity constraints are enforced in two ways.

First, any independent

$$p_j = P_{\mu\nu} \tag{87}$$

has bounds

$$0 \leq |P_{\mu\nu}| \leq 1 \tag{88}$$

and self-terms

$$p_j = P_{\mu\mu} \tag{89}$$

must be real.

Second, in an iterative procedure, or descent method, one can set up 3 or 4 stages in each iteration.

1) Calculate a descent step to move the parameters a distance d given by

$$p' = p + d\ (p, F_{obs}) \tag{90}$$

2) Using one of the purification methods, equation (43) or equation (46), generate a P-matrix whose independent variables p'_i , $1 < i < N(m-N)$, are those chosen by equation (87).

3) Calculate $F_{cal}(p')$ and $\epsilon_n[p']$.

4) (possibly) Select a new subset of N(m-N) independent P matrix elements.

A computer subroutine for step 2) is given in Appendix F.

Which elements $P_{\mu\nu}$ should be selected in step 4 above? All should be on or above the diagonal, with the Hermitivity constraint giving those below the diagonal simply as

$$P_{\nu\mu} = P_{\mu\nu}{}^{*} \tag{91}$$

All but the largest self-term P_{AA} should be used. The largest self-term is given by the normalization constraint as

$$P_{AA}=N-\sum_{\mu\neq A} P_{\mu\mu} \tag{92}$$

For the one-electron case,

$$N(m-N) = m - 1 \tag{93}$$

and all of the independent P matrix elements have been accounted for.

If N > 1, some cross-terms are also independent. I do not know which should be used. There is no reason to think that the same choice is appropriate both for McWeeny's method and for Mestechkin's method.

Since both McWeeny's and Mestechkin's purification processes are iterative, a starting guess for the independent elements of P in the idempotency step 2 is needed. On all but the first iteration, the corresponding elements from the previous iterations can be used. Zeros should not be used, since if, for example, one starts from

$$P_{init}= \begin{bmatrix} P_{11} & 0 & 0 \\ 0 & P_{22} & P_{23} \\ 0 & P_{32} & (N-P_{11}-P_{22}) \end{bmatrix} \tag{94}$$

then

$$3P^2 - 2P^3 = \begin{pmatrix} P'_{11} & 0 & 0 \\ 0 & P'_{22} & P'_{23} \\ 0 & P'_{32} & P'_{33} \end{pmatrix} \tag{95}$$

P_{12} and P_{13} are always zero if one starts them out at zero, and McWeeny's process will diverge or fail. An excellent starting guess is

$$P'_{\mu\nu} = \pm \frac{1}{\sqrt{N}} \left(\sqrt{P_{\mu\mu}} \sqrt{P_{\nu\nu}} \right) \tag{96}$$

In the one-electron case, Equation (96) is the exact solution, and no further purification is necessary.

Equation (96) introduces a new problem, or perhaps merely reveals an old problem. Since the P-matrix is the square of a wavefunction, $P = CC^+$, then

$$P_{\mu\mu} = (|C_\mu| e^{i\theta})(|C_\mu| e^{-i\theta}) \quad \forall \theta \tag{97}$$

By choosing the self-terms as independent elements, there arises a "phase problem." Not all values of the phase θ yield the same P-matrix. As a simple example, consider N = 1, m = 2, with 1 complex parameter, C_μ , defined by

$$C_\mu = |C_\mu| e^{i\theta_\mu} \tag{98}$$

Since the total phase of the orbital ψ is arbitrary, one can write absolute value signs on the expression

$$\psi = \begin{pmatrix} C_\mu & |\sqrt{1-C_\mu C_\mu^*}| \end{pmatrix} \begin{pmatrix} g_1 \\ g_2 \end{pmatrix} \tag{99}$$

then

$$P = \begin{pmatrix} |C_\mu|^2 & |C_\mu||\sqrt{1-C_\mu C_\mu^*}| e^{i\theta_\mu} \\ |C_\mu||\sqrt{1-C_\mu C_\mu^*}| e^{-i\theta_\mu} & 1-|C_\mu|^2 \end{pmatrix} \tag{100}$$

In the case of P real, θ_μ is either 0° or 180°. 0° corresponds to $c_1 g_1 + c_2 g_2$, a bonding orbital. 180° corresponds to $c_1 g_1 - c_2 g_2$, an antibonding orbital.

The implication for empirical wavefunction determination is that one shouild consider the self-terms as having a "hidden" phase that manifests itself in the cross-terms. For P real,

$$P_{\mu\mu} = \left(+\sqrt{P_{\mu\mu}}\right)^2 \quad \text{or} \quad \left(-\sqrt{P_{\mu\mu}}\right)^2 \tag{101}$$

for P complex,

$$P_{\mu\mu} = \left(|\sqrt{P_{\mu\mu}}| \, e^{i\theta_\mu} e^{-i\theta_\mu} \right) \tag{102}$$

$$P_{\mu\nu} = \left(|\sqrt{P_{\mu\mu}}| \, |\sqrt{P_{\nu\nu}}| e^{i(\theta_\mu - \theta_\nu)} \right) \tag{103}$$

this results because

$$P_{\mu\mu} = |C_\mu|^2 \tag{104}$$

The first step in determining any wavefunction is to choose the form of the basis functions. This is especially important with totally empirical wavefunctions. Since there are a limited number of data, one must use as few parameters as possible, and therefore as small a basis as possible, in order to have a larger number of data per parameter. It is always possible to get a low ϵ by overparametrizing the problem, but this would not be a meaningful approach to interpretation.

Since this thesis is mainly concerned with electron densities from x-ray diffraction, the effect of basis set on density is of more concern than that on energy. Including electron correlation in ab initio studies changes the density by at most about 1%(72), but basis set effects are two to three times as large(59).

The best type of basis function to use for atomic calculations is the Slater orbital. These can be forced to satisfy the electron-nuclear cusp condition (which is nice, but not relevant here),

and more importantly, they decay exponentially at large distances from the nucleus, which is a condition known to be satisfied by the exact wavefunction. However, many of the integrals required to calculate molecular properties in a Slater basis are analytically intractible, and often only numerical solutions exist(73,74,75,76,77). In contrast, Gaussian orbitals decay too fast, have no cusps, but all integrals over such a basis(19,21,49,77,78) are not only closed-form and analytic, they are usually quite simple. In order to simulate the desirable properties of a Slater orbital, one can superimpose several Gaussian "primitives" in a fixed ratio(79). Some are made very "tight" (large exponent) to simulate the cusp. Others are very "loose" to simulate the gradual decay of a Slater (although this is unsatisfactory for very large distances). The remainder of the Gaussians can be optimized in an ab initio calculation either to least-squares fit a Slater orbital, called STO-nG, or to minimize the energy. This set of Gaussians is treated as a single function, referred to as a "contracted" Gaussian. To improve an atomic calculation, one can add basis functions either of different radial dependence, or functions with higher angular momentum. The general formula for an atom-centered contracted Cartesian Gaussian orbital is

$$g=(x-x_{atom})^{A}(y-y_{atom})^{B}(z-z_{atom})^{C}\times$$

$$\left(\sum_{j} c_j e^{-a_j(r-r_{atom})^2}\right) \times \frac{1}{\sqrt{Nor}} \qquad (105)$$

where

$$r_{atom} = (x_{atom}, y_{atom}, z_{atom}) \tag{106}$$

is the position of the nuclear center; a_j is the j'th exponent (large exponents are "tight" primitives); the c_j are the contraction coefficients;and (Nor) is the normalization factor. The sum of a+b+c is the angular momentum quantum number; with 0 being s, 1 as p, 2 as d, 3 as f,etc. Note that the radial dependence is that of a 1s orbital. This is always taken to be the case. No analytic formulas over Gaussian 2s,4s,... primitives exist. Huzinaga has shown(80) that using 3s primitives has no advantages over 1s primitives, and it takes more effort to evaluate the integrals. To convert from Cartesian Gaussian orbitals to spherical harmonic Gaussians is not overly difficult. The matrices in Table 5 below show the process for s,p,d, and f orbitals. For example, the 4f orbital $z(x^2-y^2)$ is
$-1/\sqrt{2}\ g(0,2,1)+ 1/\sqrt{2}\ g(2,0,1)$.

For molecular or crystal wavefunctions, atom-centered basis functions are not necessarily appropriate. A crucial feature of the density when two atoms bond to each other is a shift of the density from near the nuclei and from the opposite side of the atom to the bonding region. The Hellmann-Feynman Theorem dictates that the basis functions in a finite atom-centered expansion also move into the bonding region. There are two ways of modeling this effect. One way is to introduce higher-momentum atom-centered "polarization" functions,

Table 5

Conversion Between Cartesian Forms $x^A y^B z^C$
and Real Spherical Harmonics

		A+B+C=0 (0,0,0)
ls		1

		A+B+C=1 (1,0,0)	(0,1,0)	(0,0,1)
2p:	x	1	0	0
	y	0	1	0
	z	0	0	1

		A+B+C=2 (2,0,0)	(0,2,0)	(0,0,2)	(1,1,0)	(1,0,1)	(0,1,1)
	3s	$1/\sqrt{3}$	$1/\sqrt{3}$	$1/\sqrt{3}$	0	0	0
3d:	z^2	$-1/\sqrt{6}$	$-1/\sqrt{6}$	2/ 6	0	0	0
	x^2-y^2	$1/\sqrt{2}$	$-1/\sqrt{2}$	0	0	0	0
	xy	0	0	0	1	0	0
	xz	0	0	0	0	1	0
	yz	0	0	0	0	0	1

		A+B+C=3 (cubic convention) (300)	(210)	(120)	(030)	(021)	(012)	(003)	(102)	(201)	(111)
4p:	x	$1/\sqrt{3}$	0	$1/\sqrt{3}$	0	0	0	0	$1/\sqrt{3}$	0	0
	y	0	$1/\sqrt{3}$	0	$1/\sqrt{3}$	0	$1/\sqrt{3}$	0	0	0	0
	z	0	0	0	0	$1/\sqrt{3}$	0	$1/\sqrt{3}$	0	$1/\sqrt{3}$	0
4f:	$z(x^2-y^2)$	0	0	0	0	$-1/\sqrt{2}$	0	0	0	$1/\sqrt{2}$	
	$y(z^2-x^2)$	0	$-1/\sqrt{2}$	0	0	0	$1/\sqrt{2}$	0	0	0	0
	$x(y^2-z^2)$	0	0	$1/\sqrt{2}$	0	0	0	0	$-1/\sqrt{2}$	0	0
	x^3	2/ 6	0	-1/ 6	0	0	0	0	$-1/\sqrt{6}$	0	0
	y^3	0	$-1/\sqrt{6}$	0	$2/\sqrt{6}$	0	$-1/\sqrt{6}$	0	0	0	0
	z^3	0	0	0	0	$-1/\sqrt{6}$	0	$2/\sqrt{6}$	0	$-1/\sqrt{6}$	0
	xyz	0	0	0	0	0	0	0	0	0	1

such as 2p orbitals on hydrogen,which are combined to form hybrid orbitals with the desired features. Another way is to introduce functions which are not atom-centered(81); their positions are treated as another set of parameters to be optimized. Comparative ab initio studies(82,83) show that equally good descriptions of molecular bonds can be obtained with only 1/3 to 1/2 as many extra basis functions by using these floating functions instead of polarization functions. These floating functions are usually taken, for purposes of simplicity(84), to be 1s-type Gaussian primitives, called Floating Spherical Gaussian Orbitals, FSGO, bond functions, or simply floaters. The main reason that theoretical calculations don't use FSGO more often is that using them properly requires optimizing their positions and exponents separately for each new molecule - there is inherently no such thing as a "standard FSGO exponent." Also, each time one changes the position or exponent of a floater, or the position of an atom in a geometry optimization, all integrals involving floaters must be re-evaluated. Since up to half, and commonly 1/3, of the computer time in an ab initio Hartree-Fock calculation is spent evaluating integrals once, recalculating many of them on each iteration is an unpopular option. One compromise which is used(85) is to arbitrarily fix the floater position at the bond midpoint, and optimize only the exponent (to the nearest .05 $a.u.^{-2}$). Sometimes, to compensate for this limitation, a set of 2p primitives is also placed at the bond midpoint, either with the same exponent as the 1s-type floater, or with exponent

separately optimized. Optimizing the FSGO position makes the resultant wavefunction easier to interpret in terms of charge partitioning, and this partitioning is remarkably close to a separation into virial regions(86).

In a system with symmetry higher than C_1, one uses a contracted floater, with all primitives having the same exponent, but at positions related by symmetry. This is in contrast to a contracted atom-centered Gaussian,where the positions are the same, but the exponents differ. The FSGO contraction coefficients depend on the irreducible representation of the symmetry group desired. For example, in symmetry group C_i, with coordinate origin at the inversion center, one would get 2 sets of 2 floaters

$$\psi_{A_g} = (\text{norm})(e^{-a(r-r_{FSGO})^2} + e^{-a(r-r_{FSGO})^2}) \qquad (107)$$

$$\psi_{A_u} = (\text{norm})(e^{-a(r-r_{FSGO})^2} - e^{-a(r-r_{FSGO})^2}) \qquad (108)$$

A more complicated example, shown in Table 6 and Figure 9, is that of group D_{3h}, which is the atomic site symmetry in beryllium metal (see chapter 3 below) and graphite (see chapter 4 below). Here it is convenient to define the floater positions in terms of the polar coordinates r, θ, ϕ. The 12 floater positions are placed at $Q(r, \theta, \phi)$, where Q is one of the 12 operations (E, $2C_3$, $3C_2$, σ_h,

Figure 9

Floating Spherical Gaussian Orbitals

in D_{3h} (6m2) Symmetry

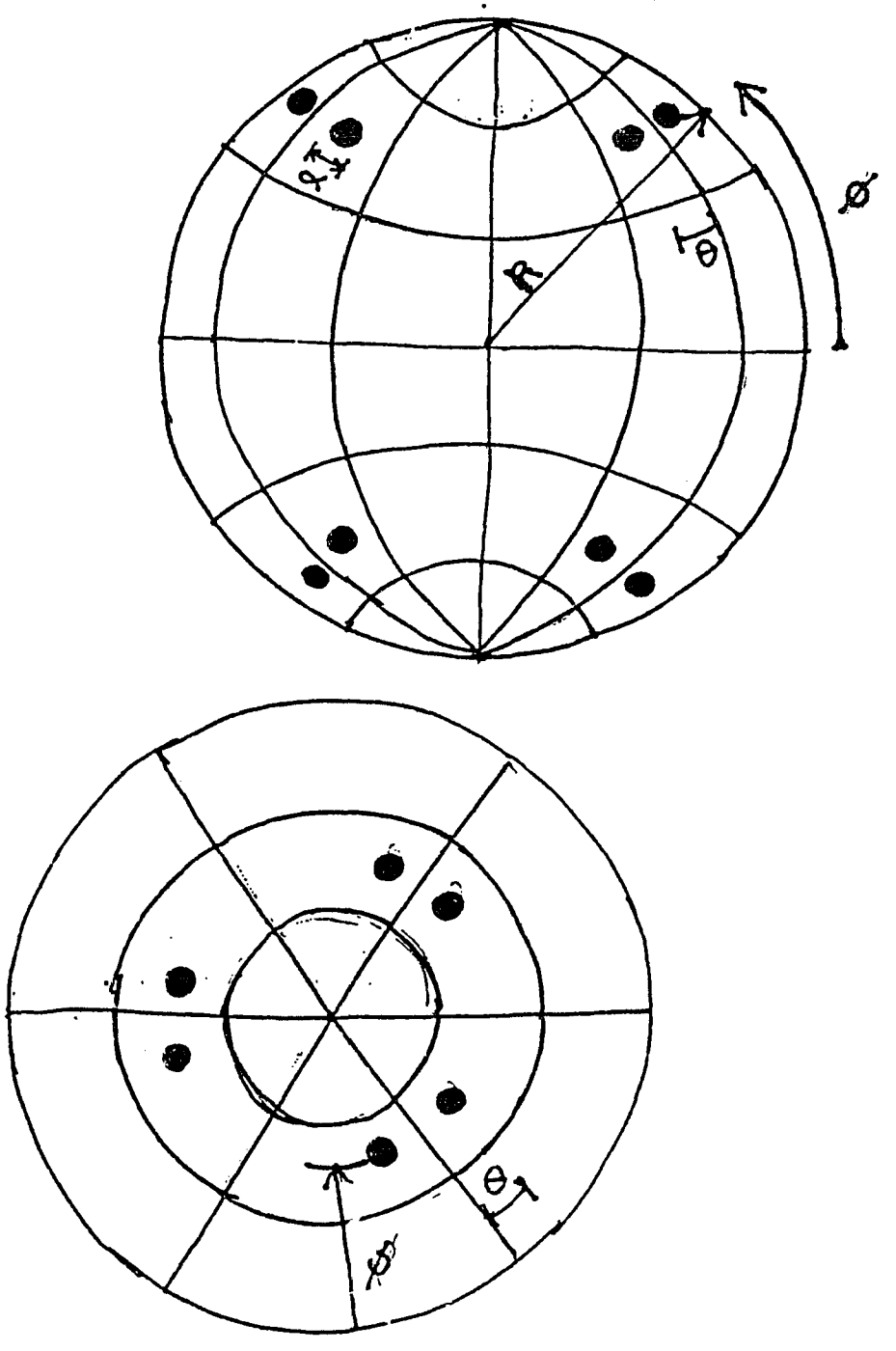

Table 6

Floating Spherical Gaussians in D_{3h} Symmetry
and Their Contraction Coefficients
for All Irreducible Representations

#	Distance	Long-itude	Lat-itude	Representation A_1'	A_2'	E_{1a}'	E_{1b}'	E_{2a}'	E_{2b}'	A_1''	A_2''	E_{1a}''	E_{1b}''	E_{2a}''	E_{2b}''
1	r	Θ	ϕ	1	1	1	1	1	1	1	1	1	1	1	1
2	r	120-Θ	ϕ	1	-1	2	0	-2	0	-1	1	2	0	-2	0
3	r	120+Θ	ϕ	1	1	1	-1	1	-1	1	1	1	-1	1	-1
4	r	240-Θ	ϕ	1	-1	-1	-1	1	1	-1	1	-1	-1	1	1
5	r	240+Θ	ϕ	1	1	-2	0	-2	0	1	1	-2	0	-2	0
6	r	-Θ	ϕ	1	-1	-1	1	1	-1	-1	1	-1	1	1	-1
7	r	Θ	-ϕ	1	1	1	1	1	1	-1	-1	-1	-1	-1	-1
8	r	120-Θ	-ϕ	1	-1	2	0	-2	0	1	-1	-2	0	2	0
9	r	120+Θ	-ϕ	1	1	1	-1	1	-1	-1	-1	-1	1	-1	1
10	r	240-Θ	-ϕ	1	-1	-1	-1	1	1	1	-1	1	1	-1	-1
11	r	240+Θ	-ϕ	1	1	-2	0	-2	0	-1	-1	2	0	2	0
12	r	-Θ	-ϕ	1	-1	-1	1	1	-1	1	-1	1	-1	-1	1
	(1/ Normalizer)^2			12	12	24	8	24	8	12	12	24	8	24	8

$2S_3$, $3\sigma_v$) of D_{3h} . All irreducible representations are spanned at least once by the set of 12 floater primitives.

Figure 9 shows a set of 12 FSGO in D_{3h} symmetry from two views. In the upper view, looking down the x axis, the z axis (poles) appears as a vertical line, and both the y axis and xy plane (equator) appear as a horizontal line. The floaters, represented as shaded circles, are at a distance r_{FSGO} from the central atom, at the six longitudes $\{0^\circ, 120^\circ, 240^\circ\} \pm \theta$, times the two latitudes $\pm\phi$, for a total of 1 distance times 6 longitudes times 2 latitudes equals 12 FSGO. The lower view, looking down the z axis (polar projection), shows the x axis as a horizontal line. The y axis, not drawn in here, would be a vertical line. The equator appears as the outermost circle.

The 12 floater positions, numbered 1 to 12 in column 1 of Table 6, are explicitly related to the 3 parameters r, θ, ϕ by columns 2,3, and 4 respectively. The 12 symmetrized representations of the point group D_{3h} that can be formed from the 12 FSGO by a unitary transformation are shown with the transform matrix in the remainder of Table 6. For example, the floaters can be combined into an a_1'' basis function as $g_{a_1''} = 1/\sqrt{12}\,(g_1 - g_2 + g_3 - g_4 + g_5 - g_6 + g_7 - g_8 + g_9 - g_{10} + g_{11} - g_{12})$ or into one part of a doubly-degenerate rep as

$g_{e_{1a}''} = 1/\sqrt{24}\,(g_1 + 2g_2 + g_3 - g_4 - 2g_5 - g_6 - g_7 - 2g_8 - g_9 + g_{10} + 2g_{11} + g_{12})$.

The use of Floating Spherical Slater Orbitals is inadvisable, since

that would put a cusp where none belongs. Also, there is no reason to expect exponential die-off from the bonding region towards the constituent atoms.

Atom-centered polarization functions and FSGO are both ways of describing "deformation density;" the difference between atoms and a molecule. There is no easy way to convert from one to the other - a set of floaters can be expanded in an infinite series of polarization functions, and vice versa, but there is no one-to-one correspondence. Although it is more convenient to think in terms of atom-centered functions, this is an educational prejudice. Neither polarization functions nor floaters is inherently a "fundamental" approach, nor is one more "contrived" or ad-hoc than the other. The advantages of each are that FSGO yield a more compact representation, while polarization functions are less costly of computer time to use. No one has ever actually expanded any wavefunction in a truly infinite series; where to truncate the finite expansion, and whether to go to more centers or to higher angular momentum, is largely a matter of taste and convenience. For totally empirical wavefunctions of small systems, there is a leaning towards floaters because of their relatively fewer parameters, but for larger systems economic considerations dictate the use of polarization functions. The strongest argument against FSGO is that to directly compare ab initio and totally empirical wavefunctions for the same system, one would prefer to use the same LCAO basis for both; since the existing ab initio calculation is almost certain to not use floaters, the totally empirical function shouldn't either.

Another common type of basis function, used mainly in ab initio solid-state wavefunctions, is the plane wave, either as the only functions, as Orthogonalized Plane Waves(87) Schmidt-orthogonalized to the atom-centered basis, or as a mixed Plane Wave/Gaussian basis(88,89). These plane waves have been used for crystallography(90). They are in general unsuited for totally empirical calculations, since one must use hundreds of them to get satisfactory convergence.

A common technique both in ab initio calculations and in non-quantum models of Bragg scattering is the frozen-core approximation. Only the valence orbitals of a molecule or crystal are allowed to change; the core orbitals are all(91) kept "frozen" at the values determined by an atomic ab initio calculation. This approximation has at most about a 0.3% effect on the density(72). Totally empirical wavefunctions should certainly use the frozen-core approximation in almost all cases - one gets the core described excellently with no added parameters. Also in view of reference(72), appeals to "core expansion" should be viewed with some suspicion.

Ab initio calculations involving large atoms often use pseudo-orbitals(92), and thus all core electrons are eliminated entirely from the calculations. A totally empirical wavefunction could use the same idea.

Pseudo-orbitals are of 2 types, core and valence. The requirement of orthogonality to the core fixes the form of the valence basis pseudo-orbitals. The prescription for ab initio calculation of valence pseudo-orbital bases is well defined(92). The pseudo-core is obtainable from atomic ab initio calculations, and is used without modification. That is, the molecular pseudo-core is an atomic core. Note that using a pseudo-core is not eliminating the density "near" the nucleus; it is eliminating the canonical core orbitals from the calculation entirely. Valence electron density near the nuclei and its modification from one molecule to the next will still be described in using valence pseudo-orbital basis functions.

Note that using core pseudo-orbitals exclusively - assuming that all electrons are in the "core" and hence are unperturbed by molecule formation or crystal formation - is exactly the superposition of free spherical atoms approximation, also called the "promolecule," that is commonly used in crystallography.

In addition to the reduction in the size of the problem from using the frozen-core approximation, one can reduce the size of the problem still further by symmetry-blocking of the P matrix. In a symmetry-adapted basis, the P matrix can be written as

$$P = P_{\Gamma_1} \oplus P_{\Gamma_2} \oplus \ldots \tag{109}$$

where each P_{Γ} satisfies

$$P_\Gamma = P_\Gamma^+ \quad ; \quad P_\Gamma^2 = P_\Gamma \quad ; \quad Tr\, P_\Gamma = N_\Gamma \tag{110}$$

and cross-terms between basis functions of different reps are necessarily zero by symmetry - each orbital in a symmetry-adapted basis must belong to one and only one irreducible representation of the group. Each rep must be assigned N_Γ electrons. In the single-determinant approximation, the N_Γ are constrained to be integer, and each assignment of the N_Γ corresponds to a different electron configuration of the system. The ground state of the system, in doubtful cases, will be the set of N_Γ which best fits the available data.

This symmetry-blocking has reduced the number of parameters. Since

$$N = \sum_\Gamma N_\Gamma \quad ; \quad m = \sum_\Gamma m_\Gamma \tag{111}$$

the number of P matrix parameters has gone from

$$\left(\sum_\Gamma N_\Gamma\right)\left(\sum_{\Gamma'} m_{\Gamma'} - N_{\Gamma'}\right) = \sum_{\Gamma\Gamma'} N_\Gamma \left(m_{\Gamma'} - N_{\Gamma'}\right) \tag{112}$$

to

$$\sum_\Gamma N_\Gamma \left(m_\Gamma - N_\Gamma\right) \tag{113}$$

and the number of parameters symmetry-constrained to zero is

$$\sum_{\Gamma} \sum_{\Gamma' \neq \Gamma} N_{\Gamma} \left(m_{\Gamma'} - N_{\Gamma} \right) \tag{114}$$

For the degenerate representations E,T,G, and H, one gets further reduction, since if the basis functions are arranged within each sub-representation in the same order,

$$P_E = P_E \ , \ P_{T_x} = P_{T_y} = P_{T_z} \text{, etc.} \tag{115}$$

and thus for purposes of counting parameters, degenerate reps are counted once only, not 2,3,4, or 5 times.

Chapter 4 below makes use of the preceding symmetry discussion to outline a procedure for determining totally empirical Bragg wavefunctions for graphite and for diamond.

In the preceding discussion, it was assumed that the basis functions were orthonormal and symmetry-adapted. If one uses a non-symmetrized basis, great care must be exercised. The observable density $\rho(r)$ always belongs to the totally symmetric representation Γ_1 of any group. An orbital ψ belonging to any irreducible representation of the group will yield a density of the proper symmetry. However, non-symmetrized basis functions, which belong in general to a reducible representation, will usually yield a density of the wrong symmetry. As a trivial example, in C_{ζ},

$$(\text{odd})^2 = (\text{even})^2 = \text{even, but } (\text{odd} + \text{even})^2 = (\text{odd} + \text{even}) \qquad (116)$$

If one has hybrid orbitals, say a set of sp^2 orbitals in a C_3 environment, these must be viewed as members of a degenerate set, and populated according to equation (115). Better yet would be to always use symmetry-adapted basis functions. The three sp_2 hybrids mentioned above span A and E of C_3, not just one rep.

It has been suggested(41) that one can further reduce the number of parameters in the P matrix by making the approximation that certain cross-terms are zero, not by symmetry, but because they are "expected" to be small.

One can, for example, treat each water molecule in an ice crystal separately, with no cross-terms in P between functions on different waters. A refinement of sodium azide could be constrained to have one P matrix for Na^+ and another for N_3^-. When doing this, keep in mind that a quantum P matrix has an integer trace - one cannot have separate P matrices for $Na^{(1-\chi)-}$ and $N_3^{(1-\chi)-}$.

The two most common types of constraint are called the "two-center" and "one-center" approximations. In the "two-center approximation" this expectation of negligibility comes from the two basis functions involved in the cross-term being on atoms not considered bonded to each other. For example, in the molecule $\begin{matrix} H \\ F \end{matrix}\!\!>C=O$

$$P = \begin{pmatrix} P_{HH} & 0 & P_{CH} & 0 \\ 0 & P_{FF} & P_{CF} & 0 \\ P_{HC} & P_{FC} & P_{CC} & P_{CO} \\ \end{pmatrix} \tag{117}$$

This can be implemented by defining p parameters which use the same basis functions, but each corresponds to either an atomic or a bonding feature, e.g.

$$p=p_{CH\ \text{bond}}+p_{F\ \text{atom}}+p_{CF\ \text{bond}}+p_{C\ \text{atom}}+p_{C=O\ \text{bonds}} + p_{O\ \text{atom}} + p_{H\ \text{atom}} \tag{118}$$

A problem with this is that, since the P sub-matrices do not refer to disjoint sets of basis functions, one could conceivably wind up overpopulating a particular basis function, violating the quantum constraint of equation (88). One solution would be to check any wavefunction refinement using equation (118) once every few iterations to be sure that the total P matrix is idempotent, normalized, and Hermitian; if not it should be fixed up and possibly the two-center approach should be modified.

The most extremely constrained approach is the one-center method, wherein the P matrix is treated as the direct sum of each atom's P sub-matrix. In the $\begin{matrix} H \\ F \end{matrix}\!\!>\!C=O$ example,

$$P = \begin{pmatrix} P_{HH} & 0 & 0 & 0 \\ 0 & P_{FF} & 0 & 0 \\ 0 & 0 & P_{CC} & 0 \\ 0 & 0 & 0 & P_{OO} \end{pmatrix} \tag{119}$$

Each atom then has an integer charge, and covalent bonding cannot be described. This is the approximation to use when comparing quantum Bragg refinements to multipole Bragg refinements, where the one-center approximation is almost always used to prevent over-parametrization.

A one-center quantum P-matrix is exactly equivalent to a multipole refinement with quantum constraints, as I will now proceed to show. Given m orbital basis functions g_i, one can construct m(m+1)/2 density basis functions, or multipole functions,

$$M_{ij} = g_i g_j \tag{120}$$

Table 7 displays the correspondence between one-center orbital products of Cartesian Gaussians and Hirshfeld-type(42) multipoles. Thus, one could convert a multipole refinement program to a one-center totally empirical wavefunction refinement program with only a small amount of effort. Note that the correspondence equation (120) is one—>many. The results of a multipole refinement cannot uniquely be converted to a wavefunction, not even to a wavefunction that violates quantum constraints.

Table 7

Conversion Between Cartesian Gaussians and Hirshfeld Multipoles

Orbital to Multipole

Angular Exponents g_1 A B C	Angular Exponents g_2 A B C	Orbitals	Multipole	Angular Exponents M A B C
0 0 0	0 0 0	s s	Monopole	0 0 0
0 0 0	1 0 0	s p_x	Dipole	1 0 0
0 0 0	2 0 0	s d_{xx}	Quadrupole	2 0 0
0 0 0	3 0 0	s f_{xxx}	Octupole	3 0 0
1 0 0	1 0 0	p_x p_x	Quadrupole	2 0 0
1 0 0	0 1 0	p_x p_y	Quadrupole	1 1 0
1 0 0	2 0 0	p_x d_{xx}	Octupole	3 0 0
0 1 0	1 0 0	p_y p_x	Quadrupole	1 1 0
1 0 0	2 0 0	p_x d_{xx}	Octupole	3 0 0

Multipole to Orbital

M A B C	Name	g_1 A B C	g_2 A B C	Name
0 0 0	Monopole	0 0 0	0 0 0	s s
1 0 0	Dipole	1 0 0	0 0 0	p_x s
2 0 0	Quadrupole	2 0 0	0 0 0	d_{xx} s
		1 0 0	1 0 0	p_x p_x
1 1 0	Quadrupole	1 1 0	0 0 0	d_{xy} s
		1 0 0	0 1 0	p_x p_y
3 0 0	Octupole	3 0 0	0 0 0	f_{xxx} s
		2 0 0	1 0 0	d_{xx} p_x
2 1 0	Octupole	2 1 0	0 0 0	f_{xxy} s
		2 0 0	0 1 0	d_{xx} p_y
		1 1 0	1 0 0	d_{xy} p_x

To take an example, we see that an orbital sp basis leads uniquely to monopoles from s-s terms, dipoles from s-p terms, and quadrupoles both mixed (1 1 0 from p_x-p_y terms, 1 0 1 from p_x-p_z, and 0 1 1 from p_y-p_z) and unidirectional (2 0 0 from p_x^2 , 0 2 0 from p_y^2 , and 0 0 2 from p_z^2). However, multipoles cannot be decomposed uniquely into orbitals. For example, we see that the mixed quadrupole 1 1 0 can be decomposed either into a p_x-p_y product, or an s-d_{xy} product.

If the basis g is not orthonormal, one must correct for this by the use of an overlap matrix S(91) with elements

$$S_{ij} = < g_i \mid g_j > \tag{121}$$

The equation for scattering amplitude is modified to

$$F_{cal}(K) = \text{Tr } PS^{-1/2} f(K) S^{-1/2} = \text{Tr } S^{-1/2} PS^{-1/2} f(K) \tag{122}$$

In equation (122), the two versions are correcting respectively the basis and the P matrix. When using the P iterative equations (67), it is more convenient to correct the basis. When using the descent method of equation (90), either convention is equally good. To see what the wavefunction looks like in the original basis, one can examine the matrix R defined by

$$R = S^{-1/2}PS^{-1/2} \tag{123}$$

When adding a new basis function, the initial guess at P' should be

$$P' = (S')^{+1/2} \begin{bmatrix} S^{-1/2}PS^{-1/2} & 0 \\ 0 & 0 \end{bmatrix} (S')^{+1/2} \tag{124}$$

Chapter III. Beryllium Metal

The only example in this thesis, or indeed anywhere in the literature as of March 1984, of applying the method of chapter 2 to real data from an actual experiment on a real crystal - in no sense artificial data - is this chapter, wherein the formalism is applied to beryllium metal.

The (as yet unpublished) x-ray diffraction study of beryllium metal by Larsen and Hansen(56) provides a sensitive test of the formalism. Beryllium crystallizes in space group $P6_3/mmc$, #194, at the 2 positions "c" of the Wyckoff notation. There are 2 asymmetric units per cell, with one atom in each. The site symmetry is $\bar{6}m2$, or D_{3h}. The structure is illustrated in Figure 10. There are several reasons why beryllium is a good first case.

First - it's a simple structure. Beryllium is nearly hexagonal-close-packed. There is only atom per asymmetric unit. The position of that atom is fixed by symmetry. In the spin-paired approximation, this one atom has only one valence orbital.

Second - beryllium is interesting. It has a very high Debye temperature for a metal: 1440^{o} K. The large diamagnetic susceptibility, and the fact that beryllium is brittle at room temperature, point to beryllium being not quite metallic. As a

consequence of these facts, beryllium has been extensively studied both experimentally and theoretically(56).

Third - beryllium has half its electrons in the valence shell, so the electron redistribution might be easy to spot. Unfortunately, this is not the case. 97% of the scattering power comes from the 1s core, and less than half of one percent can be attributed to bonding effects.

Fourth - because reason three didn't work out, and bonding and deformation effects are so small, the phases of all reflections are determined by the free-atom model.

Fifth - the diffraction data for beryllium are excellent. Larsen and Hansen have recently done a very careful study(56), and their 58 data extend out to 1.2 $\mathring{A}^{-1}$, with an average reported error of only 0.39% in $\sigma(F)/F$. In fact, the errors are even less than this, as will be explained below.

Several models of beryllium were tried. The first was the free-atom model. The beryllium atomic wavefunction expansion in 10 s-type Gaussians by Huzinaga(80), shown in Table 8, was used. Only three parameters were refined - an experimental scale factor 1/S, and the two vibrational parameters U_{11} and U_{33}. From symmetry,

$$U_{11}=U_{22} \quad , \quad U_{12}=U_{13}=U_{23}=0 \tag{125}$$

Table 8

The 10-Gaussian Beryllium Atom Basis of Huzinaga(80)

i	a_i	1s coefficient	2s coefficient
1	3.66826	.43211	-.10274
2	32.6562	.08689	-.01628
3	117.799	.02239	-.00414
4	532.280	.00422	-.00077
5	1.35431	.33942	-.15719
6	0.38905	.03710	.04809
7	0.15023	-.00791	.59099
8	10.4801	.24152	-.04911
9	3630.38	.00053	-.00010
10	.052406	.00183	.47194

$$g_j = \sum_{i=1}^{10} \left(\frac{2\pi}{a_i}\right)^{.75} c_{ij} e^{-a_i r^2}$$

This lead to the results of Table 9. Refining on ϵ_3' lead to wR_3 of .00419, R_1 of .00544, with a goodness of fit $GOF_3^w = 1.67$. Adding the only symmetry-allowed third cumulant C_{112} led to wR_3 of .00385, R_1 .00532, and $GOF_3^w = 1.55$, as shown in Table 9.

Thus it can be seen that any deviation from free-atom behavior in beryllium is small. The cumulant expansion is illustrated in Figure 11.

When approaching the limit of the data so closely, and with such good data, it is advisable to examine closely the data itself. Larsen and Hansen collected a full sphere of data on two wavelengths (Mo and Ag) and yet only report 58 numbers. Appendix C contains the averaged intensities for each radiation separately, for those symmetry-unique reflections that were judged by the experimentalists to be of "significant" intensity. The errors reported for the 58 fully averaged reflections are listed with the F_{obs} values in Appendix C, and these errors are graphed in Figure 12.

The errors fall naturally into 2 groups; high angle data with minute errors averaging .0017 electrons, and low-angle data with 4 times as much error in $\sigma(F)/F$ and 10 times as large an absolute error $\sigma(F)$. This is not a result of the experiment itself. It is a result of the low-angle data being artificially weighted out relative to that

Figure 10

Nuclear Positions in Beryllium Metal

from Reference(56)

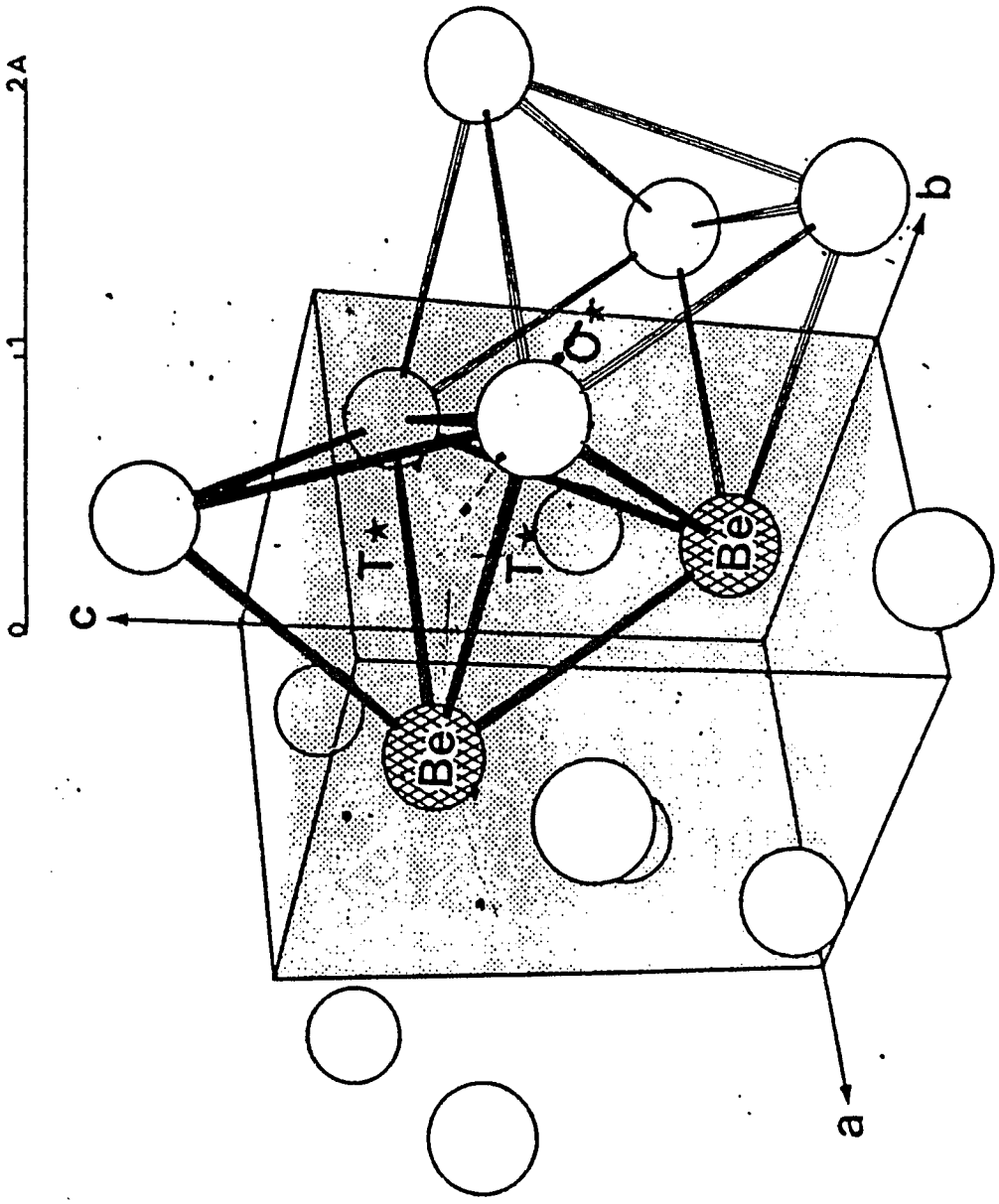

Figure 11

Cumulant Expansion for Beryllium Nuclei

$$F^{\text{RIGID BODY}}_{\text{Thermally Smeared}} = F_{\text{at-rest}} \times$$

$$\exp\left(2\pi i \underbrace{\sum_i h_i x_i}_{\text{1st cumulant}} - \underbrace{\sum_{ij} h_i h_j U_{ij}}_{\text{2nd cumulant}} - i \underbrace{\sum_{ijk} h_i h_j h_k C_{ijk}}_{\text{3rd cumulant}} + \ldots\right)$$

1st cumulant — position; 2nd cumulant — width; 3rd cumulant — skewness

Cumulants allowed by D_{3h} symmetry in Be

1st- NONE

2nd-

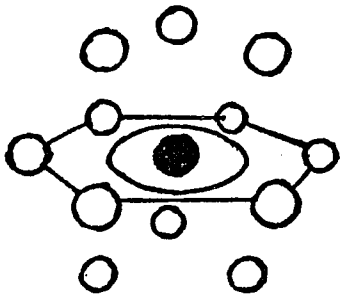

U_{11}

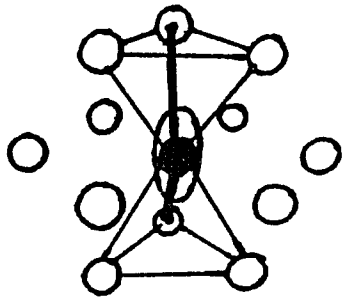

U_{33}

3rd-

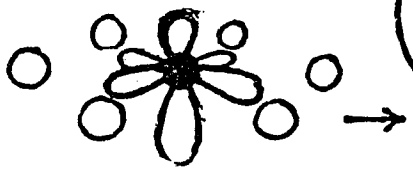

C_{112}

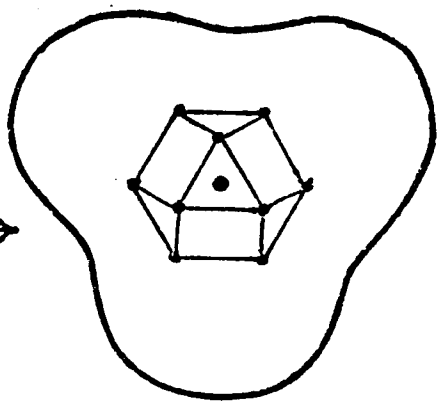

Figure 12

Errors in Larsen's(56) Beryllium Data

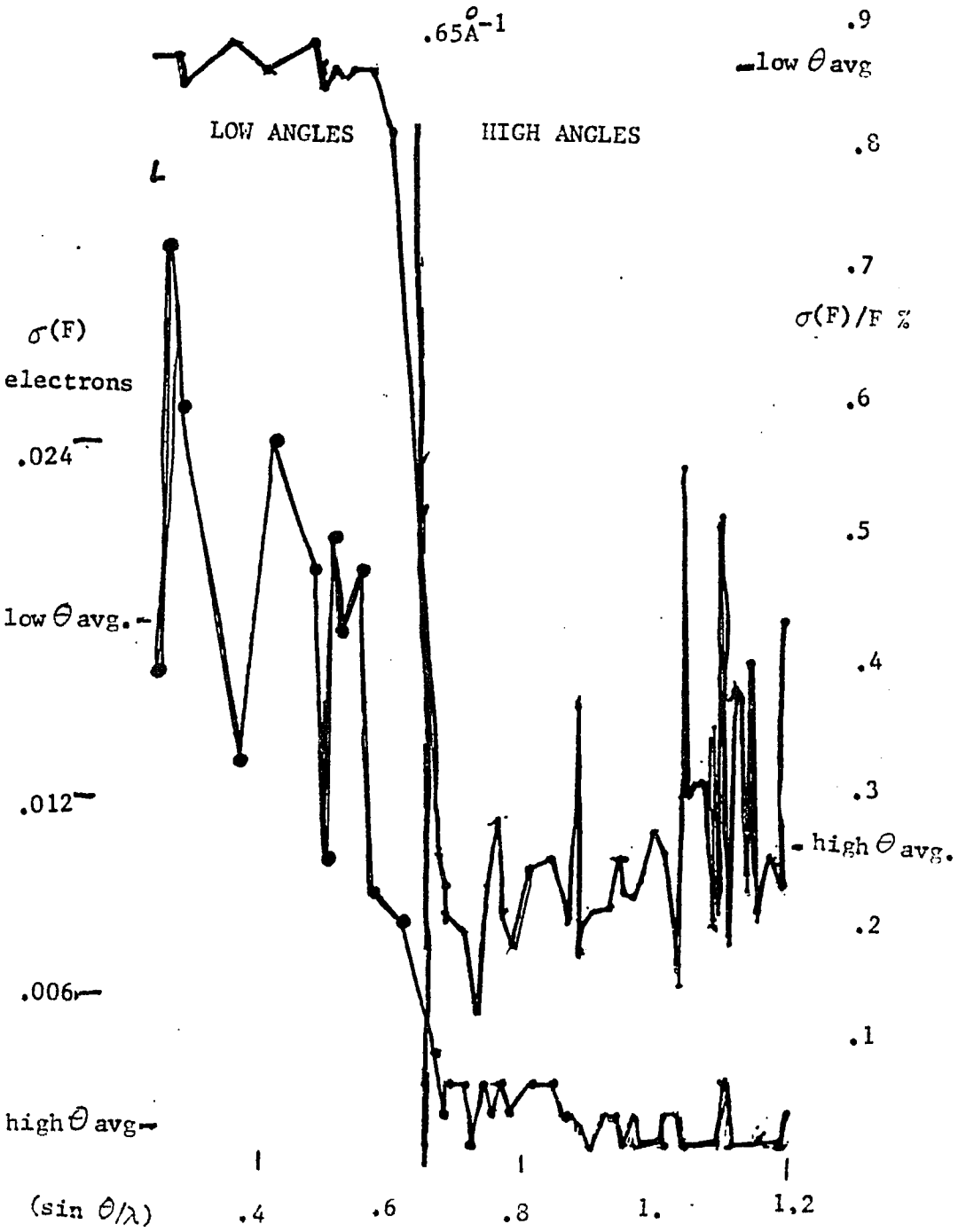

Table 9

Beryllium Model One: The Free Atom

wR_3, 3 parameters

	%	covariance with:	U_{11}	U_{33}	
U_{11}	.022114(86)				wR_3 .00419
U_{33}	.019438(99)		58.9		R_1 .00544
1/S	.9936 (17)		88.8	78.0	

R_3, 3 parameters

	%	covariance with:	U_{11}	U_{33}	
U_{11}	.02244(80)				R_3 .01040
U_{33}	.01972(96)		11.2		R_1 .00542
1/S	.9996 (69)		60.8	52.7	

wR_3, 4 parameters

	%	covariance with:	C_{112}	U_{11}	U_{33}	
C_{112}	.0033(10)					wR_3 .00385
U_{11}	.022113(80)		-.5			R_1 .00532
U_{33}	.019434(92)		-1.2	58.9		
1/S	.9936(16)		.01	88.8	78.0	

R_3, 4 parameters

	%	covariance with:	C_{112}	U_{11}	U_{33}	
C_{112}	-.00008(2200)					R_3 .01040
U_{11}	.02244(80)		-3.0			R_1 .00542
U_{33}	.01972(97)		-1.0	11.2		
1/S	.9996(70)		-1.7	60.8	52.8	

Table 10

Beryllium Model Two: The Spherical Atom

wR_3, 5 parameters

% covariance with:	U_{11}	U_{33}	1/S	ζ_{1s}	
U_{11} .02214(50)					wR_3 .00418
U_{33} .01946(50)	98.6				R_1 .00543
1/S .9936 (60)	-90.2	-89.8			
ζ_{1s} 1.000 (21)	92.9	92.4	-92.6		
ζ_{2s} 1.009 (73)	11.9	12.3	-5.0	-21.6	

R_3, 5 parameters

% covariance with:	U_{11}	U_{33}	1/S	ζ_{1s}	
U_{11} .0225(40)					R_3 .01040
U_{33} .0198(38)	96.4				R_1 .00552
1/S .999 (19)	-83.6	-83.1			
ζ_{1s} 1.00 (13)	98.3	97.6	-89.0		
ζ_{2s} 1.02 (14)	66.1	66.3	-79.5	66.7	

wR_3, 6 parameters

% covariance with:	C_{112}	U_{11}	U_{33}	1/S	ζ_{1s}	
C_{112} .0033(10)						wR_3 .00384
U_{11} .02214(48)	-9.7					R_1 .00530
U_{33} .01946(50)	-9.9	98.6				
1/S .9936(62)	9.1	-90.3	-90.0			
ζ_{1s} 1.00(2)	-7.5	93.0	92.4	-92.6		
ζ_{2s} 1.01(6)	-6.4	12.4	12.8	-5.5	-21.1	

R_3, 6 parameters

% covariance with:	C_{112}	U_{11}	U_{33}	1/S	ζ_{1s}	
C .00002(2300)						R_3 .01040
U_{11} .0225(40)	-2.4					R_1 .00552
U_{33} .0198(49)	-2.1	96.4				
1/S .999(23)	0.4	-83.6	-83.1			
ζ_{1s} 1.00(13)	-1.9	98.3	97.6	-89.0		
ζ_{2s} 1.02(14)	0.5	66.1	66.3	-79.5	66.7	

Table 11

Beryllium Model Three: Quantum Wavefunction

Refined on Unweighted ϵ_3
6 Parameters

% covariance with:	C_F	r_F	a_F	U_{11}	U_{33}	
C .37(20)						R_3 .00247
r 3.29(24)	85.3					R_1 .00249
a .363(14)	-29.8	-71.5				
U .02226(29)	-76.3	-74.3	23.0			
U .01946(22)	-49.8	-46.0	-1.1	36.4		
1/S 1.000(28)	-99.8	-86.2	29.7	79.0	52.1	

Note that ϕ refined to 92(7) degrees, and θ was unrefineable.

The R matrix was

	2s	FSGO
2s	.974	.159
FSGO	.159	.026

Table 12

Beryllium Model Four: Multipole Expansion

Refined on Unweighted ϵ_3
6 Parameters

% covariance with:	W_F	r_F	a_F	U_{11}	U_{33}	
W .53(12)						R_3 .00242
r 2.42(50)	6.7					R_1 .00237
a .190(32)	-95.9	-3.0				
U .02196(39)	-84.5	-20.1	78.7			
U .01912(38)	-81.0	-11.8	73.4	72.9		
1/S .9982(25)	-70.2	-30.8	63.8	84.0	78.3	

Note that ϕ refined to 93(8) degrees, and Θ was unrefineable.

Table 13

Wavefunction Predictions of F(K)

Type of Wavefunction	Authors	R_I for Larsen Data
"ab initio" density functional	Chou, Lam, Cohen(93)	.012
ab initio LCAO	Dovesi, Pisani, Ricca, Roetti(94)	.008
atomic SCF (free atom)	Huzinaga(80)	.00542
totally empirical	Goldberg, Massa, Frishberg, Boehme, LaPlaca(29)	.00249
ERROR IN DATA	Larsen, Hansen(56)	.00491

at low angles. This was imposed by Larsen(56) in order, he says,to "achieve even weighting over the total data set."

This approach tends to obscure the inadequacies of their free-atom model in the regions where charge redistribution contributes most heavily. In view of this, all refinements were performed on the unweighted error ϵ_3 . Goodnesses-of-fit are of doubtful value when the data weighting scheme is in doubt, and are not reported here.

Re-refining the free-atom model led to the results of Table 9. Note that much has changed - the largest shift in parameters is in C_{112} , which has gone from .0033(10) to -.0001(100).

To check for core expansion, and to reoptimize the 2s exponent, two orbital scaling factors ζ were put in as adjustable parameters according to

$$g_{1s} = \left(\sum_{j=1}^{10} c_{j,1s}\, \zeta_{1s}^{n_j} g_j\right)(\text{Norm}) \tag{126}$$

$$g_{2s} = \left(\sum_{j=1}^{} c_{j,2s}\, \zeta_{2s}^{n_j} g_j\right)(\text{Norm}) \tag{127}$$

ζ = 1 corresponds to Huzinaga's value. Coppens(16) refers to this model 2 as a "kappa refinement," or "spherical atoms." As Table 10 shows, the frozen core approximation holds remarkably (the core optimizes to its free-atom value to $\pm$.01%) and the 2s shell is optimal to within experimental error at its free-atom value. Also note that

the 1s scaling factor (which multiplies all 10 Gaussian exponents) is an ill-defined parameter with enormous covariances to the other parameters. Any appeal to core expansion is definitely not justified in this model.

Model 3 adds a set of 12 FSGO to the basis. This model thus has 8 parameters: 1/S, U_{11} , U_{33} non-electronic; r, θ, ϕ, a for the floater, and its population parameter C_F as electronic parameters. Since, in the spin-paired approximation, there is only one valence orbital, and from the excellent fit to a free-atom model, this must be mainly beryllium 2s, the wavefunction is written as

$$\Psi = \mathcal{A}\left(\psi_{1s}\alpha\beta \quad (C_1\psi_{2s} + C_2 g_F^{a_1'})\alpha\beta\right) \tag{128}$$

and the contracted set of 12 floaters is set to the A_1' rep, to which the 2s orbital belongs. The frozen core approximation is invoked. This leads to R_3 = .00247, R_1 = .00249. Adding the third cumulant yields no change; the third cumulant refines to 0. The results are presented in Table 11.

The quantum model 3 uses several approximations. First, it is not truly a molecular description. Rather it is a quasi-molecular description of a single asymmetric unit; basically a one-center expansion. The effects of crystal formation are included implicitly in a crystal-field way; the bound Be atom is deformed quantum-mechanically in accordance with the site symmetry. In other words, the model is a

one-center quantum-constrained multipole expansion. This will facilitate comparison with the V-M multipole model 4.

Second, the P matrix has been constrained to be real, even though the site symmetry does not require it. This approximation could be eliminated in a future refinement.

Third, the model uses only a single determinant, even though the Be atom has an extremely low-lying $1s^2 2p^2$ excited state of the same symmetry. The model fits the data well enough that this approximation seems justified with the current data.

Fourth, both models 3 and 4 use a small basis set of only 2 valence functions. As will be shown below, this was necessary.

In the quantum model 3, the density ρ can be written as

$$\rho = \psi\psi^{+} = \psi_{1s}^{2} + R_{2s2s}g_{2s}^{2} + R_{2sF}g_{2s}g_{F} + R_{FF}g_{F}^{2} \tag{129}$$

or, in terms of the basis of 22 primitive Gaussians,

$$\rho = \left(\sum_{i=1}^{10}(c_i^{1s} + C_{2s}c_i^{2s})g_i + \sum_{j=1}^{12} C_{FSGO}(Nor_{FSGO})\cdot 1/\sqrt{12}\, g_j\right)^2 \tag{130}$$

The full expression for the structure factor is

$$F_{cal}(K) = \frac{1}{S} e^{-U_{11}(K_x^2+K_y^2)-U_{33}K_z^2} \times \mathrm{Tr}\,(PS^{-1/2}f(K)S^{-1/2}) \tag{131}$$

where

$$f_{\mu\nu}(K) = \langle g_\mu | e^{ik\cdot r} | g_\nu \rangle \; ; \; S_{\mu\nu} = f_{\mu\nu}(0) \qquad (132)$$

A Varghese-Mason non-quantum model, model 4, in the same basis of Huzinaga's STO-10G expansion of the atomic 1s and 2s orbitals, and a set of 12 floaters, was also refined - see Table 12. As expected(104), the non-quantum model fits the data somewhat better. The density is written as a sum of additive density pieces

$$\rho = \rho_{1s} + W_{2s}\rho_{2s} + W_F\left(\sum_{i=1}^{10} \rho_{F_i}\right) \qquad (133)$$

where the density is normalized as a constraint, but the density pieces are not orthogonal. Each floater set is a simple sum of 12 overlapping density pieces. There are no cross-terms between the 12 FSGO, nor between any of the floaters and the $2s^2$ density piece.

The normalization condition is simply

$$W_{2s} + W_{FSGO} = N \text{ (1 in this case)} \qquad (134)$$

The model cannot be decomposed uniquely into orbitals. If some of the W_i were sufficiently less than zero, positron regions would appear. This did not happen in the case of beryllium metal with this particular basis.

Adding a second set of floaters seems to not be possible with this data. Although an attempt was made to do so,the computer program was unable to refine such a model. In the case of a quantum 2-floater basis, covariances between parameters often exceeded 99%. The V-M

2-floater refinement caused the program to crash due to 100% correlations.

All calculations were done using the program TREFOIL, listed in Appendix D.

The true test of whether a non-free-atom model is justified by the data is Hamilton's R-ratio test(68), which is set up for refinements on wR_3. The ratio of model 1 without third cumulant to model 1 with third cumulant is

$$.00419/.00385 = 1.088 \qquad (135)$$

for 58 data, and adding a fourth parameter, the various significance levels are :

1.033 = .05 (95% certain to be significant);

1.050 = .01 (99% significant);

and the most stringent test -

1.085 = .005;

Thus it is justified at the 99.5% level to say that the thermal motion is anharmonic.

Comparing model 2 to model 1, both without third cumulant, wR_3 (2)/wR_3 (1) = 1, which is insignificant at any level.

Comparing models 1 and 3, or models 1 and 4, the final refinement added 3 parameters r_{FSGO}, C_{FSGO} or W_{FSGO}, and a_{FSGO}. The significance test for adding 3 parameters requires an R-ratio of at least 1.13 to be 99.5% sure. Both models improve R_3 by far more than this. The improvement is certainly significant at all levels.

Although Hamilton's test is not really set up for unweighted refinements, one can use them if a standard deviation of .001 electrons is used for all reflections. Note that use of σ=1. electron would cause the calculated GOF to be .001 times as large as it should be. Unit wighting does not mean a weight of 1.000, it means assuming equal errors in all data of 1 in the least significant digit.

The model 3 value of U_{33} agrees within the error bars of each with the neutron value. The U_{11} is 6.5σ, or 3.4%, off. The free-atom model 1 is also in agreement with the neutron-scattering value for U_{33}, and 7σ off for U_{11}. U_{11} is .02132 from neutrons(56); U_{33} is .01929.

Compare the scattering factor predictions from various wave functions in Table 13. As you see, the totallly empirical wave function fits the data best. The lowest energy comes from Cohen's group, which, surprisingly, fits the data worst. This may be due to Cohen's plane wave basis, which converges very slowly.

The results clearly show that one can indeed distinguish vibrational from electronic effects. The J matrix elements connecting the 2 are quite small in most cases. An exception is W^{VM}_{FSGO}.

Compare the results of the quantum and V-M models. Since the multipole model used has no cross-terms, and the cross-term 2s-FSGO in the quantum model contributes about 20 times as much scattering power as the self-term $FSGO^2$, one would expect the multipole floater distance to be quite near to the quantum cross-term distance,

$$2.42 \text{ au} = r_F^{VM} \sim \frac{a_F^{QM} r_F^{QM}}{a_{2s_2} + a_F^{QM}} = (.363)(3.29)/(.150+.363) = 2.33 \text{ au} \qquad (136)$$

The exponent on the V-M floater, which is a density basis function, ought to be equal to the quantum cross-term exponent,

$$a_F^{VM} \sim .150+.363=.513 \text{ au}^{-2} = a_{2s_2} + a_F^{QM} \qquad (137)$$

but is in fact .190 au^{-2}, much more diffuse. This could be due to the multipole trying to smear out so as to mimic the elongation of the quantum model.

With a non-quantum model, the lack of cross-terms means that one cannot say which atom "owns" which floater. The quantum model, however, can uniquely assign FSGO to atoms since each FSGO has two positions - a self-term and a cross-term.

In a comparison of the results of free-atom, quantum, and non-quantum model refinements of Larsen's data, quantum and non-quantum both fit the data well, so a comparison of the two must be based on how each can be interpreted. The non-electronic parameters come out about the same, which shows that both quantum and non-quantum models can separate vibrational and electronic effects.

The covariance matrices J are quite different. The quantum model has far more uncoupled of electronic and vibrational parameters. That is, no quantum model electronic parameter can be modeled as well by a combination of vibrational parameters as in the more correlated non-quantum case. However, the quantum model shows severe correlation between floater coefficient and overall scale. Curiously, a quantum electronic model has reduced the correlation between vibrations from large (72.9%) to insignificant (36.4%), even though the difference between the models has nothing to do with vibration.

The non-quantum model has a much higher fraction of its charge localized on the floaters, because the lack of cross-terms prevents charge from being shared between 2s and FSGO. This ability to describe charge sharing with a quantum model leads to a more meaningful physical interpretation, since most chemical interactions are to some degree covalent.

A detail of both the quantum and non-quantum calculations which is important for experimental crystallographers is the weighting scheme employed. The usual practice in charge-density refinements is to

refine the non-electronic parameters using a free-atom model and high-angle data, and then to hold these values fixed while refining the electron-density parameters from "low-angle" data. This can lead to severe errors at the nuclear positions(95) and hence poor values for electric field gradients and the Fermi contact interaction. Low-angle data also contain information on vibration and scale factor, and high-angle intensities contain some information on charge density. The residual error for the beryllium refinement does not suffer from such drastic errors. This is partly because all parameters were refined simultaneously using the full data set, and the same data weighting scheme for both electronic and non-electronic parameters. No artifical high-angle or low-angle cutoffs were used, as these would have biased the result. Every data point should be allowed to influence every parameter(96,97,98). Let the model itself separate out vibrations and electron density - as was shown before, it can do that.

The proper comparison is the absolute error, not the relative error(97) - an error of .001 electrons is as severe for a strong reflection as for a weak one. Based on these results, it would seem that experimentalists should aim for a constant error σ(F) in their Bragg amplitudes(98). This is especially important for strong reflections, where the extra measuring time would not be prohibitive, and could have a large effect on the result.

The quantum model is consistent with the bonding in beryllium being

a five-center interaction, with all pointing to the trigonal bipyramid. The non-quantum model is consistent with a four-center tetrahedral interaction(99). The planes of Be atoms are 3.3866(2) au apart along the c axis. If the floater were at exactly $\phi = 90^{\circ}$, r=3.3866, it would be in the middle of the trigonal bipyramidal hole, at special position "c" of the Wyckoff notation, surrounded by 2 equidistant "axial" atoms along the c axis, and 3 equidistant "equatorial" atoms in the ab plane. This would be a 5-center bond. The center of the tetrahedral hole is 2.5400(2) au away, also along the c axis. This position is surrounded by a tetrahedron of equidistant Be atoms. In both the refinements of models 3 and 4, the angle of the floater refined to a value insignificantly different from 90°; both quantum and non-quantum floaters refined from a set of 12 at general position "1" to a set of 2 at special position "f" of the Wyckoff notation; in both models the floaters are directly above and below the atoms. Since the quantum distance refines to 3.2(2) au, and the V-M distance to 2.42(5) au, one can say that the quantum model points to a 5-center bond, and the non-quantum model to a 4-center bond.

See Figure 13.

Figure 13

Chemical Bonding in Beryllium

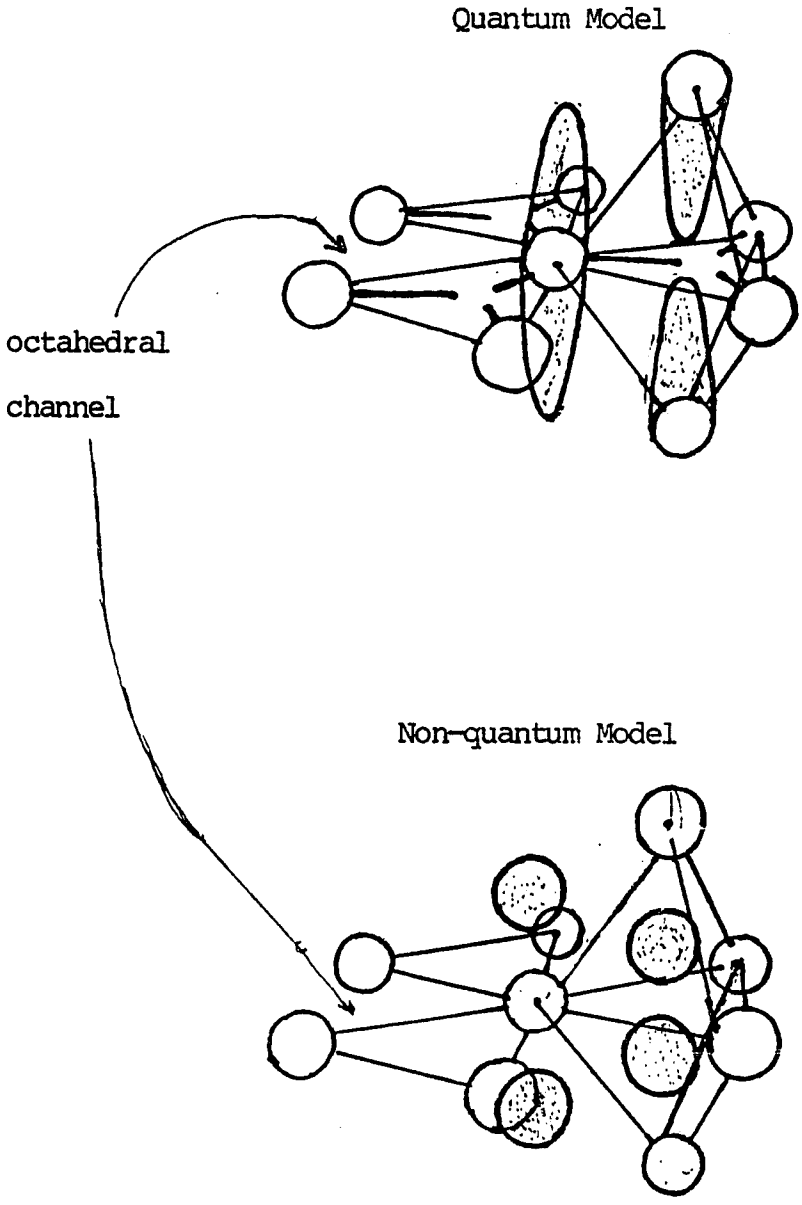

Chapter IV. Graphite and Diamond

In this chapter, two structures will be reviewed in detail, outlining how to obtain totally empirical wavefunctions for graphite, an infinite sheet structure, and diamond, an infinite network. This is not to say that the method cannot be applied to molecular crystals - indeed, molecular crystals are much easier.

For a molecular crystal, the P matrix refers to one molecule, and there aren't any complications due to intercell bonds. In graphite and diamond, the problem is more complicated. It is not possible to construct a unit cell with an entire molecule of graphite or diamond inside. Any unit cell will have bonds "sticking out" of it. To properly describe covalent bonding, one must have cross-terms in P between the two bonded atoms. This means that the P matrix for one cell must include basis functions centered on the neighboring cells. Even if one uses a basis of Wannier functions, this is the case - what is causing the extra complication is not the symmetry, but the bonding. Every basis function for an atom involved in these intercell bonds will be referred to by at least two P matrices: its own and that of each other cell to which it is bonded. The scattering power for the self-terms f_{ii} are identical in both cells; what allows the refinement to succeed is the existence of cross-terms P_{ij} and f_{ij} where i and j refer to basis functions in different unit cells. This

scattering element f_{ij} is not the same as, nor can it be simulated properly by, any intracell cross-terms.

In more mathematical terms, if the bonding orbital

$$\psi_{bond} = c_1 g_1 + c_2 g_2 \tag{138}$$

then the associated density

$$\rho(r) = \mathrm{Tr}\left(\begin{pmatrix} c_1 c_1^* & c_1 c_2^* \\ c_2 c_1^* & c_2 c_2^* \end{pmatrix}\begin{pmatrix} g_1^* g_1 & g_1^* g_2 \\ g_2^* g_1 & g_2^* g_2 \end{pmatrix}\right) \tag{139}$$

and if one does not include both g_1 and g_2 in the list of basis functions, no adequate description of ψ_{bond} is possible.

In order to make all these considerations clearer, the two examples of graphite and diamond will each be considered in detail.

Graphite(C) crystallizes in space group #194, $P6_3/mmc$, the same as beryllium. Each unit cell has 4 atoms, at positions "b" and "c" in the Wyckoff notation (0 0 1/4 and 1/3 2/3 1/4 , and symmetry-related atoms at 0 0 3/4 and 2/3 1/3 3/4). Describing one of the two asymmetric units, say the sheet at z = 1/4, is sufficient - the symmetry completely describes one in terms of the other. Describing one of the two atoms per asymmetric unit is not sufficient - they are not related by any symmetry operation. Directly above and below each "b" atom is another "b" atom. Above and below each "c" atom is the middle of a phenyl ring. Nonetheless, one could approximate each parameter for the two as being equal,

$$p^b \sim p^c \tag{140}$$

either to reduce the number of parameters or as a starting guess. As of the end of 1983, the best x-ray diffraction data available for graphite were those of Chen, Trucano, and Stewart(100), with $a = 2.461(4)\mathring{A}$, $c = 6.706(2)\mathring{A}$ at $293^{\circ}K$. All 99 unique reflections of intensity $>2\sigma$ are displayed in Table 14, courtesy of Dr. Robert F. Stewart(101). These values are corrected for all the appropriate experimental problems, and the only experimental parameter needed to model these data is an overall scale factor 1/S. The internal error $R_I \sim 3\%$.

The simplest possible model has 3 parameters : scale factor 1/S, an in-plane vibrational amplitude $U_{//}$ and out-of-plane U_{33} , where the approximation has been made that equation (140) holds, and the electron distribution of a spherically averaged free carbon atom is used.

Model 2 has 5 paramters : 1/S, $U_{//}^b$, $U_{//}^c$, U_{33}^b , and U_{33}^c . In Chen et al's paper(100), this model is found to yield $R_I = 6.0\%$, which indicates that the data is precise enough to merit a better treatment.

Next is a series of models which make the one-center approximation, thus not describing covalency explicitly, but only a quantum constrained multipole expansion. The ground configuration of carbon is(102) $1s^2 2s^2 2p_x 2p_y$, and the so-called "valency" configuration is $1s^2 2s 2p_x 2p_y 2p_z$. It is useful to note that this implies that the optimum configuration is

$$1s^2 2s^{(1+\chi)} 2p_x 2p_y 2p_z^{(1-\chi)} \quad , 0 \leq \chi \leq 1 \tag{141}$$

Note that, in point group D_{3h}, which is the site symmetry in both the b and c sites of graphite, the various atom-centered s and p orbitals have symmetries as in Table 15.

Model 3 goes beyond the Independent Particle Model, and uses two valence configurations. This model describes the atoms as

$$1s^2 (a_1')^{1+\chi} (a_2'')^{1-\chi} (e_x')(e_y') \tag{142}$$

In a minimal basis set of atom-centered functions approximated as having fixed exponents, this gives 4 parameters 1/S, U_{11}, U_{33}, and the configuration weighting χ. It is important to note that x-rays cannot see spin; electron configuration (142) could be

$$1s^2 (a_1'\alpha)(a_1'\beta)^{\chi} (a_2''\alpha)^{1-\chi} (e_x'\alpha)(e_y'\alpha) \xrightarrow[\chi=0]{} \text{spin 2} \tag{143}$$

or

$$1s^2 (a_1'\alpha)(a_1'\beta)^{\chi} (a_2''\beta)^{1-\chi} (e_x'\alpha)(e_y'\alpha) \xrightarrow[\chi=0]{} \text{spin 1} \tag{144}$$

or

Table 14

99 Bragg Data For Graphite

from Reference(101)

-5	2	5	1.080	0.033	-1	0	0	3.418	0.055
-5	2	7	0.874	0.036	-1	0	1	5.728	0.080
-5	3	3	1.348	0.033	-1	0	2	2.819	0.022
-5	4	0	3.148	0.051	-1	0	3	4.024	0.015
-5	4	2	2.912	0.067	-1	0	4	1.926	0.006
-5	4	4	2.526	0.046	-1	0	5	2.769	0.013
-5	4	6	2.052	0.041	-1	0	6	1.365	0.006
-5	5	0	1.175	0.153	-1	0	7	2.025	0.011
-5	5	1	1.177	0.019	-1	0	8	1.011	0.016
-5	5	3	0.877	0.034	-1	0	9	1.478	0.010
-4	2	0	4.455	0.136	-1	0	10	0.709	0.012
-4	2	2	4.219	0.062	-1	0	11	1.009	0.007
-4	2	4	3.742	0.050	-1	4	11	0.655	0.025
-4	2	6	3.136	0.029	0	0	2	18.170	0.210
-4	2	8	2.440	0.018	0	0	4	10.020	0.090
-4	2	10	1.744	0.046	0	0	6	6.050	0.050
-4	2	12	1.109	0.038	0	0	8	4.250	0.040
-4	3	0	1.136	0.073	0	0	10	3.060	0.030
-4	3	1	1.794	0.074	0	0	12	2.110	0.040
-4	3	2	1.043	0.030	0	0	14	1.280	0.070
-4	3	3	1.656	0.022	0	0	16	0.680	0.090
-4	3	4	0.908	0.034	0	1	13	0.700	0.170
-4	3	5	1.440	0.026	0	4	4	0.857	0.115
-4	3	7	1.147	0.018	0	4	6	0.790	0.150
-4	3	9	0.803	0.019	2	-5	6	0.680	0.010
-4	4	0	1.210	0.100	5	-5	2	0.840	0.120
-4	4	1	1.619	0.061					
-4	4	2	0.908	0.034					
-4	4	3	1.463	0.027					
-4	4	5	1.253	0.047					
-4	4	7	1.021	0.057					
-4	4	9	0.742	0.028					
-3	0	12	1.319	0.039					
-3	1	0	1.348	0.045					
-3	1	1	2.417	0.033					
-3	1	2	1.319	0.032					
-3	1	5	1.839	0.010					
-3	1	6	0.968	0.012					
-3	1	7	1.478	0.014					
-3	1	8	0.745	0.011					
-3	1	9	1.116	0.013					
-3	1	11	0.766	0.013					
-3	2	3	2.148	0.027					
-3	2	4	1.196	0.019					
-3	3	0	5.094	0.098					
-3	3	2	4.765	0.048					
-3	3	4	4.169	0.060					
-3	3	6	3.476	0.020					
-3	3	8	2.766	0.019					
-3	3	10	1.996	0.022					
-3	4	6	0.817	0.047					
-3	5	4	0.786	0.019					
-2	0	0	1.343	0.031					
-2	0	1	2.392	0.061					
-2	0	2	1.354	0.025					
-2	0	3	2.261	0.017					
-2	0	4	1.274	0.017					
-2	0	5	2.003	0.010					
-2	0	6	1.075	0.009					
-2	0	8	0.861	0.030					
-2	0	9	1.273	0.015					
-2	0	11	0.867	0.016					
-2	1	0	7.180	0.084					
-2	1	2	6.823	0.058					
-2	1	4	5.658	0.014					
-2	1	6	4.603	0.017					
-2	1	8	3.625	0.013					
-2	1	10	2.658	0.018					
-2	1	12	1.813	0.017					
-2	1	14	1.064	0.022					
-2	2	7	1.655	0.009					
-2	5	1	1.523	0.077					
-2	5	2	1.019	0.109					

Table 15

Symmetry of s and p Basis Functions in Graphite

Representation	Atom Basis	Neighbor Atoms
A_1'	s	$1/3\ (s^1+s^2+s^3)$ $1/3\ (p_y^1 + (1/\sqrt{2}\ p_x^2 + 1/\sqrt{6}\ p_y^2)$ $- (1/\sqrt{2}\ p_x^3 + 1/\sqrt{6}\ p_y^3))$
A_2'	none	none
E_x'	p_x^0	$1/\sqrt{6}\ (2p_x^1 - p_x^2 - p_x^3)$ $1/\sqrt{2}\ (p_y^2 - p_y^3)$ $1/\sqrt{2}\ (s^2 - s^3)$
E_y'	p_y^0	$1/\sqrt{6}\ (2p_y^1 - p_y^2 - p_y^3)$ $1/\sqrt{2}\ (p_x^2 - p_x^3)$ $1/\sqrt{6}\ (2s^1 - s^2 - s^3)$
A_1''	none	none
A_2''	p_z^0	$1/\sqrt{3}\ (p_z^1 + p_z^2 + p_z^3)$
E_x''	none	$1/\sqrt{2}\ (p_z^2 - p_z^3)$
E_y''	none	$1/\sqrt{6}\ (2p_z^1 - p_z^2 - p_z^3)$

$$1s^2(a_1'\alpha)(a_1'\beta)^{\chi}(a_2''\alpha)^{1-\chi}(e_x'\alpha)(e_y'\beta) \xrightarrow[\chi=0]{} \text{spin 1} \qquad (145)$$

or

$$1s^2(a_1'\alpha)(a_1'\beta)^{\chi}(a_2''\beta)^{1-\chi}(e_x'\alpha)(e_y'\beta) \xrightarrow[\chi=0]{} \text{spin 0} \qquad (146)$$

and all of these would scatter x-rays identically.

In a DZd (Double Zeta plus d-type polarization functions) basis set, again atom-centered, in addition to the 4 parameters already listed, model 3 has 5 new parameters C_1 through C_5 in

$$\psi_{(a_1')} = \frac{1}{(\text{Nor})}(s_{\text{tight}} + C_1 s_{\text{loose}} + C_2 d_{z^2}) \qquad (147)$$

$$\psi_{(a_2'')} = \frac{1}{(\text{Nor})}(p_{z\text{-tight}} + C_3 p_{z\text{-loose}}) \qquad (148)$$

$$\psi_{(e')} = \frac{1}{(\text{Nor})}(p_{xy\text{-tight}} + C_4 p_{xy\text{-loose}} + C_5 d) \qquad (149)$$

and the P matrix is a direct sum of such $\psi\psi^+$.

Obviously there is also a variant of model 3 with different parameter values for sites b and c. Model 3 is a minimal basis augmented with d functions (SZd) is a quantum-constrained hexadecapole refinement. Like multipole refinements, one can add an extra parameter

- an exponent scaling ζ for all valence Gaussians - instead of holding it fixed at the literature value. In a DZd basis with unequal atoms, since it is standard practice not to vary the exponent of the"tight" orbital (which is contracted, whereas the outer "loose" function consists of a single primitive(84), one gets as many as 8 extra exponent scaling parameters:

$$\zeta_s^b, \zeta_s^c, \zeta_{p_{xy}}^b, \zeta_{p_{xy}}^c, \zeta_{p_z}^b, \zeta_{p_z}^c, \zeta_d^b, \zeta_d^c$$

One could, of course, constrain some exponents to be equal to others or to literature values.

Model 4 is a many-center model, but uses only one configuration - χ =0 in equation (137). Advantage is taken of x-ray scattering's indifference to spin. Site b is populated with all valence electrons spin-up, and all site c valence electrons are spin-down. This is necessary to prevent overpopulating, as will be explained below. The orbitals on each site are described using atom-centered symmetry-adapted basis functions from that site and its three (in-plane) near neighbors as in Table 15. This is not exactly a molecular description, but it does allow for bonding. The a_2'' orbital is a "pi" orbital in organic molecular orbital notation. This antiferromagnetic model ensures that no spinorbital basis function will have more than one electron in it because all delocalization from a b site to a c site is of opposite spin to c—>b delocalization. A variant of model 4 constrains b and c site parameters equal.

Model 5 uses two configurations but is otherwise like model 4. A

problem with this is that the a_1' orbitals on each site could conceivably overpopulate the 2s basis functions, if one is not careful. Writing the a_1' spinorbitals as

$$\psi^b_{a_1'}\alpha = \frac{1}{(N_1)}(2s^b + C_1(2s^c_{a_1'}) + C_2(2p^c_{a_1'}))\alpha \tag{150}$$

$$\psi^b_{a_1'}\beta = \frac{1}{(N_2)}(2s^b + C_3(2s^c_{a_1'}) + C_4(2p^c_{a_1'}))\beta \tag{151}$$

and similarly on site c with parameters C_5 to C_8, and normalizers N_3 and N_4, the populations of the basis functions are

$$(a_1'^b\alpha)^1(a_1'^c\beta)^1(a_1'^b\beta)^{\chi_b}(a_1'^c\alpha)^{\chi_c} \tag{152}$$

so the constraints due to the Pauli principle are that

$$\frac{1}{3}\left(\frac{C_1}{N_1}\right)^2 + \frac{\chi_c}{(N_3)^2} \leq 1 \qquad \text{for the } 2s^b_\alpha \text{ spinorbital,} \tag{153}$$

$$\frac{\chi_b(C_3)^2}{3(N_2)^2} + \frac{1}{(N_4)^2} \leq 1 \qquad \text{for the } 2s^b_\beta \text{ spinorbital,} \tag{154}$$

$$\frac{1}{3}\left(\frac{C_5}{N_3}\right)^2 + \frac{\chi_b}{(N_1)^2} \leq 1 \tag{155}$$

and

$$\frac{\kappa_c}{3}\left(\frac{C_7}{N_4}\right)^2 \frac{1}{N_2^2} \leq 1 \qquad \text{for } 2s^c. \tag{156}$$

None of the other basis functions are in danger of being overpopulated.

Model 5 is a quasi-molecular model,using a near-neighbor approximation. If one considers each orbital to be an average over spin states and sites, this is a quasi-molecular description of a C_2 unit using basis functions on each of the 2 carbons and the four near neighbors; the $\bar{6}$m2 site symmetry of each site is rigorously preserved.

Model 6 is an explicitly molecular model. Each asymmetric unit contains 2 carbons, with 4 core electrons total, which are kept frozen, and 8 valence electrons. The trace of the valence P matrix is 8. The easiest way to describe the model is in a non-symmetrized basis, centered on six atoms as shown in Figure 14.

If one appropriately rotates coordinate systems for each atom, then certain blocks of the P matrix become equal from symmetry considerations. The most general possible P matrix for a six-center system with the same basis on each center is

$$P = \begin{bmatrix} P_{11} & P_{12} & P_{13} & P_{14} & P_{15} & P_{16} \\ P_{12}^{+} & P_{22} & P_{23} & P_{24} & P_{25} & P_{26} \\ P_{13}^{+} & P_{23}^{+} & P_{33} & P_{34} & P_{35} & P_{36} \\ P_{14}^{+} & P_{24}^{+} & P_{34}^{+} & P_{44} & P_{45} & P_{46} \\ P_{15}^{+} & P_{25}^{+} & P_{35}^{+} & P_{45}^{+} & P_{55} & P_{56} \\ P_{16}^{+} & P_{26}^{+} & P_{36}^{+} & P_{46}^{+} & P_{56}^{+} & P_{66} \end{bmatrix} \tag{157}$$

Figure 14

Numbering of Graphite Nuclei for

the Explicitly Molecular Model Six

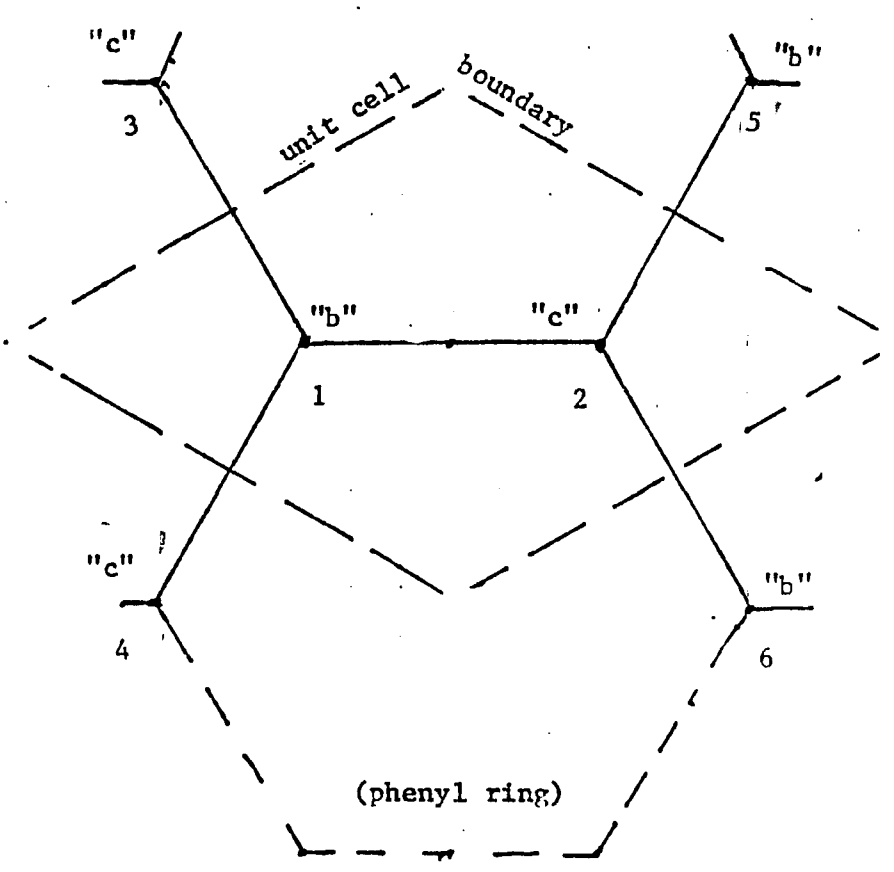

With the site symmetry, this reduces to

$$\rho = \begin{bmatrix} \rho_{11} & \rho_{12} & \rho_{13} & \rho_{13} & \rho_{12} & \rho_{12} \\ & \rho_{22} & \rho_{12}^{\dagger} & \rho_{12}^{\dagger} & \rho_{25} & \rho_{25} \\ & & \rho_{33} & \rho_{34} & \rho_{35} & \rho_{36} \\ (+) & & & \rho_{33} & \rho_{36} & \rho_{35} \\ & & & & \rho_{55} & \rho_{56} \\ & & & & & \rho_{55} \end{bmatrix} \tag{158}$$

All the P submatrices must be written out, but the number of non-equivalent elements $P_{\mu\nu}$ is larger than the number of independent parameters. If I represents an independent submatrix, and d a dependent one, then

$$P = \begin{bmatrix} I & I & d & d & d & d \\ d & I & d & d & d & d \\ d & d & d & d & d & d \\ d & d & d & d & d & d \\ d & d & d & d & d & d \\ d & d & d & d & d & d \end{bmatrix} \tag{159}$$

and there are at most three submatrices that need parametrization:

P_{11} and P_{22}, the atomic hybridizations, and P_{12}, the bond. All other P submatrices are fixed either by symmetry or by the quantum constraints.

The 2-center approximation as usually understood would dictate that P have zero blocks "0" and non-zero blocks "#" as

$$P = \begin{bmatrix} \# & \# & 0 & 0 & \# & \# \\ & \# & \# & \# & 0 & 0 \\ & & \# & 0 & 0 & 0 \\ & & & \# & 0 & 0 \\ & \text{adjoint} & & \# & 0 & \\ & & & & & \# \end{bmatrix} \quad \begin{matrix} = \\ (\text{site} \\ \text{symmetry}) \end{matrix} \quad \begin{bmatrix} P_{11} & P_{12} & 0 & 0 & P_{12} & P_{12} \\ & P_{22} & P_{12}^{+} & P_{12}^{+} & 0 & 0 \\ & & P_{33} & 0 & 0 & 0 \\ & & & P_{33} & 0 & 0 \\ & \text{adjoint} & & & P_{55} & 0 \\ & & & & & P_{55} \end{bmatrix} \tag{160}$$

but it may not be possible to construct a matrix which is both as sparse as that and also idempotent.

P2=

$$\begin{pmatrix} P_{11}^2+P_{12}^2+2P_{12}P_{12}^{+} & P_{12}P_{11}+P_{12}P_{22} & P_{12}P_{12}^{+} & P_{12}P_{12}^{+} & P_{11}P_{12}+P_{12}P_5 & P_{11}P_{12}+P_{12}P_{55} \\ & P_{12}^2+P_{22}^2+2P_{12}^{+}P_{12} & P_{22}P_{12}^{+}+P_{12}^{+}P_{33} & P_{22}P_{12}^{+}+P_{12}^{+}P_{33} & P_{12}^2 & P_{12}^2 \\ & & P_{12}P_{12}^{+}+P_{33}^2 & P_{12}P_{12}^{+} & 0 & 0 \\ & & & P_{12}P_{12}^{+}+P_{33}^2 & 0 & 0 \\ & \text{(adjoint)} & & & P_{12}^{+}P_{12}+P_{55}^2 & P_{12}^{+}P_{12}+P_{55}^2 \\ & & & & & P_{55} \end{pmatrix} \tag{161}$$

Then

$$\rho_{12}^2 = \left(\rho_{12}^{+}\right)^2 = \rho_{12}\rho_{12}^{+} = \rho_{12}^{+}\rho_{12} = 0 \tag{162}$$

$$\rho_{11}^2 = \rho_{11}\ ;\ \rho_{22}^2 = \rho_{22}\ ;\ \rho_{33}^2 = \rho_{33}\ ;\ \rho_{55}^2 = \rho_{55} \tag{163}$$

$$\rho_{12} = \rho_{12}(\rho_{11}+\rho_{22}) = \rho_{11}\rho_{22} + \rho_{12}\rho_{55} = \rho_{12}\rho_{22} + \rho_{33}\rho_{12} \tag{164}$$

It would be physically unreasonable to have delocalized a whole electron out of the eight (two out of eight in a spin-paired approximation) into the next cell in a description of the central cell. Since idempotency requires that

$$\mathrm{Tr}(P_{33}) \in \{0,1,2\};\ \mathrm{Tr}(P_{55}) \in \{0,1,2\} \tag{165}$$

then P_{33} and P_{55} must be identically zero. This makes equation (164)

$$\rho_{12} = \rho_{12}(\rho_{11}+\rho_{12}) = \rho_{11}\rho_{12} = \rho_{12}\rho_{22} \tag{166}$$

and P_{12} isn't just nilpotent of order 2, it's identically zero. This reduces the two-center approximation to

$$P = \begin{bmatrix} P_{11} & 0 & 0 & 0 & 0 & 0 \\ 0 & P_{22} & 0 & 0 & 0 & 0 \\ 0 & 0 & 0 & 0 & 0 & 0 \\ 0 & 0 & 0 & 0 & 0 & 0 \\ 0 & 0 & 0 & 0 & 0 & 0 \\ 0 & 0 & 0 & 0 & 0 & 0 \end{bmatrix} \tag{167}$$

and it seems that a two-center idempotent expansion for graphite does not allow for covalent bonding P_{12}.

The two-center approximation apparently can force itself to be a one-center approximation. Model 6 requires going beyond the two-center approximation in order not to be a one-center expansion. The submatrices P_{13}, P_{25}, P_{33}, P_{34}, P_{35}, P_{36}, P_{55}, and P_{56}, although they are determined entirely by the idempotency and symmetry constraints, are not identically zero. No free parameters are needed, but calculations of all the f submatrices are required.

Model 7 uses either d-type polarization functions on all centers, or sets of 12 floaters in the appropriate reps, in addition to the s and p atom-centered functions.

Obviously, there are many variants of models 4, 5, 6, and 7 constraining various parameters equal to each other and/or to literature values.

Diamond, silicon, germanium, and α-tin all crystallize in the diamond structure, space group #227, Fd3m, at Wyckoff position "a", of site symmetry $\bar{4}3m$ (T_d), each unit cell containing 8 symmetry-related atoms, one in each asymmetric unit. Thus, the asymmetric unit, which is what must be described, contains only one atom. The 2-configuration electron assignment of the Group IV compound above can be described as

$$(\text{core})^2 a_1^{1+\chi} t_2^{3-\chi} \quad ; \quad 0 \leq \chi \leq 1 \tag{168}$$

Keeping in mind that any basis spinorbital used can have at most one electron in it, as in equations (161), (162), and (163), one can write each of the orbitals a_1 and t_2 as a combination of s and p (and d and/or FSGO) centered on the atom and its four neighbors, appropriately symmetry-adapted. A one-center expansion in a basis with s and p exponents constrained equal cannot refine the parameter χ, because

$$p_x^2 + p_y^2 + p_z^2 = s^2 \tag{169}$$

and the densities add, being in orbitals of different reps, and thus having zero cross-terms between them. In a two- or few-center approximation, the parameter χ has meaning, because s-p bonds, s-s bonds, and p-p bonds lead to different cross-terms in scattering power.

In a more complicated structure, it may be necessary to use more elaborate equivalents of equations (161) to (163), but the basic ideas outlined above should make possible a near-neighbor treatment of any structure. To include further neighbors, one includes basis functions centered further away in the description of the central atom, but the technique is about the same. For some structures, the P matrix for one asymmetric unit will include basis functions centered on atoms there and in the neighboring cells and asymmetric units, possibly only on atoms near the boundary of the central unit. For diamond-type structures the quasi-molecular model is adequate; the next level up would include a central atom and its four near neighbors as the fundamental unit, with basis functions on the second shell used in the description of this 5-atom, 20-valence-electron unit.

In the cases of graphite and the Group IV compounds, the high site symmetry has allowed the reduction of a four- or eight-electron problem to a series of one-electron problems. This allows one to refine directly on wavefunction coefficients C and orbital populations χ. Things are not so simple when some cross-terms in the P matrix are independent of all self-terms, as is always the case when the P matrix is normalized to a number larger than one, in other words nearly always. How to adapt the method to deal with this complication is not yet known.

In the thesis so far, each atom has been treated as having an at-rest scattering factor appropriate to a molecular environment, which is nevertheless affected by vibration as though it were rigidly locked to the motion of a single nucleus. The vibrational smearing of cross-terms in f between different atoms has not been discussed. In chapter 6, the vibration problem is discussed.

The complication that the basis is not usually orthonormal at the outset can be dealt with approximately by using an S matrix the size of the P matrix, i.e. one asymmetric unit, one cell, or a few cells across. In the next chapter, a more correct way of dealing with orthogonality in an infinite lattice of basis functions is presented. The resultant Wannier functions are treated exactly the same way as atom-centered functions or contracted floater sets, for the ideas in this chapter. The Wannier-izing process is irrelevant to bonding considerations; it is purely an orthonormalization process.

Chapter V. Bloch and Wannier Orbitals

In the case of solids, electronic structure is usally described through the formalism of band theory. This approach is general enough to encompass a wide variety of properties associated with solids ranging from insulators and semiconductors to metals(87). It is worth noting that there are close formal connections among quantum descriptions of atomic, molecular, and solid systems based essentially on their orbital structure. A fundamental result of band theory requires that the "crystal orbitals" of solid systems may be written as superpositions of Bloch functions which are spinorbital basis functions having the periodicity of the lattice.

Until now our formalism has been restrictive in the sense that its application was impractical except in the approximation that neighboring unit cells are almost independent of each other, as is often the case for molecular crystals.

In the present chapter the application of the formalism is extended to the realistic description of solids. The description of interaction among unit cells will be introduced in a way applicable to insulators, semiconductors, and metals, by writing the form of the density matrices that arise naturally out of the use of a Bloch or Wannier function orbital basis. The application of the resulting formalism to the Bragg experiment has been previously reported(3,25,26,27,28,41,103,104).

Our density matrix formalism may be applied either with Bloch

orbitals, or with the equivalent Wannier orbitals, built from a variety of different lattice-centered basis functions. As a numerical example of the theory, an application is made to a model problem consisting of a one-dimensional crystal of hydrogen atoms.

Bloch's theorem takes the form

$$\psi_k(r) = e^{ik\cdot r} u_k(r) \tag{170}$$

where $u_k(r)$ is any function periodic modulo a lattice translation. A prescription for constructing the functions u_k out of lattice-centered basis functions g^L is the following:

$$u_k(r) = \sum_L e^{-ik\cdot(r-r_L)} g^L(r-r_L) \tag{171}$$

The electron density ρ may be constructed in a Bloch orbital basis as follows. The list g(k,r) of Bloch basis functions all satisfy equation (170), so that the basis matrix is

$$g(k,r)g(k,r')^\dagger = e^{ik\cdot(r-r')} u_k(r) u_k(r')^\dagger \tag{172}$$

where the $u_k(r)$ all satisfy equation (171), and the g^l are basis functions centered at lattice site l, which themselves are not periodic. Bloch orbitals are eigenfunctions of the lattice translation symmetry operations of a crystal, and the final crystal orbitals ψ_k will be linear combinations of the set g(k,r).

$$\psi_k(r) = C_k\, g(k,r) \tag{173}$$

Expanding the periodic g(k,r) in the non-periodic g^L,

$$\psi_k(r) = C_k \sum_L e^{ik\cdot r_e - ik\cdot(r-r_L)} g^L(r) \tag{174}$$

or

$$C_k \sum_L e^{ik\cdot r_L} g^L(r) \tag{175}$$

Then the matrix

$$\psi_k(r)\psi_k(r')^+ = \sum_{Ll} e^{ik\cdot(r_L-r_l)} C_k\, g^L(r) g^l(r')^+ C_k^+ \tag{176}$$

and the first-order reduced density matrix of wave vector k is

$$\rho_1^k(r;r') = \mathrm{tr}\,\psi_k\psi_k^+ = \sum_{Ll} e^{ik\cdot(r_L-r_l)}\, \mathrm{Tr} C_k^+ C_k\, g^L(r) g^l(r)^+ \tag{177}$$

Defining the projector P_k as in Reference(103) by

$$P_k = S_k^{1/2} C_k C_k^+ S_k^{1/2} \tag{178}$$

where S_k is the matrix of overlap integrals of Bloch basis functions g_k,

$$\rho_1^k(r;r') = \mathrm{Tr} P_k S_k^{-1/2} \left(\sum_L \sum_l g^L(r) g^l(r')^+ e^{ik'(r_L - r_l)} \right) S_k^{-1/2} \tag{179}$$

Expanding this explicitly,

$$\rho_1^k(r;r') = \mathrm{Tr} P_k S_k^{-1/2} \left(g(r-r_0) g(r'-r_0)^+ + 2g(r-r_0) g(r'-r_1)^+ e^{ik'(r_0-r_1)} + \ldots \right) S_k^{-1/2} \tag{180}$$

where advantage has been taken of the fact that the g^L basis is the same in each unit cell. This form makes obvious the mutual influence of cells separated by a distance $(r_L - r_l)$. Equation (179) is the density matrix of wave vector k for a Bloch orbital basis.
The structure factors

$$F(K) = \int \exp(i K \cdot r) \rho(r) \, dr \tag{181}$$

may be seen to take the form

$$F(K) = \mathrm{Tr} P_k S_k^{-1/2} \{ f_{00}(K) + 2 f_{01}(K) \exp(ik \cdot (r_0 - r_1)) + \ldots \} S_k^{-1/2} \tag{182}$$

All values of k contribute to the scattering, which is measured for a change $\Delta k = K$. One can think of $f_{ij}(K)$ as an integral over $f_{ij}(k,K)$:

$$f_{ij}(K) = \int_{BZ} n(k) f_{ij}(k,K)\, dk \tag{183}$$

where the scattering component

$$f_{ij}(k,K) = \int e^{ik\cdot r} g_i(k,r) g_j(k,r)^* dr \tag{184}$$

and $g_j(k,r)$ is orthogonal to all $g_j(k',r)$ for $k \neq k'$. $n(k)$ is the fractional occupancy at point k in the Brillouin zone and ranges from 0 for the empty part of the band to a fully occupied 1 electron (2 in a spin-free formalism).

As usual, the Hartree-Fock case will be specified by the condition that

$$P^2 = P \qquad \text{and} \qquad Tr\ (\ P\ ) = N \tag{185}$$

Hence it follows immediately that the Hartree-Fock Bloch orbital density matrix of wave vector k may be determined from the iterative equations

$$P_k' = 3P_k^2 - 2P_k^3 + \lambda_N^1 \quad + \tag{186}$$

$$\lambda \in \sum_L S_k^{-1/2} W(K) \left\{ f_{00}(K) + 2f_{01}(K) e^{ik(r_0 - r_1)} + \ldots \right\} S_k^{-1/2}$$

The physical significance of these equations is that they deliver a density matrix in a Bloch orbital basis that satisfies the restrictions of quantum mechanics and of the x-ray scattering experiment. This generalization incorporating Bloch orbitals allows one to treat equivalently the properties of a wide variety of solids, whether insulators, semiconductors, or metals. Without this, one is restricted to compounds like organic crystals, which are approximated as being composed of non-interacting unit cells.

Bloch orbitals may be transformed into their direct-space equivalents, called Wannier orbitals. The Wannier functions form an orthonormal basis; the overlap matrix for neighboring unit cells is reduced to zero, and the overlap matrix within the same cell is a unit matrix. These are discussed next.

Given a set of basis functions g^1 in each cell 1, construct a Bloch basis

$$g^k = \sum_1 e^{ik \cdot r_1} g^1 \tag{187}$$

Integrating over the occupied part of the Brillouin zone yields Wannier basis functions

$$g^L_W = \sum_1 \int_{BZ} n(k) e^{ik\cdot(r_1 - r_L)} g^1 dk \tag{188}$$

The Wannier functions can be combined to form crystal orbitals

$$\psi^L = C g^L_W \tag{189}$$

Notice that in equation (189) the crystal orbitals associated with cell L have been restricted to being built only from Wannier functions centered on the same cell. In the case of covalent bonding across cell boundaries, as in graphite and diamond, it is necessary to relax this constraint. In such a case, the dimension of the P, S, and f matrices are larger than the number of primitives g^L from which the Wannier basis is constructed. An additional constraint on the P matrix arises; the sum of those diagonal elements corresponding to the same Wannier spinorbital basis function in different cells must be at most one. The Bloch orbital analog of this is that the Bloch P is a function of k. This latter point is why a Wannier representation was considered preferable to that of Bloch for the quantum parametrization of experiments with a limited number of data - P constant instead of P(k).

The integration over the Brillouin zone can be performed separately to get a Wannier phasing

$$\omega^{1L} = \int_{BZ} e^{ik\cdot(r_L - r_1)} dk \tag{190}$$

or in the case of a partly occupied Brillouin zone

$$\omega^{lL} = \int_{BZ} n(k) e^{ik\cdot(r_L - r_l)}\, dk \tag{191}$$

and now the crystal orbitals can be expressed as a function of position only.

$$\psi^L = c \sum_l \omega^{Ll} g^l \tag{192}$$

The single-determinant crystal orbitals may be taken as orthonormal without any loss of generality(105). Defining the Wannier overlap matrices

$$S^{lL} = \int g^l (g^L)^+ dr \tag{193}$$

and

$$\mathcal{S} = \sum_l \sum_{l'} \omega^{Ll} S^{ll'} \omega^{l'L} \tag{194}$$

the orthonormal Wannier basis can be defined as

$$g^L_{WO} = \mathcal{S}^{-1/2} g^L_W = \mathcal{S}^{-1/2} \sum_l \omega^{Ll} g^l \tag{195}$$

and the crystal orbitals can be expressed in this basis as

$$\psi^L = C_o g^L_{WO} = C_o \mathcal{S}^{-1/2} \sum_1 \omega^{L1} g^1 \tag{196}$$

where the subscript o denotes orthonormality.

Define the Fourier transform matrix at the scattering vector K for products of basis functions as

$$f^{L1}(K) = \int e^{iK\cdot r} g^L (g^1)^+ dr \tag{197}$$

and

$$\mathcal{f}(K) = \sum_1 \sum_{1'} \omega^{L1} f^{11'}(K) \omega^{1'L} \tag{198}$$

In equations (194) and (198) , 1 refers to an arbitrary reference unit cell. The calculated scattering amplitudes are given by

$$F_{cal}(K) = \text{tr } P \mathcal{S}^{-1/2} \mathcal{f}(K) \mathcal{S}^{-1/2} \tag{199}$$

which is of the same form as equation (122). The density matrix for the entire crystal in terms of crystal orbitals may be seen to be

$$\rho_1(r;r') = \sum_L \text{Tr } \psi^L(r) \psi^L(r')^+ \tag{200}$$

which can be written in the basis g^L as

$$\rho_1(r;r') = \sum_L \mathrm{Tr}P\, \mathcal{S}^{-1/2} \left(\sum_{1\,1'} \omega^{L1} g^1 (g^{1'})^+ \omega^{1'L} \right) \mathcal{S}^{-1/2} \tag{201}$$

Using the orthonormal Wannier representation, identify

$$P = C_o^+ \; C_o \tag{202}$$

then the iterative equations which determine the density matrix subject to experimental constraints are

$$P' = 3P^2 - 2P^3 + \lambda_N 1 + \lambda_\epsilon \sum_K W(K) \left| F_{obs}(K) - \mathrm{Tr}P\, \mathcal{F}^{-1/2} f(K) \mathcal{S}^{-1/2} \right| \tag{203}$$

Note that there are two places where neighbor effects enter. First, there is a double sum over cells in calculating $f(K)$ and $\mathcal{S}$. This should be extended over a few neighbors - the example below uses 10.

For many shapes of Brillouin zone, the integral (191) can be performed analytically. For any one-dimensional insulator,

$$\omega^{L1} = \sin(2\pi^2 (r^L - r^1)) / (\pi (r^L - r^1)) \tag{204}$$

Note that $\omega'' = 2\pi$. For a spherical Brillouin zone, such as may be found in three-dimensional metals, see the interesting articles of Matthai et al(106,107).

In the numerical examples of some previous papers(41,104), the stress has been on the comparison of quantum and non-idempotent fits to scattering data. In this chapter, all P matrices are idempotent, but some use a one-cell basis while others refer to a Wannier basis. For this purpose, the numerical example used will be a linear array of equidistant hydrogen atoms, all spin-up.

For an assumed "exact" density matrix P_{exact}, which includes interactions among neighboring unit cells through the Wannier formalism, assumed "exact" scattering factors $F_{exact}(K)$ are calculated. These "data" $F_{exact}(K)$ are then best-fit in the least-absolute-value sense R_1 , by a single-determinant N-representable density matrix calculated in two different ways. In the first fit, hydrogen atoms in neighboring unit cells are not allowed to interact - the problem is treated as an isolated atom. The resulting isolated-atom density matrix is allowed to adjust to fit as closely as possible the scattering data F_{exact} using the given isolated-atom basis. In the second fit, a Wannier basis is formed from the isolated-atom basis, using the formalism above. The resulting Wannier density matrix is then allowed to adjust according to equation (203). Since the scattering data were calculated in a Wannier basis, it is natural that the data would be better fit in the second case. That is what will be shown.

The comparisons are made in terms of R_f . As a point of reference, the R-factors appropriate to using P_{exact} within the isolated-atom basis are given. The calculations are repeated for a series of scaled basis function exponents, which emphasize that the overlap between basis functions in different cells determines the importance of the Bloch/Wannier formalism.

The calculations were done in double precision on the CUNY IBM 3033 computer using the PL/I program EXAMPLE of Appendix D. The model line of H atoms had a repeat distance of 1.88 atomic units, which is a variational minimum-energy distance(108). A basis built from three ls-type Gaussian functions was used, with exponents a multiple of {19.2406, 2.89915, 0.653401}. This set has been used to contract the inner function on hydrogen in a double-zeta basis set(109). The results are collected in Table 16 and Table 17. For all five bases, a set of 30 "observed" structure factors was first calculated in the Wannier formalism above, using the assumed "exact" P matrix

$$P = \begin{bmatrix} 1/3 & -1/3 & -1/3 \\ -1/3 & 1/3 & 1/3 \\ -1/3 & 1/3 & 1/3 \end{bmatrix} \qquad (205)$$

Structure factors and the error R were then calculated for each of the three cases:

1) $P = P_{exact}$, isolated-atom basis

2) $P = P_{best\ fit}$, isolated-atom basis

Figure 15

Errors Incurred by Neglecting to "Wannier-ize"

the Basis Functions

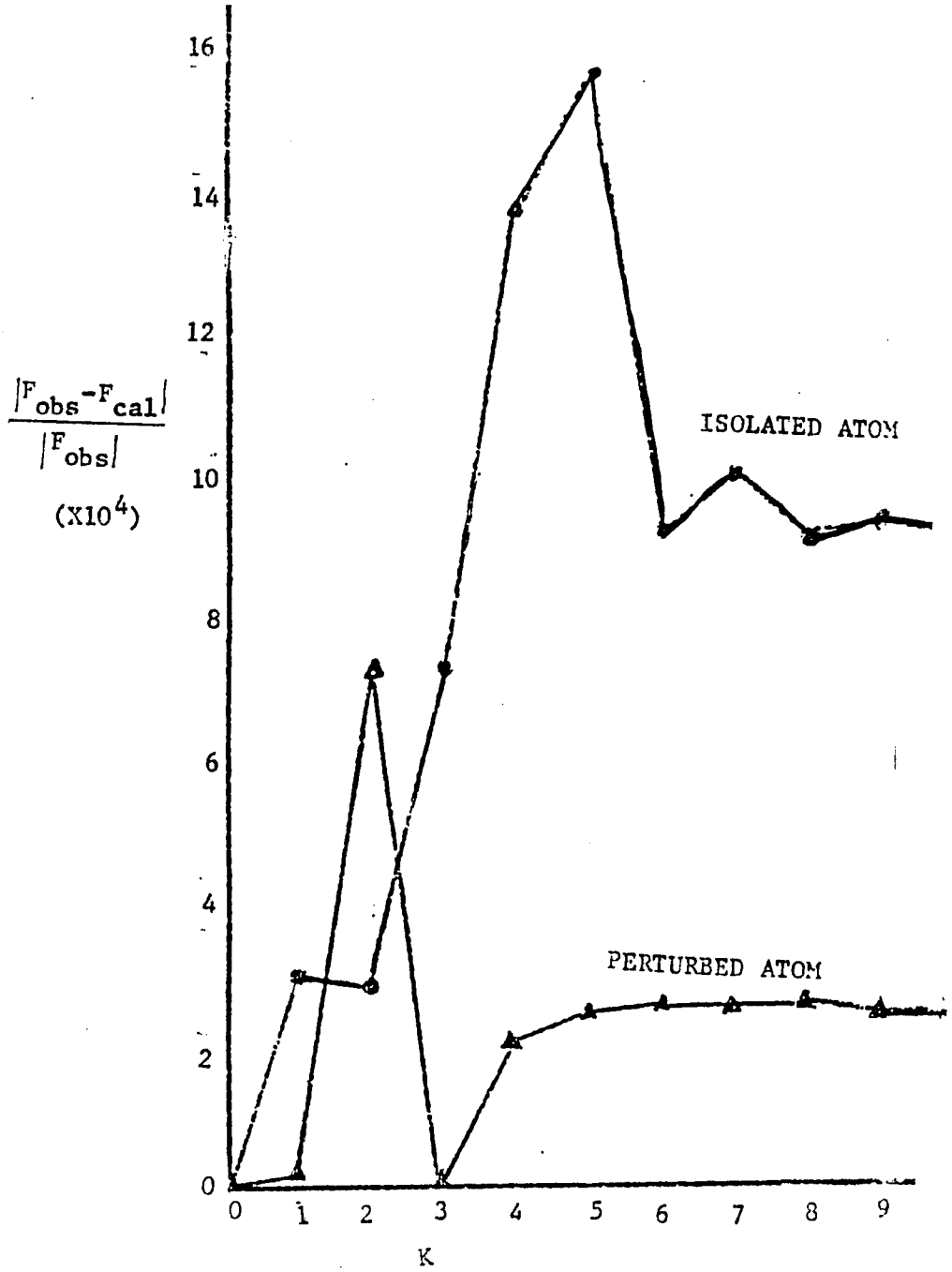

Table 16

Numerical results using the Wannier and isolated-atom approximations.

CASE	BASIS	NUMBER OF F_{obs}		R-FACTOR, EXACT P	R-FACTOR, BEST-FIT P	
		$>10^{-20}$	$>10^{-6}$	ISOLATED ATOM APPROX	ISOLATED	WANNIER
1	.192406 .0289915 .00653401	1	0	1.3×10^{-2}	*	*
2	1.92406 0.289915 0.0653401	4	2	8.9×10^{-3}	*	*
3	19.2406 2.89915 0.653401	13	7	3.9×10^{-4}	2.75×10^{-4}	4.3×10^{-8}
4	192.406 28.9915 6.53401	>30	22	6.5×10^{-9}	6.3×10^{-9}	5.0×10^{-9}
5	1924.06 289.915 65.3401	>30	>30	4.8×10^{-15}	1.2×10^{-9}	1.2×10^{-9}

* Too few data, *P* matrix undetermined.

Table 17

Density matrix solutions of the iterative equations.

CASE	BASIS	BEST-FIT P MATRIX ISOLATED ATOM APPROXIMATION	BEST-FIT P MATRIX WANNIER FORMALISM
3	19.2406 2.89915 0.653401	$\begin{bmatrix} .33346 & -.33269 & -.33404 \\ -.33269 & .33191 & .33327 \\ -.33404 & .33327 & .33462 \end{bmatrix}$	$.333\ 333 \times \begin{bmatrix} 1 & -1 & -1 \\ -1 & 1 & 1 \\ -1 & 1 & 1 \end{bmatrix}$
4	192.406 28.9915 6.53401	$.333\ 333\ 33 \times \begin{bmatrix} 1 & -1 & -1 \\ -1 & 1 & 1 \\ -1 & 1 & 1 \end{bmatrix}$	$.333\ 333\ 33 \times \begin{bmatrix} 1 & -1 & -1 \\ -1 & 1 & 1 \\ -1 & 1 & 1 \end{bmatrix}$
5	1924.06 289.915 65.3401	$.333\ 333\ 33 \times \begin{bmatrix} 1 & -1 & -1 \\ -1 & 1 & 1 \\ -1 & 1 & 1 \end{bmatrix}$	$.333\ 333\ 33 \times \begin{bmatrix} 1 & -1 & -1 \\ -1 & 1 & 1 \\ -1 & 1 & 1 \end{bmatrix}$

3) $P = P_{\text{best fit}}$, Wannier basis

The index of agreement minimized was ϵ_1 .

Each superiteration was considered complete when neither λ was larger than 10^{-10}. A run was considered complete when $\epsilon < 10^{-9}$. In case 3, an ϵ value of 10^{-8} was considered acceptable because of computer time limitations.

Case 3 is the most realistic basis considered(109), and thus merits further discussion. In column 5 of Table 27, the R-factor calculated with the exact P, but using an isolated-atom g, is .00039. Allowing the P matrix to readjust to fit the scattering "data" as closely as possible within the single-determinant approximation, without adjusting the basis, the R-factor is reduced to .000275, as indicated in column 6. Now if, in addition to allowing P to adjust, the Wannier basis is used, built from the isolated-atom basis, then the R-factor drops to .000000043, as indicated in column 7. This is just the numerical illustration desired. The error for case 3 is graphed in Figure 16.

If interactions among neighboring unit cells are important, then the Bloch/Wannier formalism ought to be important for fitting the scattering data. Cases 1, 2, 4, and 5 of Table 27 investigate the effects of scaling the basis. These four cases are much less realistic as bases for hydrogen. However, they do illustrate the manner in which overlap of orbitals among neighboring cells determines the relative

importance of a Bloch/Wannier formalism. For very large exponents, cases 4 and 5, the electron density is concentrated near the nuclei, reducing any overlap amongst unit cells. The result in case 4 is that, although the Wannier formalism is an improvement over the non-interacting unit cell case, it is not nearly as important as in the realistic case 3, where there was appreciable overlap. In case 5, the atoms are so tightly bound that there is essentially no differential overlap between cells and the more realistic Wannier calculation yields results virtually identical to the isolated-cell case. For very small exponents, cases 1 and 2, the orbitals are very diffuse, and consequently the scattering does no extend far enough into reciprocal space to provide sufficient data to fix all the elements of the density matrix. Notice, however, that neglecting interactions among unit cells in cases 1 and 2 corresponds to an error of about 1% as measured by the R-factors indicated.

Table 28 lists the P matrices calculated for cases 3, 4, and 5 of Table 27. The greatest difference between P matrices occurs for case 3, with the most realistic basis. As discussed above, for the very tightly bound orbitals of cases 4 and 5, the density matrices are virtually the same with as without the Wannier formalism, differing only after the eighth digit. For Gaussians tighter than about $\exp(-10r^2)$, the Wannier formalism seems unnecessary.

A final comment concerning the numbers in Table 27 : although the R-factors seem small, apparently exacting little penalty for the isolated atom approximation, remember that this is only a model problem. Thus, there are fewer F_{obs} than in real, three-dimensional experiments. Also, the model problem only has one electron per unit cell, so valence scattering efffects are small. Thinking of the results on an error per electron basis gives a better perspective on the significance of interactions among neighboring unit cells.

Chapter VI. Nuclear Vibration

In this chapter, a possible future extension of the formalism is discussed, namely a realistic boson oscillator model for thermal and zero-point vibrations of nuclei.

The motions of the $\mathcal{A}$ nuclei in a crystal can be partially described by the $3\mathcal{A}$ functions describing the projections of the motions on 3 independent axes. Viewing this as the diagonal of a matrix, the motion can be fully described by a $3\mathcal{A}$ by $3\mathcal{A}$ matrix, each element of which is a function, describing the covariances of the above projected motions.

The independent ellipsoid model, which is the common formalism used,and corresponds to a cumulant expansion cut off at second order, assumes that:

1) all $3\mathcal{A}$ diagonal functions are Gaussians.

2) off-diagonal couplings between different atoms are zero.

3) off-diagonal elements of the 3 X 3 submatrix for each atom's motion are such that the eigenfunctions are Gaussians along 3 principal axes.

Spectroscopic models of nuclear motion make far fewer assumptions. They try to determine a complete set of boson nuclear wavefunctions υ_n where υ_0 describes zero-point motions, and the higher (exciton) functions are represented as

$$\upsilon_n = b_n^+ \upsilon_0 \tag{206}$$

in second-quantized notation. One can expand this wavefunction in a basis of normal modes or local modes(110,111). Such a spectroscopic description can be used for the "internal" modes of a crystal(112), but this seems not to work(113) as well, and requires far too many parameters. Also, a complete normal-mode analysis is not always available, because it requires such a large amount of data. However, it can be done(114).

Not as much data on nuclear motion is available from x-ray crystallography as from spectroscopy. This is because the experiment does not actually see moving nuclei, but merely instantaneous nuclear positions. Nuclear motions are inferred from the distribution of nuclei in the various cells, as follows. The translational symmetry of the crystal requires that the equilibrium positions of all translation- or other symmetry- related nuclei be identical modulo the symmetry operation. Any deviation from exact symmetry is ascribed to either disorder or vibration. In a quantized system of vibrations, disorder can be thought of as motion in a multiple-minimum potential well with insuperably high barriers separating the several local minima.

When a system is moving in several normal modews at once, it is no longer possible to observe which nuclear motion comes from which normal mode. In x-ray scattering, the correlations between various bond stretches, bends, and torsions gives rise only to thermal diffuse scattering, called TDS(115,116,117,118). Cruikshank (115) says, "The x-ray data give average frequencies for identifiable sets of branches,

but not in general for the individual branches." Dawson et al(118) state that "it is immaterial for Bragg scattering whether the thermal motions actually relate to independent or coupled vibrational behavior."

For example, consider a crystal of linear triatomic molecules. For an asymmetric stretch, one bond is shrinking while the other elongates. For the synmetric stretch, both bonds expand and contract simultaneously.

Since correlations between electron positions and between nuclear positions are not observed in elastic scattering, that is, they appear only in the off-diagonal elements of $\rho_1(r,r')$; one only sees scattering from orbitals effectively associated with one atom. One sees a distribution of instantaneous positions, but not the correlation between local modes of vibration, as in Figure 16.

For this reason, one can, to a good approximation, treat each atom as an independent oscillator, if one is modeling elastic scattering of x-rays (and/or neutrons). A potential function for this independent oscillation can be approximated from Bragg data through a single-center expansion of the electron density and the resultant model of the second derivative of the Hellmann-Feynman force(16).

A more common approximation is merely to describe the distribution of instantaneous nuclear positions in a vibrational multipole expansion about each nuclear position without making any assumptions or

Figure 16

Indistinguishability of the Phasing of Vibrational Motions

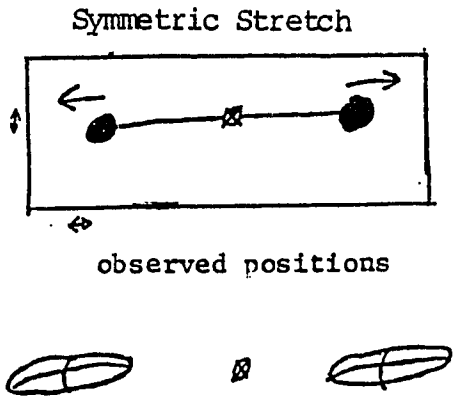

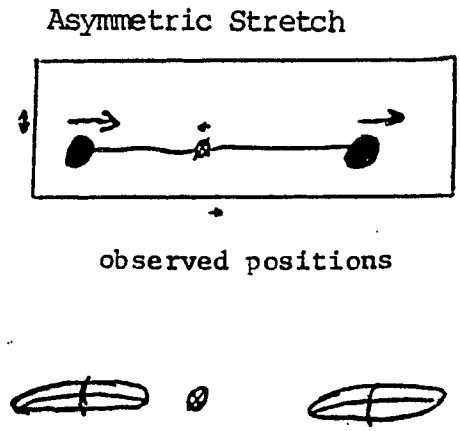

explanations about this distribution(119). Truncating the expansion at second order leads to the anisotropic harmonic "independent ellipsoid model'" also called the "Debye-Waller factor" model. Truncating at first order (if the expansion center is the average nuclear position, all first-order terms are by the definition of "average" identically zero) leads to an isotropic Debye-Waller factor - a scalar "thermal smearing." Expanding to higher order leads to one of at least four different models(120), depending on the details of the expansion. All these are known collectively as "higher cumulant models." The cumulants have the following physical meaning:

The zero'th cumulant is the r.m.s. displacement of the nucleus from the expansion center.

The three first cumulants are the average displacement of the nucleus from the expansion center.

The five second cumulants are the distortion of the thermal motion's three principal axes from equal length, and their orientation relative to the model's axis system. (N.B. the 5 second cumulants and the 1 zero'th cumulant are almost always combined into the anisotropic Debye-Waller tensor U.)

The seven third cumulants,or "skew," nine fourth "kurtosis" cumulants, etc. describe various distortions in the angular part of the

nuclear position distribution. These have the same angular depedence as the 7 f orbitals, 9 g orbitals, etc. where the negative lobes are a lessening of the probability of the nucleus being there, and the positive lobes an increasing. There is a requirement of positivity here also; the nucleus must have at least a zero chance of being somewhere, and "antimatter regions" are disallowed on physical grounds. In a non-orthonormal axis system, such as the natural crystal axis system, the relationships and mathematical formulae are more complicated(121). One can always convert to a Cartesian coordinate system describing the crystal axes in a complicated way, and the atoms themselves in the simple way above(122).

A formalism is proposed below which is more physically meaningful than a cumulant expansion in that, by making mechanistic assumptions about the nuclear motion, the parameters to be refined will have direct physical interpretations. The parameters of the model will be amplitudes of bond stretches, bends, torsions, ring bends, etc., following a suggestion of Pawley(122); no thermal ellipsoids will be used, and no Debye-Waller factors will arise(123). This makes the x-ray data very directly useful, and comparable to spectroscopic data analyses in that, ideally, our force constants will equal theirs. Spectroscopists also can use a local mode description of their data analysis(110). The concept of a group frequency in infrared spectroscopy supports this. Recent calculations of vibrational levels(111) find that, even in the frequency region of excitation of

only one normal mode to its first excited state, the normal mode description is not much superior to that of local modes.

The independent ellipsoid model is not at all equivalent to a normal/local mode analysis, even for the same number of parameters. As shown below, the mechanistic model uses 3A+15 parameters for A atoms, as opposed to 6A thermal ellipsoid parameters. A problem with atomic ellipsoids is that they obfuscate the data analysis so that it is impossible to separate internal vibrations from rigid-body translations and rotations(124,125). The assumption of negligible internal motions is incorrect, but the 21-parameter TLSρ (Translation,Libration,Screw rotation, and center of rotation(ρ-tation)) model(126) (more than 24, if one uses higher cumulants) of external rigid-body motions in a rectilinear coordinate cumulant expansion allows separating internal and external. The TLS (Translation,Libration,Screw rotation) model without higher cumulants doesn't need the 3 cumulant expansion center location parameters "ρ," so that 21 parameters are taken up by external motions, and internal motions need a different model. This internal motion must be described, since it was long ago shown(124) that "there are molecular distortions which are by no means negligible." Moreover, the ratio of internal to external motions increases with decreasing temperature(112). Since the highest quality Bragg data in future years will come from synchrotron sources such as Brookhaven's National Synchrotron Light Source, which plans to run most of its diffraction experiments at 20^{o}K(127), a good model for

vibration at these temperatures must be flexible enough to accurately describe both internal and external motions.

The 3A motions undergone by A nuclei in a crystalline environment can be described in terms of 3 rigid translations of a unit cell relative to its neighboring cells, 3 rigid rotations of the unit cell relatively to others, and 3A-6 internal vibrations which closely resemble the vibrations of isolated gas-phase molecules. The 6 external modes - 3 translations, or longitudinal acoustic modes; and 3 hindered rotations, or transverse modes; are described in detail by Shomaker and Trueblood(128) in connection with the TLS model. The modified form of the TLS model described below does not make the unphysical(129) assumption that

$$Tr(S)=0 \tag{207}$$

which is necessary when converting from thermal ellipsoids,but which in general is not needed(126).

It is proposed to use a curvilinear coordinate(130) description of the 6 independent external motions of the TLS model(128), rather than an expansion in cumulants(126) of the tangential rectilinear approximation to them.

Although the TLSρ model(126) and the modified TLSI (Internal) model described here both use 21 parameters for external motions, they are different. A potential is assumed of the form

$$V(q_i) = \mathcal{K}_i \, q_i^2 \tag{208}$$

for each coordinate q_i, and thus there are 6 force constants $\mathcal{K}_i$ as adjustable parameters.

The q_i for translation are three orthogonal axes forming a translational Principal Axis System, which intersect at the center of mass. The three Euler angles for rotation of the crystal axes into the translational PAS are adjustable parameters.

The q_i for rotation are three helices, with three independent pitches, or helix lengths, as adjustable parameters. The lines about which these helices coil are orthogonal to each other, requiring 3 Euler angles to describe their PAS. These helix axes do not intersect, and each of them require 2 parameters describing the vector displacement of the axes at their closest approach to the center of mass. These 21 parameters are summarized in Figure 17.

Briefly, there are 2 sets of 3 quadratic force constants $\mathcal{K}$; 2 sets of 3 Euler angles; and for each of the 3 screw oscillations, the model requires 1 helix length and 2 axis displacements; a total of

$$2\,(\,3\,) \;+\; 2\,(\,3\,) \;+\; 3\,(\,1+2\,) \;=\; 21 \tag{209}$$

Figure 17

The TLS Model

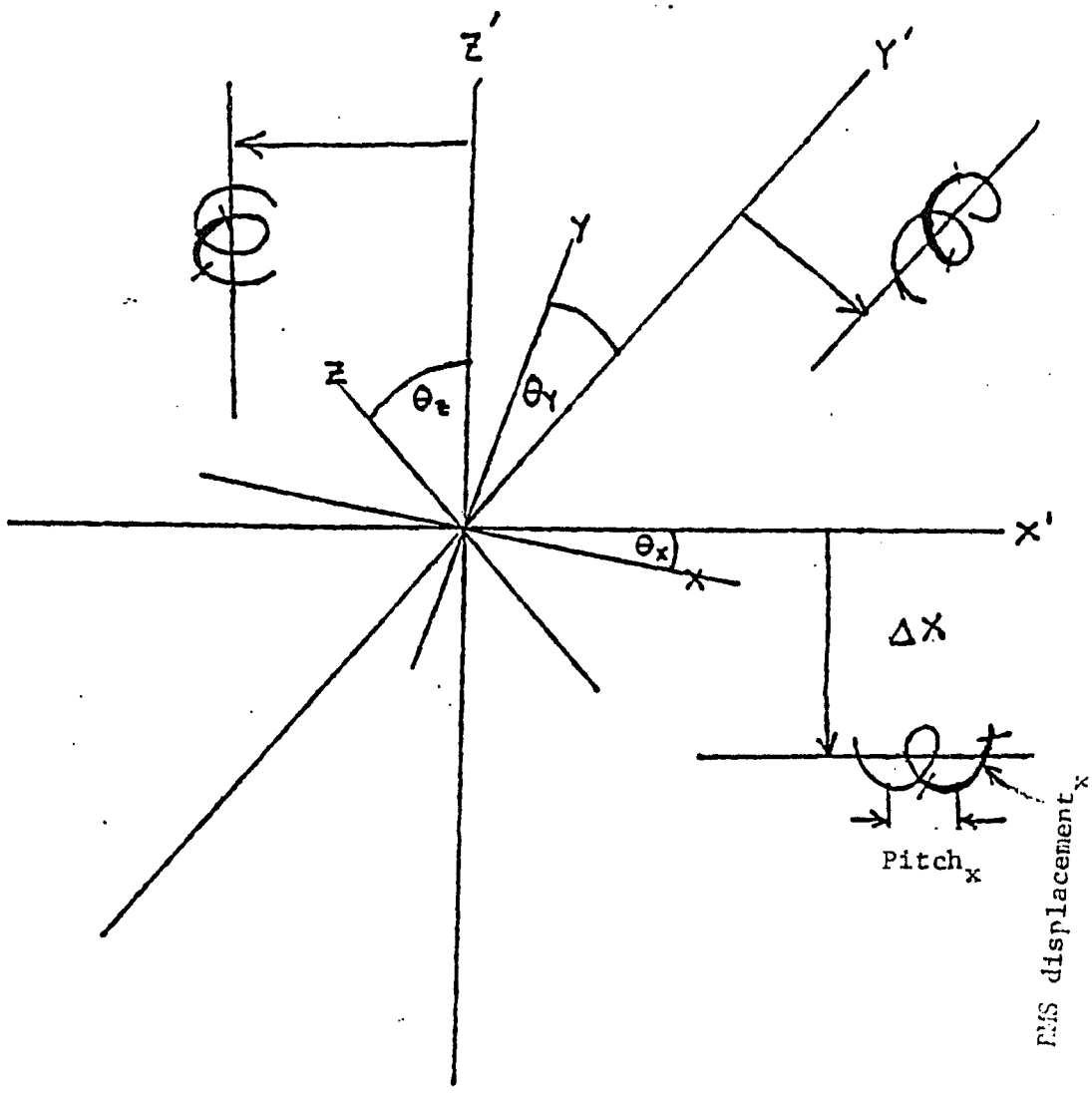

external mode parameters. It is likely that such a model is analytically intractible; the only solution possible is likely to be at least partly numerical(131).

The 3A-6 internal modes of vibration of the crystal, which cause molecular distortions, can be modeled as 3A-6 local mode quadratic oscillators, each of which is a combination of bond stretchings, angle bendings involving 3 atoms, torsions involving 4 atoms, and possibly ring motions involving 5 or more atoms.

Since the force constants associated with angle and torsional variation are roughly 10 times as large as bond stretching force constants(132), their relative amplitudes can be assessed as follows. Assuming equipartition of energy among all modes, for quadratic modes n,

$$E_n = \tfrac{1}{2} \mathcal{K}_n \Delta q_n^{\,2} \tag{210}$$

implies that

$$\frac{\langle \Delta q_{\text{bend}} \rangle}{\langle \Delta q_{\text{stretch}} \rangle} \approx \sqrt{\frac{E_{\text{bend}}\, \mathcal{K}_{\text{stretch}}}{E_{\text{stretch}}\, \mathcal{K}_{\text{bend}}}} \tag{211}$$

$$\frac{\langle \Delta q_{\text{bend}} \rangle}{\langle \Delta q_{\text{stretch}} \rangle} \sim \sqrt{\frac{1}{1} \cdot \frac{10}{1}} \sim 3 \tag{212}$$

and bends and torsions are roughly thrice as important as stretches. This explains the success of Hirshfeld's rigid-bond postulate(133), which makes the approximation

$$\mathcal{K}_{stretch} = \infty \qquad (213)$$

For finite stretching constants, especially the smaller ones associated with X - H stretches, or motion along a Van der Waals bond, it is advantageous to use the dimensionless coordinate

$$q = (r - r_{eq}) / r \qquad (214)$$

of Simons(134) where r is the internuclear disatance. This partially corrects for anharmonicity, by building into the coordinate the idea that it is easier to stretch a bond than to compress it. For example, $q = -1$ corresponds to $r=1/2\ r_{eq}$, but $q = +1$ corresponds to $r=\infty$. This method is the most satisfactory for expanding a potential in a given number of parameters, as opposed to Pade approximants or modified Morse curves(135).

There are only two 2-parameter vibrational potential functions in the literature: a quadratic oscillator in Simon's coordinate, called the Kratzer potential(136), and the harmonic oscillator. For example, the Morse function requires r_{eq}, a force constant, and a dissociation energy; only the 2 functions above require only r_{eq} and $\mathcal{K}$, and not a

Figure 18

Comparison of Harmonic, Kratzer, and RKR

Potentials for the CO Molecule

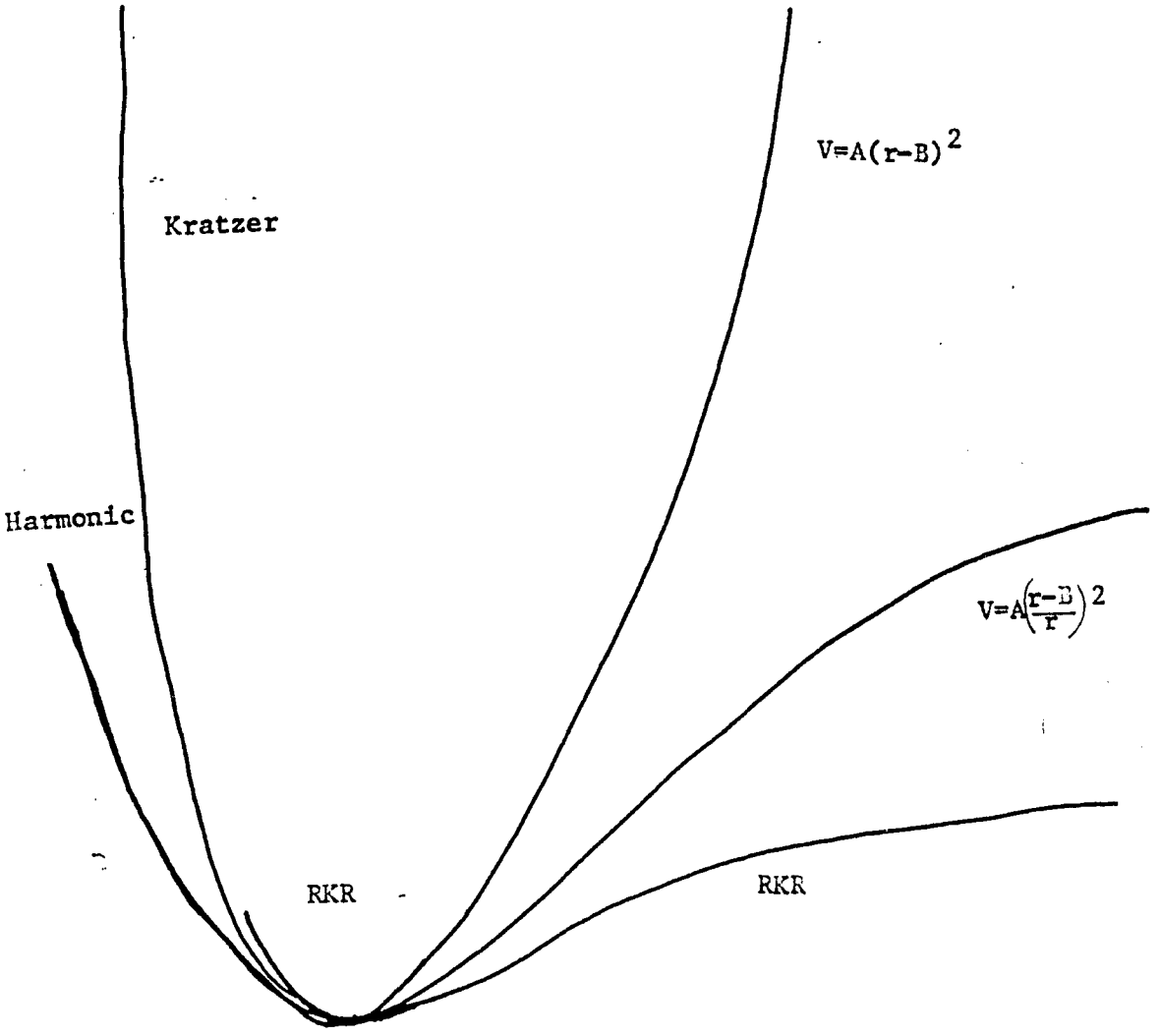

dissociation energy. Figure 18 shows a comparison of a harmonic, a Kratzer, and an RKR fit to the CO molecule.

The coordinates for bending can be the curvilinear

$$q = \theta - \theta_{eq} \quad \text{or} \quad q = \phi - \phi_{eq} \tag{215}$$

where θ is an angle and ϕ is a dihedral angle.

Since these are internal vibrations, the unit cell as a whole must neither rotate or translate. This invariance can be preserved by the "riding" motion model(137), wherein the rest of the molecule preserves as much as possible its bond lengths, angles, and dihedrals. This requires a definition of which atoms are bonded - either chemical intuition is used, or the bond orders from the electronic parametrization by the P matrix can be examined. A possibility would be to use chemical intuition for the initial guess, and the P matrix thereafter.

This highly non-linear modeling of vibration does not result in anything resembling the Debye-Waller ellipsoids(123). One could least-squares fit a set of U to this vibrational TLSI model, in a reversal of the idea of Shomaker and Trueblood(128). The TLSI equations reduce to ellipsoids only at high temperatures, when the oscillators look like pure Gaussians; and only if one treats all motions as pure translations of unconnected spherical sub-units(123), rather than as molecular fragments.

In the general case, each unit cell has a certain number of molecules, each requiring its own set of external and (if the molecule has 2 or more atoms) internal vibrational parameters. The ellipsoid model is recovered if one treats each atom as a separate molecule, as in the beryllium model of chapter 3, with the external screw motions having zero amplitude, and the external translations treated with a truncated cumulant expansion.

Vibrations of 2-center orbital products should be treated by the "center-of-density" method of Stevens et al.(138). The position of the density element is that of an imagined point in space defined by the weighted average position of the two orbital basis functions concerned. The orbital exponents determine the weighting factor. Note that this method is only defined with Gaussian orbitals, not STO. The motion of this density element depends on the motions of the 2 nuclei. If bonded, the density element is some sort of weighted average of the 2 nuclear motions. If the 2 centers are not considered bonded, the motion of the density element is the convolution of the nuclear motions.

The P matrix is not a function of the reciprocal lattice vector K. However, in the general case P is a function of the vibrational excursions q. Given

$$P(q), S^{-1/2}(q), f(K,q) \tag{216}$$

the scattering factors are(139)

$$F_c(K) = \sum_n W_n \int \upsilon_n(q)^* F(K,q) \upsilon_n(q)\, dq \qquad (217)$$

for vibrational wavefunctions υ_n with temperature-dependent weighting factors W_n.

A vast simplification has been implicitly used here. The Einstein model for vibrations has been used. In fact, since this is a crystal, the vibrational levels $\upsilon_n(q)$ are not simple functions, but bands, which need a Bloch or Wannier description. Fortunately, phonons of vibration are bosons, which means that it is not unphysical to say that W_n in equation (217) is a delta function on the center of the Brillouin zone, and thus force all phonons to sit at point Γ. This approximation is equivalent to the Einstein model(140). If desired, a Debye model of vibration could be used, which would require a Brillouin zone summation. Still more realistic, and less computationally tractable, would be an experimental vibration model, using data from Inelastic Neutron Scattering (INS), or from TDS.

The appropriate approximations are totally opposite for internal and external motions. Each internal motion in each cell should(141) be treated as totally uncoupled to all others, both those in the same cell and those in any other cell; this corresponds roughly to a uniform distribution throughout the Brillouin zone of each internal vibrational level. Matrix elements connecting electronic basis functions in

different cells should be convoluted with both internal vibrational excursion probabilities (amplitude squared) separately. External motions in any cell should be treated as totally correlated to all the rest, as shown by experiment(117). Cross-cell matrix elements have external motions perfectly in phase with each other; translations leave all distances unchanged, but screw rotations correspond to the motion of two coupled helices.

As a first approximation, one could assume that each mode is a harmonic oscillator in the appropriate coordinate system. This is only an approximation, since a quadratic oscillator is not a harmonic oscillator if the coordinate q is not the same as a simple distance; the kinetic energies are not the same. However, this approximation makes things much simpler.

Assuming each mode is a quantum boson harmonic oscillator, then

$$\sum_n W_n \upsilon_n^*(q_i)\upsilon_n(q_i) \tag{218}$$

can be represented as a probability of an instantaneous excursion $\Omega(\Delta q)$, which can be expressed in closed form(142) as

$$\Omega(\Delta q_i)dq_i = \sqrt{\frac{\gamma_i}{2\pi}}\, e^{-\frac{1}{2}\gamma_i(\Delta q_i)^2} dq_i \tag{219}$$

where the γ_i are related to spectroscopy by(142)

$$\gamma_i = \frac{2\nu_i}{\hbar} \tanh(\hbar\nu_i / 2k_B T) \tag{220}$$

for a frequency ν, and a temperature T. These frequencies ν are the parameters comparable to an IR/Raman experiment. Thus,

$$F_c(K) = \int_q Tr\, P(q) S^{-1/2}(q) F(K,q) S^{-1/2}(q) \prod_{q=1}^{3A} \sqrt{\frac{\gamma_i}{2\pi}} e^{-\frac{\gamma_i}{2} q_i^2} d\vec{q} \tag{221}$$

Now models are needed for P(q), $S^{-1/2}(q)$, and f(K,q). The model for $S^{-1/2}(q)$ and for f(K,q) has no adjustable parameters, since these matrices are determined strictly by the nuclear positions, and by the basis functions used. They could thus be evaluated explicitly as a power series expansion about the equilibrium value, or at a series of q values, and then spline fit, or something similar. Although these alternatives both require a lot of computer time, some approximations or simplifications might be possible. A Taylor series expansion in $(r - r_{equilibrium})$ would be aided by the fact that the derivative of a scattering matrix element

$$\frac{\partial f_{\mu\nu}(K)}{\partial q} = \frac{\partial}{\partial q} \langle g_\mu | e^{iK\cdot r} | g_\nu \rangle \tag{222}$$

is related to the scattering by the derivative of the basis

$$\left\langle \frac{\partial g_\mu}{\partial q} \middle| e^{iK\cdot r} \middle| g_\nu \right\rangle \tag{223}$$

The derivatives $\partial P/\partial q$ are not determined by P, but must be varied to fit the experiment. However, there are constraints on $\partial P/\partial q$. First, there is the constraint system that can be derived from the electrostatic and virial theorems(143) if the energy implied by a particular P matrix and other derived quantities are solved for in order to apply the constraints. These derived quantities involve as much time and approximations as an ab initio solid-state wavefunction not based on the data, and will not be considered further in this thesis. More importantly, for any value of q,

$$(P(q))^2 = P(q) \text{ and } Tr\ (P(q)) = N \tag{224}$$

In a Taylor series expansion of P(q), this means that

$$(P(0))^2 = P(0) \text{ and } Tr\ (P(0)) = N \tag{225}$$

$$\left(P(0)+\sum_i \frac{\partial P}{\partial q_i}\delta q_i + \frac{1}{2!}\sum_{ij}\frac{\partial^2 P}{\partial q_i \partial q_j}\delta q_i \delta q_j + \ldots\right)^2$$

$$= P(0)+\sum_i \frac{\partial P}{\partial q_i}\delta q_i + \frac{1}{2!}\sum_{i\,j}\frac{\partial^2 P}{\partial q_i \partial q_j}\delta q_i \delta q_j + \ldots \tag{226}$$

Expanding, and setting $\delta q=0$, $i \neq i'$, yields

$$P(0)^2 + \left(P(0)\frac{\partial P}{\partial q_i} + \frac{\partial P}{\partial q_i}P(0)\right)\delta q_i + \ldots \qquad = P(0) + \frac{\partial P}{\partial q_i}\delta q_i + \ldots \tag{227}$$

In addition to the equilibrium term (225), results can be obtained from equating terms of the same order in δq. In particular,

$$\left(P(0)\ (\partial P/\partial q_i)+(\partial P/\partial q_i)P(0)\right)\delta q_i=(\partial P/\partial q_i)\delta q_i \tag{228}$$

and

$$P''\ (P')^2+.5P(0)P''+P''P(0)\ )\delta^2 q_i=.5P''\delta^2 q_i \tag{229}$$

and so forth, leading to equations of constraint like

$$(\partial P/\partial q)=P(0)(\partial P/\partial q)+(\partial P/\partial q)P(0) \tag{230}$$

from the linear term (228), and another for each order of δq, which equations must be applied separately to each type of motion q_i.

Let us examine the simplest case - two orbitals and one electron. Then

$$P(0)=\begin{pmatrix}\cos^2\theta & -\sin\theta\cos\theta\\ -\sin\theta\cos\theta & \sin^2\theta\end{pmatrix}\ \text{and}\ \frac{\partial P}{\partial q}=\begin{pmatrix}a & b\\ b & c\end{pmatrix} \tag{231}$$

From formula (230) above, it can be seen that

$$\begin{pmatrix} a & b \\ b & c \end{pmatrix} = \begin{pmatrix} a & b \\ b & c \end{pmatrix} \begin{pmatrix} \cos^2\theta & -\sin\theta\cos\theta \\ -\sin\theta\cos\theta & \sin^2\theta \end{pmatrix} +$$

$$\begin{pmatrix} \cos^2\theta & -\sin\theta\cos\theta \\ -\sin\theta\cos\theta & \sin^2\theta \end{pmatrix} \begin{pmatrix} a & b \\ b & c \end{pmatrix} \tag{232}$$

Multiplying out gives

$$\begin{pmatrix} a & b \\ b & c \end{pmatrix} \begin{pmatrix} 2a\cos^2\theta - 2b\sin\theta\cos\theta & b - (a+c)\sin\theta\cos\theta \\ b-(a+c)\sin\theta\cos\theta & 2c\sin^2\theta - 2b\sin\theta\cos\theta \end{pmatrix} \tag{233}$$

which leads to the values

$$a = -c = b\tan\theta \tag{234}$$

where b is a free parameter. Put another way,

$$\frac{\partial P}{\partial q} = \begin{pmatrix} a & a\cot 2\theta \\ a\cot 2\theta & -a \end{pmatrix} \tag{235}$$

and the number of new parameters for each q_i is the same. In order to stem the proliferation of parameters to be fit, the approximation

$$\partial P/\partial q = 0 \qquad (236)$$

should be used unless there is likely to be a really good reason not to, such as a high-spin/low-spin transition as a result of a particular vibrational motion. Approximation (236) is similar to the convolution approximation(144), but superior, since the overlap matrix is allowed to adjust in the TLSI model, but not in that of Coulson and Thomas(144).

The result of equation (221) is that, even with approximation (236), the model takes vibronic effects partially into account, without any new free parameters. The total number of parameters to optimize is 3A nuclear position projections onto the 3 axes, 21 external mode parameters (assuming no added cumulants), 3A-6 internal vibration force constants, and N(m-N) P matrix parameters (assuming a fixed basis); a total of 6A+15+N(m-N). This reduction in the dimensionality of the parametrization is the ultimate justification for approximation (236), even though it is inconsistent with, and worse than, the adiabatic approximation(137). Note that all 6A+15 non-electronic parameters could be refined from neutron scattering, or an X+N joint refinement.

If approximation (236) is made for all vibrational modes, the effective matrix $P_{average}$ is not in general the same as $P_{equilibrium}$, since the data being fit is vibrationally averaged. Rather,

$$P_{average} = \int_q P(q)\,\Omega(q)\,dq \qquad (237)$$

and consequently

$$F_{cal}(K)=Tr\int_q\left\{\int_{q'}P(q')\Omega(q')dq'\times S^{-1/2}(q)f(K,q)S^{-1/2}(q)\Omega(q)\right\}dq \tag{238}$$

Replacing equation (238) with

$$F_{cal}(K)=Tr\langle P\rangle\langle S^{-1/2}\rangle\langle f(K)\rangle\langle S^{-1/2}\rangle \tag{239}$$

is a worse approximation, since the three latter terms ought to be averaged exactly in phase with each other, and scrambling this phasing throws out information that can be retained without any extra effort.

Compare this $\langle P\rangle$ to the following;

1) The "perfectly following" approximation(145) wherein the electron density is partitioned amongst the nuclei and each piece is assumed to move unchanged with its nucleus.

2) The "convolution" approximation(144), wherein

$$\rho(r,q)=\sum_{\mu L}\rho_\mu(r-r_{equilibrium,L}-v_{\mu L}) \tag{240}$$

where the pieces ρ_μ of the density assigned to atom k in cell L move with the vibrations v_{kL} of the nuclei k. This approximation has been studied for N_2, CO, BF, and HF(146), and Epstein and Stewart find that

$$\left\langle I^{\text{x-ray}}_{\text{elastic}} \right\rangle - \left\langle I^{\text{rigid}}_{\text{elastic}} \right\rangle \leq .06\% \qquad (241)$$

compared to vibrational anharmonicity errors of -.26%. The much larger errors found for the H monopole(147) may be due to using a multipole expansion about nuclei rather than about charge centroids. X-H bonds are known to be troublesome since the bond is weak, and H atoms have no core electrons. Epstein and Stewart find(147) a 5.0% anharmonicity correction for the H monopole. Any errors made by using approximation (236) are four or five times less severe than the errors made in truncating the vibrational cumulant expansion.

A simple analogy is a camera mounted on a moving truck. Any blurring in the picture due to imperfect lenses in the camera is negligible compared to the problems caused by poor shock absorbers on the truck.

As suggested by Mills(148), all vibrational parameters ought to be in dimensionless coordinates so that the units for stretching and bending will be identical. Bond stretches could be expressed in the dimensionless Simon's coordinate(132), angle variations in $\Delta\theta$, and torsions in $\Delta\phi$. There is an added advantage to this in that least-squares fits vary with the coordinate system(149), so that the less arbitrary the coordinate system, the less arbitrary the point of best fit. Coordinates must, however, be in arbitrary units, with

dimensions of length. Following Pawley(122), atomic positions can be expressed in orthogonal Å, or orthogonal au, coordinates.

This vibration model in curvilinear dimensionless coordinates uses, in the approximations of this chapter, 3A-6 local-mode quadratic force constants. This can lead to, at most, errors of 5%(150). Mills(148) feels that ignoring anharmonic bending forces is "80% valid." Scheringer(151) finds that the riding model(137) underestimates the spectroscopically calculated amplitudes by .004 to .011 Å, but that ignoring the intramolecular response to a vibration entirely ("uncorrelated atoms") yields amplitudes that are far too large. A "damped" riding model might be useful, but the damping factor parameters cannot be refined from Bragg scattering. The riding model is the best alternative.

The various parameters could be refined sequentially, as in TREFOIL, or simultaneously, as shown by Rae for the 2X2 case(152). The refinement should be started with a fairly good (as judged by R-factor) model. An initial guess for internal mode amplitudes is that they are all zero. The PAS of translation and libration could start out as the unit-cell-fixed frame. The P matrix of the free atom model is a good starting guess. Ruysink and Vos(153) recommend assigning as much thermal motion as possible to the 6 external modes of the crystal. The bond-stretch amplitude should be refined last, since it is likely to be smallest, and make the least difference in the R-factor.

This chapter is not complete or detailed enough of information to

write a computer program implementing this TLSI model. The chapter is only a suggestion - a very detailed suggestion - for future work.

Chapter VII. Computational Considerations

The Lowdin orthonormalization procedure(154) takes an arbitrary basis g' and converts it to an orthonormal set g. This is very convenient, because the P matrix must refer to an orthonormal set, or else the requirements of idempotency, normalization, and Hermitivity take on a very complex form(103). This procedure is simple:

$$g_o = S^{-1/2} g' \tag{242}$$

The scattering tensor f^K is given by

$$f^K = S^{-1/2} |g'\rangle e^{iK\cdot r} \langle g'| S^{-1/2} \tag{243}$$

or alternatively one can use the non-orthonormal basis and use, not P, but instead

$$R = S^{-1/2} P S^{-1/2} \tag{244}$$

Either requires evaluation of $S^{-1/2}$. The overlap matrix has elements

$$S_{\mu\nu} = \langle g_\mu | g_\nu \rangle \tag{245}$$

which can be calculated in a Gaussian basis as the forward scattering matrix f(0 0 0) using the formulas of reference(78). The inverse square root of a matrix can be calculated from the matrix by the iterative procedure of Igolkin and Mestechkin(155). Start with a guess

at $S^{-1/2}$ given by

$$S^{-1/2}_{0} = \frac{1}{\sqrt{Dim(g)}} 1 \tag{246}$$

and iterate on the formula

$$(S^{-1/2})' = 3/2\ (S^{-1/2}) - 1/4\ ((S^{-1/2})S(S^{-1/2})^2 + (S^{-1/2})^2\ S(S^{-1/2})\ ) \tag{247}$$

until

$$\left(\sum_{\mu}\sum_{\nu}\left[(S^{-1/2})'_{\mu\nu} - (S^{-1/2})_{\mu\nu}\right]\right)^2 Tr\, S \text{ is sufficiently small.} \tag{248}$$

If the convergence criterion is about 10^{-20}, and Dim(g)=3, this takes about 10 iterations.

Reference has been made above to changing the local coordinate system so that P submatrices are equal. This requires rotating and translating the coordinates into a Principal Axis System. Rotation of coordinates is a bit tricky. It requires three parameters. One way of defining the rotation is by Euler angles(156), but this process has

problems with 180^{o} angles. Another way is described by Scheringer(157), and coded in PL/I in Appendix F, and this has problems at 90^{o}. The best thing to do is to use one method sometimes, and another at other times, depending on the rotation angles involved. The ab initio program GAUSSIAN-80 uses only Euler angles, and when an angle being optimized hits 180^{o}, the program crashes. Any rotation method has a singularity somewhere, so at least two must be used.

In a cubic crystal, the crystal coordinate system is Cartesian. All 3 axes are of equal length, and 90^{o} apart. The other six Bravais lattices require a metric tensor to convert to a Cartesian system. Alternatively, one can use fractional coordinates x. The same considerations apply to the reciprocal lattice. Pawley(122) gives a conversion procedure, and propagandizes in favor of a Cartesian system.

From a computational viewpoint, the problem of this thesis is: Given some highly non-linear functional $\epsilon[p]$, and some equality and inequality constraints

$$\Xi_{eq}(\rho) = 0 \quad ; \quad \Xi_{in}(\rho) \geq 0 \tag{249}$$

minimize ϵ subject to Ξ.

Non-linear optimization theory(158) is a rapidly expanding field of applied mathematics concerned with exactly this problem - to minimize a functional, with or without some constraints. Methods for non-linear optimization fall into three categories: Newton-Raphson methods, where

second derivatives are used; quasi-Newton methods, where first derivatives are used, and direct search methods, where no derivatives are used.

Derivatives can be calculated in two different ways. In some cases, $\nabla\epsilon$ can be derived analytically from ϵ. In almost all cases, $\nabla\epsilon$ can be approximated numerically as the finite difference

$$\frac{\partial\epsilon}{\partial p_i} \sim \frac{\epsilon[p+\Delta p_i] - \epsilon[p]}{\Delta p_i} \tag{250}$$

It is recommended that if the parameter vector p is defined to an accuracy of η digits,

$$\frac{\Delta p_i}{p_i} = 10^{-\frac{1}{2}\eta} \tag{251}$$

For example, if p is defined as DECIMAL FLOAT(12), then

$$\frac{\Delta p_i}{p_i} = 10^{-6} \tag{252}$$

Numerical derivatives are less accurate than analytic derivatives. If a number z is accurate to $\pm\sigma$, then a rough estimate is that ∂z is good to $\pm\sigma$, and Δz to $\pm 10\sigma$.

What is desired is a global minimum in ϵ. However, no method of non-linear optimization can guarantee that. Only local minima can be found. A local minimum is defined(159) in Newton-Raphson methods as

$$\nabla \epsilon = 0 \tag{253}$$

$$\nabla^2 \epsilon > 0 \tag{254}$$

In quasi-Newton methods, equation (253) is satisfied, and an approximation to equation (254) is sometimes used. For direct searches, one aims for convergence (p' = p), rather than testing for (253) or (254). The program EXAMPLE of chapter 5 eventually gives up when it can't lower ϵ to ϵ_{goal} in 3000 iterations. The program TREFOIL for chapter 3 never gives up; one controls it by only giving it a finite amount of computer time. TREFOIL, which uses a direct-search method, seems quite susceptible to local "false" minima(160).

The only way to feel confident that a global minimum may have been found is to start with several initial guesses widely separated in parameter space, and if all converge to the same place, it's probably the global minimum. If not, choose the lowest local minimum, and maybe try some more initial guesses.

Direct search methods work by controlled trial and error. One varies the parameter vector p a distance Λ in direction s, to lead to

$$p' = p + d = p + \Lambda s \tag{255}$$

If $\epsilon[p']$ is less than $\epsilon[p]$, the step is accepted, and if not, rejected. After that, a step in some other direction is tried. The various methods differ in the ways in which they determine Λ and s. Some take steps along each parameter in turn. The program TREFOIL does this, and when no step along any direction is accepted, TREFOIL divides Λ by 10. In other methods, steps are taken along certain preferred directions, say along eigenvectors of the covariance matrix(161), or in directions that had been most successful previously and orthogonal to that.

Quasi-Newton and Newton-Raphson methods update the parameter vector by a change d given by

$$p' = p + d = p + \Lambda H G \tag{256}$$

where

$$G = \nabla\epsilon = \frac{\partial \epsilon}{\partial p} \tag{257}$$

and H is related to, or an approximation of, the inverse Hessian matrix. For a recent article, which reviews many of the quasi-Newton methods, see reference(162). An excellent textbook is Bazaraa and Shetty(159).

The method of steepest descents is defined by equation (256) and

$$H = 1 \tag{258}$$

Although this method works, it is slow. The problem is that it is far too sensitive to local changes in slope, and the Markov chain of the steepest descent path usually zigzags toward the solution, rather than following a smooth or regular trajectory. Minimization methods need not throw out all memory of previous iterations. The path so far can give clues as to which direction s to update in. The various quasi-Newton methods fold in information about previous function and gradient values to the H matrix, and the steepest-descent path G is deflected in a plausible direction. The best H seems to be that of Broyden, Fletcher, Goldfarb, and Shanno (BFGS or BFS)(163).

The steplength Λ is determined in one of several ways. The "acceptable-point" method tries $\Lambda=1$, and if this leads to lower ϵ, the move is accepted, and if not, $\Lambda=1/2$, then 1/4, etc. are tried. The cubic interpolation of Davidon(164) finds a nearly optimal Λ, but takes so much extra computer time to do so that the acceptable-point method is often preferred. The program TREFOIL uses the method of Davies, Swann, and Campey(165). It steps some predetermined Λ, and if this lowers ϵ, another 2Λ, and then maybe 4Λ, and so on until the step is unsuccessful. ϵ is then evaluated at a point midway between the two most recent steps, and quadratic interpolation is performed. Several other variants are known.

Due to the peculiar nature of the idempotency constraint, only one method of imposing the constraints of idempotency, normalization, Hermitivity, symmetry, and positivity of the vibrational cumulant expansion will be mentioned here. Normalization and Hermitivity are imposed by the method in which dependent $P_{\mu\nu}$ are calculated; symmetry by construction also; I don't know about positivity of U. The idempotency cannot be imposed by Lagrangian multipliers nor by any other one-step method. A two-step tangential approach(166,167) is required.

$$\text{STEP 1: } p'' = p + \Lambda H G \tag{259}$$

$$\text{STEP 2: } p' = \widehat{\text{constraints}}(p''); \text{ evaluate } \epsilon[p''] \tag{260}$$

Many of the programs and subroutines mentioned in this thesis are coded in PL/I in the Appendices. As yet, no quasi-Newton programs for quantum crystallography have had fast enough computation times to be useful - this is likely to be due to programming errors, and not inherent defects in the methods. Also, quasi-Newton methods and least-absolute-values error measures are incompatible(164) due to a singularity in the gradient at convergence. Most quasi-Newton methods assume the existence of $\epsilon'''[p]$; the singularity at $\epsilon'''[p_{optimal}]$ means, by definition, that least-absolute-value measures are not well-behaved in an optimization theory sense.

All parameters should be refined simultaneously. Just because a free-atom refinement comes up with certain positions and thermal parameters, this doesn't mean that a quantum (or even a non-quantum) refinement should keep v fixed while refining electronic parameters. This fixing of v is commonly done, either due to computer time limitations, or because of fear that certain elements of J, especially those connecting dipoles with position, and monopoles and quadrupoles with vibration, will be enormous (>95%) and then the parameters aren't independent; the problem has become overparametrized. However, the electronic and non-electronic parameters have quite a different dependence on K, and this hopefully will alleviate the correlations if a sufficient number of reflections are measured(133). A commonly used technique is called the "X minus X-high" refinement(81), where some "cutoff" is taken, usually .65 $\mathring{A}^{-1}$, and the $F_{obs}(K)$ are divided into "high-angle" and "low-angle" scattering factors by

$$K_{low} < .65\mathring{A}^{-1} < K_{high} \tag{261}$$

High angle reflections are used to refine v with free atoms, and then low angles are used to fix P. This procedure has a few problems. First, there is no justification for throwing out perfectly good data for some parameters, and pretending that J has no elements between v and P. By definition, it will find a false minimum which may or may not be close(81) to the true minimum. All data should be used to fix

each parameter, and if a certain datum has no effect on a parameter, it won't affect the refinement. Second, X-X-high arbitrarily refines first v, then P, in effect pretending that the X-high experiment is infinitely more important than X-low. Third, Price et al.(38) find that "residual two-centre scattering, i.e. that which is not accounted for accurately by one-centre terms, is a high-Bragg angle phenomenon." In other words, cross-terms in P show up mainly above the cutoff, where a free-atom model is being used.

Another questionable refinement technique is the "X minus N"(168) method. Here, neutron scattering is used to find v, which is then held fixed while x-rays are used to refine P. This assumes that neutron data is infinitely better than x-ray data. Contrast this with the laudable "X plus N" method(5) where one refines both data sets with the same model, with an overall weighting ratio w_X/w_N based on experimental considerations, internal consistency of each data set, etc.

A measure of internal consistency is needed. One is the comparison of experimental numbers which ought to be equal, say F(K) and F(-K) in a centrosymmetric crystal. This is not entirely satisfactory, since the absorption in an odd-shaped specimen is not centrosymmetric. A very nice measure is the internal R-factor, which is an R-factor where

$$F_{cal}(K) = F_{obs}(K) + \sigma F_{obs}(K) \qquad (262)$$

Despite Scherinmger's caveat(151) that mixing data sets of different quality "has a disastrous effect" on refinements, one should follow Hirshfeld(133) and use all reflections for refining all parameters. Preferably, reflections will be measured out as far as possible. No data should be thrown out, even if the measured intensity is negative(169). Oldfield(104) has shown the remarkable insensitivity of P to random error in measured Bragg intensities. Arnberg et al(97) refined the structure of $C_{30}H_{18}O_2$ until it "converged to acceptable coordinate values" based solely on data with $\sigma(I)/I > 0.30$. They conclude(97) that "no set of reflections should therefore be excluded from a least-squares refinement on the pretext of having too large $\sigma(I)/I$ values."

Error bars and covariance matrices are a necessary part of any interpretation of experimental data(170), which data always have error bars of their own. The propagation of errors from data to parametrization proceeds as follows.

Define G_μ^K as the gradient of one $F_{cal}(K)$ with respect to a parameter p_μ.

$$G_\mu^K = \frac{\partial F_{cal}(K)}{\partial p_\mu} \tag{263}$$

E is a square matrix Dim(p) by Dim(p) with elements

$$E_{\mu\nu} = \sum_K G_\mu^K G_\nu^K \sigma(F_{obs}(K)) \tag{264}$$

Then the error bars $\sigma(p)$ and covariance matrix J are, for ϵ_3',

$$\sigma(p_\mu) = \sqrt{\frac{1}{\Phi}(E^{-1})_{\mu\mu}\,\epsilon} \tag{265}$$

$$J_{\mu\nu} = (E^{-1})_{\mu\nu} \Big/ \sqrt{(E^{-1})_{\mu\mu}(E^{-1})_{\nu\nu}} \tag{266}$$

where E^{-1} is the inverse of E. The goodness of fit is

$$\mathrm{GOF} = \sqrt{\epsilon / \Phi} \tag{267}$$

where

$$\Phi = \mathrm{Dim(F)} - \mathrm{Dim(p)} \tag{268}$$

A GOF of 1.00 is as good as the data itself. Any method which gets a GOF<1 with "chemistry quality" data is unlikely. The goodness of fit will get worse as the model becomes overparametrized. GOF is what really should be minimized in a totally empirical wavefunction; the dependence on Φ, the number of observations minus the number of parameters, should be kept in mind. Be sure that each extra parameter is justified. A good discussion of statistical sloppiness is Lonsdale's article(171).

Some directions for future work have been suggested above. The application of the fitting procedure in cases of more than one orbital of the same symmetry is still not fully delineated. Although beryllium metal has been modeled, no semiconductors or insulators have had their x-ray diffraction data fit by totally empirical wavefunctions. Possibilities are graphite; the series diamond,silicon, germanium, and α-tin; and the organic crystal oxalic acid dihydrate. Whether it is more efficient to use McWeeny's or Mestechkin's purification method is still an open question. The Wannier formalism has not been applied to any real 3-dimensional crystals. The vibrational TLSI formalism of Chapter VI is totally lacking in computational considerations. The thesis does provide a fairly complete framework for these investigations, however.

VIII. Conclusions

Molecular systems can best be modeled by a quantum mechanical wavefunction. It is possible to obtain a wavefunction purely from experimental data, without recourse to energy evaluations, by imposing quantum constraints on the interpretation of one or more experiments. This totally empirical wavefunction formalism is applicable to insulators, semiconductors, and metals.

Information from many different kinds of experiment can simultaneously be fit by a totally empirical wavefunction. In this thesis, attention has been focussed on Bragg scattering. Two-state experiments; i.e. absorption or emission spectroscopy, have not been treated in this thesis; the formalism is thus restricted as of now to resonance and scattering experiments. Only two types of measurement provide a large enough sample of unambiguous data for use as the only experiment to be fit. The fundamental object to be modeled, according to the Hohenberg-Kohn theorem(10), is the electron density. Bragg scattering measures the real space electron density $\rho(r)$; Compton scattering and positron annihilation measure the momentum space density $\rho(k)$. The scope of coherent scattering measurements is certainly sufficient for determining a totally empirical wavefunction. Magnetic resonance, inelastic scattering, and the like do not of themselves measure the electron density unambiguously at all points in space; although useful in conjunction with Bragg diffraction, they are not

sufficient in themselves. Neutron scattering cannot see paired spins. Compton scattering and positron annihilation have not been dealt with in this thesis simply because my predecessors(13,103,104) have concentrated on Bragg scattering.

The totally empirical wavefunction must be determined from the data using some fitting procedure. The iterative equation method of Clinton et al.(13), using the unweighted least-absolute-value error measure ϵ_1, has been the only fitting procedure used until now. Table 3 and equations (67) to (69) detail the extension of Clinton's algorithm to all 8 crystallographic error measures: weighted or unweighted; amplitude-based or intensity-based; least-absolute-value or least-squares. The measure most faithful to a properly designed experiment is the unweighted intensity-based least-squares measure ϵ_4. The "best" electron density is given by ϵ_3 or ϵ_3'. Due to the nature of the idempotency constraint, a one-step minimization method must treat idempotency as a quality to be maximized, and smallness of the error as an auxiliary constraint. A two-step method has been devised, which alternates between unconstrained optimization of ϵ and satisfaction of the quantum constraints. Although this method is related to generalized reduced gradient techniques found in the literature(71,166,167), its use in quantum crystallography is new. The advantages of this two-step method over the iterative equations (67) are:

1. any parameter, not just P matrix elements, can be optimized.

2. the number of independent fitting parameters is explicitly shown, as opposed to the old method which updated the entire P matrix as a unit regardless of how many $P_{\mu\nu}$ were entirely determined by the constraints and the other P elements.
3. error bars and a covariance matrix can easily be obtained for the parameter values.
4. far less computer time is needed than for the iterative equation method.
5. any unconstrained optimization method in the computer science literature can be used without major modifications, if the (ill-behaved) least-absolute-value error measures are avoided.

The totally empirical wavefunction model has been extended to include three effects not found in the case of isolated gas-phase atoms. First, the requirements for describing a bond or antibond between two atoms have been discussed, and in the case of Model 6 for graphite, an explicitly molecular wavefunction model including intercell and intracell bonds has been delineated. The dangers of a "two-center" approximation, in which some P matrix elements, assumed on the basis of chemical intuition to be zero, have been described. A distinction has been drawn between bonding and antibonding terms in the P matrix.

Second, in Chapter V, solid-state effects on the orbital basis have been explicitly described by means of a Wannier formalism. Associated with each cell is a damped wave of isolated-atom basis functions

extending out into neighboring unit cells. Although the details of the damping depend on the Compton profile of the orbitals being modeled, an approximate treatment of the band structure leads to a simple and computationally tractable model, equations (191) to (199), for the "Wannier-izing" of the basis.

Finally, a TLSI (Translation, Libration, Screw rotation, and Internal vibration) model for thermal and zero-point nuclear motions has been outlined. The TLSI model combines the 21-parameter TLS model of Schomaker and Trueblood(128) with a 3A-6 - parameter spectroscopic-like model of internal motions in a curvilinear(130) Simons'-coordinate(134) local-mode(110) description.

For the first time, the totally empirical wavefunction model has been applied to actual experimental data - the beryllium metal Bragg data of Larsen and Hansen(56). Several approximations were made. The data was assumed free of errors due to absorption, extinction, etc., and only an overall scale factor was optimized. The quantum wavefunction was restricted to a frozen core plus a single determinant of spin-paired orbitals with real coefficients. The core was taken from the atomic calculation of Huzinaga(80). The valence orbital was modeled in a basis of only 2 functions: the atomic(80) 2s orbital and a set of 12 Floating Spherical Gaussian Orbitals. The effects of crystal formation were approximated by a sum of overlapping perturbed atoms. The nuclear motion was assumed rigidly coupled to the electron density of each atom, and totally independent of the motion of all other

atoms. A vibrational cumulant expansion truncated at third cumulants was used. Thus, the electronic problem was reduced to the modeling of a single electron, using 5 parameters; the nuclear problem to a single nucleus modeled with 3 parameters; the experimental problem reduced to a single parameter. Two of the electronic parameters and one of the vibrational parameters were dropped from the refinement. the resultant quantum wavefunction is shown in Table 11. An excellent fit, with conventional R-factor .00249, was obtained. For comparison, a Varghese-Mason multipole model,model 4, was refined in the same basis. The fit to experiment was even better - R_1 was .00237. The two models were compared. The non-quantum model does not lend itself as readily to the interpretation or prediction of other phenomena or experiments. As shown in Figure 13 , the quantum model suggests a trigonal bipyramidal 5-center bonding unit, and the non-quantum model a tetrahedral 4-center interaction.

Appendix A - Notation

SYMBOL	MEANING	EQUATION
A	number of nuclei	
C	wavefunction coefficient	34
	vibrational third cumulant	Figure 10
D	$\partial \epsilon / \partial \rho$	Table 3
E	Error Matrix	257
F	Scattering Amplitude	5, 175
G	Gradient Vector	68, 250
H	inverse Hessian Matrix	249
I	Scattering Intensity	175
J	Covariance Matrix	266
K	Reciprocal Lattice Vector	
L	A Lattice Site	166
M	Multipole Basis Function	16
N	Number of Electrons	23
	Normalizer	145
O	Operator Matrix for a Property	1
P	Density Matrix	38
Q	Symmetry Operation	
R	Error Measure	Table 3
	Scattering Weight Matrix	123
S	Overlap Matrix	121
	Experimental Scale Factor	Figure 20
T	Reduction Factor	70
	Temperature	213

U	Vibrational Tensor	125
V	Potential Function	201
W	Weight of a Multipole Function	21
	Wannier Function	181
	Vibrational Weighting	210
Y	Mestechkin Residual	45
Z	Robust/Resistant Functional	62
$\mathcal{A}$	Number of Nuclei in a Crystal	
$\mathcal{A}$	Antisymmetrizer	
$\mathcal{S}$	Wannier Overlap Matrix	187
a	Exponent, Usually Gaussian	17
c	Contraction Coefficient	106
d	Change in Parameters	90
e	exp(1) = 2.718...	
f	Scattering Tensor	4
g	Basis Function	17
i	$\sqrt{-1}$	
k	Reciprocal Space Wavevector	
	in the Brillouin Zone	165
	Boltzmann's Constant	213
l	Lattice Site	170
m	Number of Basis Functions	
n	Fractional Occupancy of a Band	176
o	Orthonormal	235
	Observed	Table 3
p	Parameter Vector	83

q	Vibrational Excursion Coordinate	
r	distance	
s	Direction for Changing p	248
u	Periodic Function	165
v	Variables Unrelated to P	83
w	Weight of an Observation	
f	Wannier Scattering Tensor	190
1	Unit Matrix	
'	Next Iterate	
•	Dot Product	
$<\|$	Dirac Bra	1
Γ	1-Body Density Matrix	38
	Irreducible Representation	109
	Center of Brillouin Zone	
Δ	Change	
∇	Gradient	
Λ	Steplength	248
Ξ	Constraint Function	242
Π	Product	
Σ	Sum	
Ψ	Many-Body Wavefunction	33
Φ	Degrees of Statistical Freedom	268

Ω	Probability of an Instantaneous Excursion	212
α	Spin-Up	
β	Spin-Down	
γ	A Fitting Parameter Related to Spectroscopy	213
δ	Kronecker Delta	
	Variation	219
∂	Partial Derivative	
ϵ	Error Functional	60
ξ	Exponent Scaling	126
η	Number of Significant Figures	244
θ	Angle	
$\varkappa$	Vibrational Force Constant	201
λ	Lagrange Multiplier	69
μ	General Matrix	Page 28
ν	Vibrational Frequency	220
π	3.14159...	
ρ	Physically Meaningful Density	12
σ	Error Bar	265
υ	Boson Nuclear Wavefunction	206
ϕ	Dihedral Angle	
χ	Weight of 1 Determinant	33
ψ	Orbital	13
ω	Wannier Phasing	190

The PL/I Program TREFOIL

```
1.      //MJGPCNEG JOB MJCPC500,TIME=1,50),REGION=4PCK
2.      //  EXEC  PLIXCG
3.      //*MAIN LINES=20
4.      //PLI.SYSIN  DD  *
1000.    TREFOIL:PROCEDURE OPTIONS(MAIN);
1001.    /*CODED BY MARTIN GOLDBERG IN MAY THROUGH DECEMBER 1983 */
1010.      /*THIS FOURTH-TRY PROGRAM FITS FINN LARSEN'S DATA
1020.          TO A GAUSSIAN WAVEFN IN A SMALL BASIS,WITH THE
1030.          SCATTERING FROM ONE CENTER BEING DESCRIBED BY
1040.          BASISFNS CENTERED ON THE BE ATOM OF INTEREST
1050.          AND TWELVE FSGO'S FLOATING NEARBY IN D3H SYMMETRY.THE CORE IS
1060.         FIXED TO ITS ATOMIC VALUE, FROM HUZINAGA'S TABLE
1070.          14 IN JCP VOL.42,(1965)P.1293    */
1080.
1090.     DCL EPSWAY DECIMAL FIXED(2) ;DCL RMAT(3,3) FLOAT(12);
1100.    DCL FTABLE(C:58,4,4)
1110.      COMPLEX FLOAT(12);DCL (EPSLAST,EPSCY,DUN) FLOAT(12);
1115.    DCL(FC(58),PATTERN(3),TRIAL(20),ZETY(25,2),EPSY,PY(3,3))FLOAT(12);
1120.    DCL(ZETAS(25,2),HKLAL(C:58,3),CENTER(3),VARY(20),SCALE,P(3,3),
1130.      SINV2(3,3),FLO1(12,3),FLO2(12,3),FCAL(58),EPS)FLOAT(12);
1133.       DCL VIB(58,2) COMPLEX FLOAT(12);
1135.       EPSWAY= 4;
1136.       DCL FOBS(58) FLOAT(12)  INIT(3.348,2.216,1.212,.590,1.839,
1135.2   2.815,1.473,2.151,.995,1.307,.551,.68,.273,1.188,2.CC7,1.C44,
1136.4   1.55,.727,.977,.418,.524,1.408,1.251,.902,.549,.364,.623,.234,
1136.6   .513,.247,2.068,2.335,1.6C6,.919,.463,.863,1.449,.762,1.142,.541,
1136.8   .741,.327,.416,.484,.811,.436,.657,.321,.449,.488,.443,1.056,.948,
1137.    .599,.286,.481,.260,.402          );
1137.2     DCL ERROBS(58)  FLOAT(12) INIT (29,19,3,3,16,24,13,19,8,3,1,2,
1137.4   1,10,17,9,4,2,2,1,1,3,3,2,1,2,2,1,1,1,23,20,3,2,2,2,3,1,2,2,2,
1137.6     1,1,1,2,1,1,1,1,1,1,2,2,2,2,1,1,1,1     );
1137.8   IF EPSWAY>4 THEN ERROBS=2*FOBS*ERROBS;
1138.    DCL (NCUT,NPARM)DECIMAL FIXED(2);NCUT=58;NPARM=11;
1140.       ERROBS=.001*ERROBS;ERROBS=1./(ERROBS*ERROBS);EPSLAST=1.E6;
1145.    IF ((EPSWAY=2)|(EPSWAY=4)|(EPSWAY=6)|(EPSWAY=8)) THEN ERROBS=.1;
1150.    DCL (IT,FL) DECIMAL FIXED(2), CYCLE DECIMAL FIXED(6) INIT(0);
1151.    DCL (A,I,J,K,#PARM,#PIJ) DECIMAL FIXED(2);
1152.    EPS,EPSY,EPSCY,EPSLAST=1.E10;
1153.    /* #PARM IS THE NUMBER OF PARAMETERS.  #PIJ DETERMINES THE REFINEMENT
1154.     TECHNIQUE.  0 IS THE FREE ATOM,1 AND 2 ARE THE NUMBER OF QUANTUM
1154.1   FSGO.  -1 AND -2 ARE THE NUMBER OF NON-QUANTUM FSGO.
1154.3    IF STATS_NOW = 0 , NO ERROR BARS ARE CALCULATED.       */
1155.    DCL STATS_NOW DECIMAL FIXED(1);STATS_NOW=2;#PIJ=-2;
1157.    DCL STEP(20)FLOAT(12) INIT(.005,.005,.005,.1,10,10,.1,.1,10,10,.01,
1158.       .CCCC1,.CCCC1,.CCCC1,.C001,.01,.01,0,0,0);STEP=STEP/10;
1160.    /* FTABLE IS THE TABLE OF FOURIER TRANSFORMS OF BASIS
1170.       FUNCTIONS.
1200.           ZETAS
1210.       IS THE LIST OF GAUSSIAN EXPONENTS AND THEIR CONTRACTION
1220.       COEFFICIENTS.  HKLAL IS THE LIST OF BRAGG VECTORS IN
1230.       ORTHOGONAL ATOMIC UNITS.  CENTER IS (1/3,2/3,1/4) IN
1240.       ORTHOGONAL ATOMIC UNITS.
1250.       VARY IS THE GUESS VECTOR. ***************************
1250.1        1 - 2-S COEFFICIENT IN PSI
1250.2          2-  FLO1      "       "   "
1250.3          3-  FLO2      "       "   "
1250.4          4-  R_FLO1
1250.5          5-  THETA_FLO1
1250.6          6-  PHI_FLO1
1250.7          7-  ALPHA_FLO1
1250.8          8-  R_FLO2
1250.9          9-  THETA_FLO2
1251.          10-  PHI_FLO2
1251.1         11-  ALPHA_FLO2
1251.2         12-  THIRD CUMULANT,EDGEWORTH CONVENTION(NOT GRAM-CHARLIER)
1251.3         13-  U_11  (NEUTRON VALUE .02132(11) )
1251.4         14-  U_33  (NEUTRON VALUE .01929(11) )
1251.5         15-  FCAL SCALE FACTOR (GAMMA-RAY VALUE 1.00(.01)  )
1251.6         16-  1-S EXPONENT SCALING (AB INIT VALUE 1  )
1251.7         17-  2-S EXPONENT SCALING ("   "      "   1  )
1251.8         18-  NOT USED
1251.9         19-  NOT USED
1252.          20-  NOT USED
1260.       P IS THE DENSITY MATRIX REPRESENTATIVE. FLO 1 AND 2 IS
1270.       THE LIST OF FSGO POSITIONS.
1280.       VIB IS THE LIST OF THERMAL SMEARINGS. SCALE IS THE
1290.       SCALE FACTOR, WHICH WAS SUPPOSED 1 .00 BY LARSEN.
1300.       FCAL ARE THE CALCULATED SCATTERING AMPLITUDES. FOBS
1310.       ARE LARSEN'S SCATTERING AMPLITUDES, FROM
1320.       HIS MANUSCRIPT.  ERROBS ARE THE ERRORS IN HIS
1330.       MEASUREMENTS.    CYCLE
1340.       IS HOW MANY ITERATIONS SO FAR */
1350.
```

```
1355.       ON UNDERFLOW ;
1360.       CALL STARTUP(ZETAS,HKLAU,CENTER);
1362.       DCL ZETAL(25,2)FLOAT(12);ZETAL=ZETAS;
1365.        PUT SKIP;
1370.        CALL INITGUESS(VARY,P);
1371.
1375.       CALL VIBFIX(VARY,HKLAU,VIB);
1377.       PUT SKIP LIST(VARY(13),VARY(14));
1380.       INWARDS: /* START NEXT ITERATION */
1385.       CALL FIXUP(#PIJ,P,3,1,VARY,ZETAS,ZETAL);
1390.       PATTERN(2)=VARY(5);PATTERN(1)=VARY(4);PATTERN(3)=VARY(6);
1395.       CALL LPOS(PATTERN,FLO1);PATTERN(1)=VARY(8);PATTERN(2)=VARY(9);
1397.       PATTERN(3)=VARY(10);CALL LPOS(PATTERN,FLO2);
1400.        CALL VIBFIX(VARY,HKLAU,VIB);
1410.       CALL CALCINTS(#PIJ,FTABLE,FLO1,FLO2,HKLAU,ZETAS,SINV2,FL);
1411.       IF SINV2(1,1)<9000.  THEN GO TO SAFE;
1411.5      ELSE DO;VARY(7)=VARY(7)*.1;VARY(11)=VARY(11)*.1;
1411.6       GO TO INWARDS;END;
1412.
1413.
1414.       SAFE:FL=0;
1415.
1420.       CALL CALCF(#PIJ,P,FTABLE,SINV2,VIB,VARY,CENTER,HKLAU,FCAL);
1421.       CALL FIXEPS(FOBS,ERROBS,FCAL,EPSWAY,EPS,RFAC);EPSCY=EPS;
1421.1      CALL MATMULT(P,SINV2,3,PY);CALL MATMULT(SINV2,PY,3,RMAT);
1421.2       PUT SKIP DATA(RMAT);
1422.       DO I=1 TO 58;PUT SKIP LIST(I,FCAL(I),ABS(FCAL(I))-FOBS(I));
1422.3      END;
1422.5
1423.5      PUT SKIP DATA(CYCLE,EPS,RFAC,VARY,SINV2,P);
1425.        RFAC=0;SELECT(EPSWAY);
1430.        WHEN(1)DO; DO I=1 TO 58;RFAC=RFAC+ERROBS(I)*FOBS(I);END;
1431.                   RFAC=ABS(EPS/RFAC);END;
1435.        WHEN(2)DO; DO I=1 TO 58;RFAC=RFAC+FOBS(I);END;
1436.                   RFAC=ABS(EPS/RFAC);END;
1440.        WHEN(3)DO; DO I=1 TO 58;RFAC=RFAC+ERROBS(I)*FOBS(I)**2;END;
1441.                   RFAC=SQRT(EPS/RFAC);END;
1445.        WHEN(4)DO; DO I=1 TO 58;RFAC=RFAC+FOBS(I)*FOBS(I);END;
1446.                   RFAC=SQRT(EPS/RFAC);END;
1450.        WHEN(5)DO; DO I=1 TO 58;RFAC=RFAC+ERROBS(I)*FOBS(I)**2;END;
1451.                   RFAC=SQRT(EPS/RFAC);END;
1455.        WHEN(6)DO; DO I=1 TO 58;RFAC=RFAC+FOBS(I)*FOBS(I);END;
1456.                   RFAC=SQRT(EPS/RFAC);END;
1460.        WHEN(7)DO; DO I=1 TO 58;RFAC=RFAC+ERROBS(I)*FOBS(I)**4;END;
1461.                   RFAC=SQRT(SQRT(EPS/RFAC));END;
1465.        WHEN(1)DO; DO I=1 TO 58;RFAC=RFAC+FOBS(I)**4;END;
1466.                   RFAC=SQRT(SQRT(EPS/RFAC));END;
1470.        OTHERWISE RFAC=1.00/0.00; END;
1475.
2050.       PUT SKIP LIST(EPSWAY,'TYPE R= ',RFAC);PUT SKIP;
2060.       ONWARDS:ZETY=ZETAS;DO I=2,3,12,13,14,15;
2090.       UNIVAR:/*DAVIES,SWANN,AND CAMPEY ALGORITHM*/
2092.       DCL S DECIMAL FIXED(1);
2094.       DCL (X(3),Y(3),N) FLOAT(12);
2096.       S=1;N=1.;TRIAL=VARY;Y(1)=EPS;X(1)=TRIAL(I);
2098.       TRY: TRIAL(I)= TRIAL(I) + STEP(I)*N;
2102.        CALL FIXUP(#PIJ,PY,3,1,TRIAL,ZETY,ZETAL);
2104.       IF ((I>3)&(I<11)) THEN DO;
2104.5      PATTERN(2)=TRIAL(5);PATTERN(1)=TRIAL(4);PATTERN(3)=TRIAL(6);
2104.6       CALL LPOS(PATTERN,FLO1);
2104.8      PATTERN(1)=TRIAL(8);PATTERN(2)=TRIAL(9);PATTERN(3)=TRIAL(10);
2105.1      CALL LPOS(PATTERN,FLO2); END;
2106.       IF ((I=12)|(I=13)|(I=14)) THEN CALL VIBFIX(TRIAL,HKLAU,VIB);
2108.       IF ((I>3)&(I<12))|(I>15)) THEN
2110.        CALL CALCINTS(#PIJ,FTABLE,FLO1,FLO2,HKLAU,ZETY,SINV2,FL);
2114.       CALL CALCF(#PIJ,PY,FTABLE,SINV2,VIB,TRIAL,CENTER,HKLAU,FCAL);
2116.       CALL FIXEPS(FOBS,ERROBS,FCAL,EPSWAY,EPSY,RFAC);
2118.       PUT SKIP DATA(TRIAL(I));PUT LIST(EPSY);
2120.       IF((EPSY>EPS)&(S=1)&(N>0.)) THEN DO;
2122.       N=-1.5;GO TO TRY;END;
2124.       IF((EPSY>EPS)&(S=1)&(N<0.)) THEN GO TO NEXTI;
2126.       IF S=1 THEN DO;
2128.        S=2;N=N*2.;EPS,Y(2)=EPSY;X(2)=TRIAL(I);GO TO TRY;END;
2130.       IF S=2 THEN DO;
2132.        X(3)=TRIAL(I);Y(3)=EPSY;
2134.        IF EPSY<EPS THEN DO;
2136.         S=3;N=N*2.;END;ELSE DO;S=5;N=-N*.5;END;
2138.        GO TO TRY;END;
2140.       IF S=3 THEN DO;
2141.       IF((Y(1)<Y(2)))THEN DO;EPSY=1.E9;GO TO DSC;END;
2142.        X(1)=X(2);X(2)=X(3);X(3)=TRIAL(I);
2144.        Y(1)=Y(2);Y(2)=Y(3);Y(3)=EPSY;
2146.        IF EPSY<EPS THEN DO;EPS=EPSY;N=N*2.;END;ELSE DO;S=5;N=-N*.5;END;
2148.        GO TO TRY;END;
2150.       IF S=6 THEN GO TO DSC;
2152.       /*S=5.  EITHER Y(2) OR EPSY IS SMALLEST.THROW OUT ONE ENDPOINT
2154.         AND INTERPOLATE.  */
2156.       IF Y(2)<EPSY THEN DO;Y(3)=EPSY;X(3)=TRIAL(I);END;
2158.        ELSE DO; X(1)=X(2);X(2)=Y(2);X(3)=TRIAL(I);Y(3)=EPSY;END;
```

```
2150.       X=6;TRIAL(I)=X(3) + .5*(X(2)-X(2))*(Y(1)-Y(3))/
2152.        (Y(1)-2*Y(2)+Y(3));
2163.        GO TO TRY;
2164.       DOC: IF ((EPSY<Y(2))&(EPSY<Y(1))&(EPSY<Y(3))) THEN DO;
2165.         VARY(I)=TRIAL(I);EPS=EPSY;ZETAS=ZETY;P=PY;GO TO NEXTI;END;
2168.         ELSE DO;
2170.          IF((Y(2)<Y(1))&(Y(2)<Y(3))) THEN DO;VARY(I)=X(2);EPS=Y(2);END;ELSE
2170.5      IF(Y(1)<Y(3)) THEN DO;VARY(I)=X(1);EPS=Y(1);END;ELSE DO;
2171.         VARY(I)=X(3);EPS=Y(3);END;
2172.         CALL FIXUP(#PIJ,PY,3,I,TRIAL,ZETY,ZETAL);
2172.2      IF ((I>3)&(I<11)) THEN DO;
2172.4      PATTERN(2)=TRIAL(5);PATTERN(1)=TRIAL(4);PATTERN(3)=TRIAL(6);
2172.6        CALL LPOS(PATTERN,FLO1);
2172.8      PATTERN(1)=TRIAL(8);PATTERN(2)=TRIAL(9);PATTERN(3)=TRIAL(10);
2173.       CALL LPOS(PATTERN,FLO2); END;
2173.2      IF ((I=12)|(I=13)|(I=14)) THEN CALL VIBFIX(TRIAL,HKLAU,VIB);
2173.4      IF ((I>3)&(I<12))|(I>15)) THEN
2173.6        CALL CALCINTS(#PIJ,FTABLE,FLO1,FLO2,HKLAU,ZETY,SINV2,FL);
2173.8      CALL CALCF(#PIJ,PY,FTABLE,SINV2,VIB,TRIAL,CENTER,HKLAU,FCAL);
2188.                 END;
2190.       NEXTI:END;IF EPS=EPSOY THEN STEP=STEP/10;EPSOY=EPS;
2192.       PUT SKIP DATA(STEP(4));
2300.        CYCLE=CYCLE+1;
2305.        IF STATS_NOW = 0. THEN GO TO INWARDS;
2600.        FULMAT: /*FULL-MATRIX LEAST-SQUARES A LA STOUT AND JENSEN */
2610.          DCL(FLO1Y(12,3),FLO2Y(12,3),V(17),EX(17),SIG(17))  FLOAT(12);
2515.          DCL VIBY(58,2) COMPLEX FLOAT(12);
2520.
2625.        DCL (A#(58,17),AIJ(17,17),FDEL(58),BIJ(17,17))  FLOAT(12);
2530.       A#=0;AIJ,BIJ=0;FDEL=0;ZETY=ZETAS;PY=P;VIBY=VIB;IT=0;    J=0;
2535.          #PARM=14;DO A=2,3,4,5,6,7,8,9,10,11,12,13,14,15;
2640.       J=J+1;I=A;
2645.       ZETY=ZETAS;PY=P;VIBY=VIB;
2550.       TRIAL=VARY;TRIAL(I)=VARY(I)*1.CCC01;
2655.        CALL FIXUP(#PIJ,PY,3,I,TRIAL,ZETY,ZETAL);
2655.2      IF ((I>3)&(I<11)) THEN DO;
2555.4      PATTERN(2)=TRIAL(5);PATTERN(1)=TRIAL(4);PATTERN(3)=TRIAL(6);
2555.6        CALL LPOS(PATTERN,FLO1Y);
2655.8      PATTERN(1)=TRIAL(8);PATTERN(2)=TRIAL(9);PATTERN(3)=TRIAL(10);
2556.       CALL LPOS(PATTERN,FLO2Y); END;
2656.2      IF ((I=12)|(I=13)|(I=14)) THEN CALL VIBFIX(TRIAL,HKLAU,VIBY);
2656.4      IF ((I>3)&(I<12))|(I>15)) THEN
2656.6        CALL CALCINTS(#PIJ,FTABLE,FLO1Y,FLO2Y,HKLAU,ZETY,SINV2,FL);
2556.8      CALL CALCF(#PIJ,PY,FTABLE,SINV2,VIBY,TRIAL,CENTER,HKLAU,FDEL);
2695.       DO K=1 TO 58;
2700.       A#(K,J)=(ABS(FCAL(K))-ABS(FDEL(K)))/.CCC01/VARY(I);
2705.       END;NEXT:END;IF IT=5 THEN GO TO INWARDS;ELSE PUT LIST('STATISTICS');
2710.       V=0.;AIJ=0.;
2715.        DO I=1 TO #PARM;DO K=1 TO 58;
2717.       /*THIS ONLY SET UP TO DO STATISTICS ON EPSWAY 3 OR 4 */
2720.       V(I)=V(I)-(FOBS(K)-ABS(FCAL(K)))*A#(K,I)*ERROBS(K);
2725.        DO J=1 TO #PARM;AIJ(I,J)=AIJ(I,J)+A#(K,I)*A#(K,J)*ERROBS(K);
2730.       END;END;END;
2735.       DCL NOPE DECIMAL FIXED(2) INIT(0);
2740.       CALL INVSYM(AIJ,#PARM,NOPE);
2745.       IF NOPE>0 THEN DO;PUT LIST('SINGULARITY');V=V/0.;END;
2750.       DO I=1 TO #PARM-1;DO J=I+1 TO #PARM;AIJ(J,I)=AIJ(I,J);END;END;
2755.       DO I=1 TO #PARM;SIG(I)=SQRT(ABS(AIJ(I,I))*EPS/(58-#PARM));END;
2760.       PUT SKIP DATA(SIG);
2765.       DO  I=1 TO #PARM;
2770.        DO J=1 TO #PARM;
2775.       IF ((AIJ(I,I)>0)&(AIJ(J,J)>0)) THEN
2780.        BIJ(I,J)=AIJ(I,J)/SQRT(AIJ(I,I)*AIJ(J,J));
2785.       PUT DATA(BIJ(I,J));
2790.       END;END;
2793.       /*THIS ONLY SET UP TO DO STATISTICS ON EPSWAY 3 OR 4 */
2795.       BIJ(2,3)=SQRT(EPS/(58-#PARM));PUT SKIP LIST('GOF=',BIJ(2,3));
2800.       CALL KET(AIJ,V,#PARM,EX);
2805.       PUT SKIP DATA(EX);
2810.
2815.       GO TO INWARDS;
2850.        /*   HOW TO RUN THE PROGRAM: TYPE
2860.            M 1,1135,1155,1158,2C6C,2635,1236C/12390
2870.            LINE 1 RENAMES THE RUN AND SETS THE TIME IN MINUTES
2880.            LINE 1135 SETS WHICH ERROR MEASURE TO USE,3 IS STANDARD.
2890.            LINE 1155 SETS WHETHER TO CALCULATE STATISTICS (NOT = 0)
2900.                      AND THE NUMBER OF ESGO
2910.            LINE 1158 SETS THE STEPLENGTH MULTIPLIER
2915.            LINE 2C6C LISTS ALL PARAMETERS TO BE OPTIMIZED
2917.            LINE 2635 CONTROLS WHICH PARAMETERS ARE UNCERTAIN
2920.            LINES 1236C/12390 LIST THE STARTING VALUES OF EACH VARIABLE
2922.               THE PROGRAM DOESN'T KNOW WHEN TO STOP,SO THE TIME MUST
2922.1              BE USED INSTEAD. FOR NO OPT,SET TIME=1
2925.                          */
2930.
3000.       /*  LIST  OF SUBROUTINES
3010.
3020.            LINE      NAME          FUNCTION
```

```
3030.
3040.
3050.          35CC      INVSYM      FINDS THE INVERSE OF A SYMMETRIC REAL
3060.                                SQUARE MATRIX AND OVERWRITES IT
3070.
3080.          8170      VIBFIX      CALCULATES  U-11(K) AND U-33(K) INCLUDING
3090.                                THE THIRD COMPLANT PART OF U-11
3100.
3110.          9330      ORTHAU      CONVERTS K TO ORTHOGONAL ATOMIC UNITS
3120.
3130.          9520      FT          CALCULATES THE FOURIER TRANSFORM OF
3140.                                A BASIS PAIR AT A SPECIFIED K
3150.
3160.          974C      LEFTFN      PART OF THE FT ALGORITHM
3170.          9800      CHOOSE       "   "  "  "      "
3180.          986C      RIGHTFN      "   "  "  "      "
3190.
3200.         10000      INPROC      INNER PRODUCT OF 2 REAL VECTORS
3210.         10010      INPRODX     INNER PRODUCT OF 2 COMPLEX VECTORS
3220.         10020      OUTPROD     OUTER PRODUCT OF 2 REAL VECTORS
3230.         10030      OUTPRODX    OUTER PRODUCT OF 2 COMPLEX VECTORS
3232.
3235.         10100      FIXEPS      CALCULATES SOME ERROR MEASURE 'EPS'
3240.
3245.         12280      INITGUES    INITIAL GUESS AT VARIABLES
3250.
3255.         12520      STARTUP     OVERHEAD AND INITIALIZATION
3260.
3265.         14CCC      CALCINTS    CALCULATES FTABLE AND OVERLAPS
3270.
3275.         17710      CALCF       FINDS  F_CALCULATED
3280.
3285.         17870      FIXUP       IMPOSES CONSTRAINTS ON P MATRIX
3290.                                AND OTHER VARIABLES
3295.
3300.         18C60      TRACE       TRACE OF A MATRIX
3305.         18200      TRACEX      TRACE OF A COMPLEX MATRIX
3310.
3315.         19CCC      MATMULX     COMPLEX MATRIX MULTIPLY
3320.         19100      MATMULT     REAL    MATRIX MULTIPLY
3322.
3325.         2000C      KET         MATRIX : VECTOR > = : VECTOR >
3330.
3335.         21000      POWER      MATRIX **-1/2 OR  **-1
3340.
3345.         3CCCC      LPOS        POSITIONS 12 FLOATERS IN D3H SYMMETRY
3350.                                AT  (R,THETA,PHI)
3355.
3360.         35CCC      RP          START A 3 BY 3 P-MATRIX WHERE
3365.                                        ( 1 0 C )
3370.                                   R = ( 0 0 0 )
3375.                                        ( 0 0 0 )                    */
3380.
3500.   INVSYM: PROCEDURE(A,NN,IFAIL);
3510.  /* INVERTS SYMMETRIC MATRICES-METHOD OF H. RUTISHAUSER,
3520.     ALGORITHM # 150,COMM. ACM 6(1963)P. 66
3530.     CODED IN PL/I BY MARTIN GOLDBERG ON 7-JULY-1983 */
3540.  DCL(A(*,*),P(200),C(200),BIGA) FLOAT(12);
3550.  DCL( I,J,K,R(200),IFAIL,N,NN,J1,KM1) DECIMAL FIXED(2);
3560.  IFAIL=0;R=0;N=NN;
3570.  DO I=1 TO N;
3580.  BIGA=0.0;
3590.   DO J=1 TO N;
3600.    IF((R(J)=1)|(ABS(A(J,J))<BIGA)) THEN GO TO TWO;
3610.    BIGA=ABS(A(J,J));
3620.    K=J;
3630.   TWO: END;
3640.   IF BIGA=0. THEN GO TO EIGHT;
3650.   R(K)=1;
3660.   P(K)=1./A(K,K);
3670.   C(K)=1.;
3680.   A(K,K)=0.;
3690.   IF K=1 THEN GO TO FOUR;
3700.   KM1=K-1;
3710.   DO J=1 TO KM1;
3720.    P(J)=A(J,K);
3730.    IF R(J)=0 THEN A(J,K)=-A(J,K);
3740.    Q(J)=A(J,K)*C(K);
3750.    A(J,K)=0.;
3760.   END;
3770.   IF K=N THEN GO TO SIX;
3780.   FOUR: J1=K+1;
3790.   DO J=J1 TO N;
3800.    C(J)=-A(K,J)*C(K);
3810.    IF R(J)=0 THEN A(K,J)=-A(K,J);
3820.    P(J)=-A(K,J);
3830.    A(K,J)=0.;
3840.  END;
```

```
9850.         SIX: DO J=1  TO N;
9860.           DO K=J TO N;
9870.             A(J,K)=A(J,K)+P(J)*C(K);
9880.         END;END;END;
9890.         GO TO  NINE;
9900.         EIGHT  : IFAIL=1;
9910.         NINE: RETURN;END INVSYM;
5165.
5170.
8170.         VIB=IX:PROCEDURE(VARY,HKLAU,VIB);
8171.         /*CODED BY MARTIN GOLDBERG ON MAY 23,1983*/
8180.         DCL(VARY(*),HKLAU(*,*),PI)FLOAT(12);PI=3.14159265359;
8185.           DCL VIB(*,*) COMPLEX FLOAT(12);
8190.         DCL(I,J,K) DECIMAL FIXED(2);
8200.
8210.
8215.
8220.         DO K=1 TO 58;
8230.             VIB(K,1)=EXP(-2.*PI*PI*VARY(13)*(HKLAU(K,1)*HKLAU(K,1)
8240.                 +HKLAU(K,2)*HKLAU(K,2)));
9243.           VIB(K,1)=VIB(K,1)*EXP(VARY(12)*-1.I*((3*HKLAU(K,1)**2*HKLAU(K,2))-
8245.             (HKLAU(K,2)**3)));
8247.
9250.             VIB(K,2)=EXP(-2*PI*PI*VARY(14)*HKLAU(K,3)*HKLAU(K,3));
8260.         END;
8270.         RETURN; END VIBFIX;
9320.
9330.         ORTHAU: PROCEDURE(FRACT,ORTH,N,CELCON);
9331.         /*CODED BY MARTIN GOLDBERG ON MAY 23,1983*/
9340.         /* THIS CONVERTS FRACTIONAL COORDS TO ORTHOGONAL ATOMIC UNITS*/
9350.         DCL(CELCON(*),FRACT(*,*),ORTH(*,*),SINN(3),COSS(3),
9370.         THINGY(5)) FLOAT(12);
9380.         DCL(I,J,N) DECIMAL FIXED(2);
9385.         DCL(A,B,K(2)) FLOAT(12) ;
9390.         DO I=4 TO 6; SINN(I-3)=SIND(CELCON(I)); COSS(I-3)=COSD(CELCON(I));END;
9392.         A=COSD(30);B=SIND(30);
9395.
9400.         THINGY(1) = CELCON(3)*(COSS(2)-COSS(1)*COSS(3))/SINN(3);
9410.         THINGY(2) = CELCON(1)*COSS(3);
9420.         THINGY(3) = CELCON(3)*COSS(1);
9430.         THINGY(5) = SQRT(1-COSS(1)**2-COSS(2)**2-COSS(3)**2+
9440.         2*COSS(1)*COSS(2)*COSS(3) ) /SINN(3);
9450.         DO J=0 TO N;
9460.         ORTH(J,2) = FRACT(J,2)*CELCON(2)*SINN(3);
9470.         ORTH(J,1) = FRACT(J,1)*CELCON(1)+FRACT(J,2)*THINGY(2)+FRACT(J,3)*
9480.                     THINGY(3);
9490.         ORTH(J,3) = FRACT(J,3)*CELCON(3)*THINGY(5);
9491.         /*NOW TO ROTATE A*B* WRT AB */
9492.5        K(1)=ORTH(J,1);K(2)=ORTH(J,2);
9493.         ORTH(J,1)=A*K(1)-B*K(2);
9493.5        ORTH(J,2)=A*K(2)+B*K(1);
9494.         /*ROTATED*/
9500.         END; RETURN; END ORTHAU;
9510.
9520.         FT: PROCEDURE(RA,RB,NA,NB,EXPA,EXPB,KVEC)RETURNS(COMPLEX FLOAT(12));
9520.1        /*CODED BY MARTIN GOLDBERG ON MAY 23,1983*/
9530.         /* RA, RB IN ORTHOGONAL ATOMIC UNITS, KVEC IN AL**-1.  NA, NB
9540.            ANGULAR DEPENDENCE, THIS FROM G.S. CHANDLER AND M.A. SPACKMAN,
9550.            ACTA CRYST A34(1978)P.342 EQUATION 7 */
9560.         DCL (NA(*),NB(*),I,J,K,STEST) DECIMAL FIXED(2);
9570.         DCL (RA(*),RB(*),PI,EXPA,EXPB, KVEC(*), PEA)FLOAT (12);
9580.         DCL (BBG(4),EFFT(3),KEW(3),ANGULAR) COMPLEX FLOAT (12);
9584.         ON ZERODIVIDE BEGIN;PUT DATA(RA,RB,NA,NB,EXPA,EXPB,KVEC);PUT FLOW;END;
9590.         PI = 3.14159265359; PEA = EXPA + EXPB; BBG=0;
9600.         KEW = EXPA*RA+EXPB*RB+.5I*KVEC*2.*PI;
9610.         DO I =1 TO 3;
9620.         BBG(1) = BBG(1) + (RA(I)-RB(I))**2;
9630.         BBG(2) = BBG(2) + 2.I*PI*KVEC(I)*(EXPA*RA(I)+EXPB*RB(I));
9540.         BBG(3) = BBG(3) - PI*PI*KVEC(I)*KVEC(I);
9550.         END; BBG(1)=(BBG(2)+BBG(3)-BBG(1)*EXPA*EXPB)/PEA;
9660.         BBG(4)=EXP(BBG(1));     STEST=0;
9670.         ANGULAR = 1;EFFT=0;DO I=1 TO 3;STEST=STEST+NA(I)+NB(I);END;
9673.          /*THIS NORM ONLY FOR IS GAUSSIANS */
9675.          ANGULAR=(4.*EXPA*EXPB/PI/PI)**.75;
9676.
9580.         IF STEST=0 THEN GO TO EASY; /*S-ORBS*/
9590.         DO I=1 TO 3; DO J=0 TO (NA(I)+NB(I));
9700.         EFFT(I)=EFFT(I)+LEFTFN(J,NA(I),NB(I),-RA(I),-RB(I))*
9710.            RIGHTFN(J,PEA,KEW(I));
9720.         END; ANGULAR = ANGULAR*EFFT(I); END;
9730.         EASY: RETURN(PI/PEA*SQRT(PI/PEA)*BBG(4)*ANGULAR); END FT;
9740.         LEFTFN: PROCEDURE(J,L,M,A,B) RETURNS(FLOAT(12));
9740.1        /*CODED BY MARTIN GOLDBERG ON MAY 23,1983*/
9750.         DCL(I,J,L,M,N) DECIMAL FIXED (2),(A,B,C,D,FN) FLOAT(12);
9760.         FN=0; DO I=MAX(0,J-M) TO MIN(J,L);
9765.         IF L-I=0 THEN C=1;ELSE C=A**(L-I);
9766.         IF M+I-J=0 THEN D=1; ELSE D=B**(M+I-J);
9770.         FN=FN+FLOAT(CHOOSE(L,I))*FLOAT(CHOOSE(N,J+I))*C*D;
```

```
 9790.       END; RETURN (FN); END LEFTFN;
 9800.       CHOOSE: PROCEDURE(N,M) RETURNS(DECIMAL FIXED(6));
 9800.1      /*CODED BY MARTIN GOLDBERG ON MAY 23,1983*/
 9810.       /* N /(M (N-M) )*/
 9820.       DCL(J,N,M) DECIMAL FIXED(2), I DECIMAL FIXED(6); I=1;
 9830.       IF N>1 THEN DO J=(M+1) TO N; I = I*J; END;
 9840.       IF (N-M)>1 THEN DO J=2 TO (N-M); I=I/J; END;
 9850.       RETURN (I); END CHOOSE;
 9860.       RIGHTFN: PROCEDURE(N,PEA,KEW) RETURNS(COMPLEX FLOAT(12));
 9860.1      /*CODED BY MARTIN GOLDBERG ON MAY 23,1983*/
 9870.       DCL N DECIMAL FIXED(2), PEA FLOAT(12), KEW COMPLEX FLOAT (12);
 9880.       SELECT (N);
 9890.       WHEN (0) RETURN (1.);
 9900.       WHEN (1) RETURN (KEW/PEA);
 9910.       WHEN (2) RETURN (1./PEA*(.5+KEW*KEW/PEA));
 9920.       WHEN (3) RETURN (KEW/PEA/PEA*(1.5+KEW*KEW/PEA));
 9930.       WHEN (4) RETURN (1./PEA/PEA*(.75+KEW*KEW/PEA*(3+KEW*KEW/PEA)));
 9940.       WHEN (5) RETURN (KEW/PEA/PEA/PEA*(3.75+KEW*KEW/PEA*
 9950.          (5.+KEW*KEW/PEA)));
 9960.       WHEN (6) RETURN (1./PEA/PEA/PEA*(1.875+KEW*KEW/PEA*
 9970.          (11.25+KEW*KEW/PEA*(7.5+KEW*KEW/PEA))));
 9980.       OTHERWISE RETURN (0.); END; END RIGHTFN;
10000.       INPROD:PROCEDURE(A,B,N)/* <A(N BY 1):B(1 BY N)>=C(SCALAR) */
10001.         RETURNS(FLOAT(12)); DCL (A(*),B(*),C) FLOAT(12),(I,N)
10002.         REAL FIXED(2);C=0.;
10003.         DO I=1 TO N;
10004.            C=C+A(I)*B(I);       END;
10005.         RETURN (C); END INPROD;
10006.
10010.       INPRODX:PROCEDURE(A,B,N)/* <A(N BY 1):B(1 BY N)>=C(SCALAR) */
10011.         RETURNS(FLOAT(12)); DCL A(*) COMPLEX FLOAT(12),
10012.         (B(*),C) FLOAT(12),(I,N) REAL FIXED(2);C=0.;
10013.         DO I=1 TO N;
10014.            C=C+REAL(A(I))*B(I);       END;
10015.         RETURN (C);END INPRODX;
10020.       OUTPROD:PROCEDURE(A,B,N,C);/* :A><B: =C (N BY N ) */
10021.         DCL(A(*),B(*)) FLOAT(12);DCL(I,J,N)REAL FIXED(2);
10022.       DCL C(*,*) COMPLEX FLOAT(12); C=0.;
10023.       DO I=1 TO N;DO J=1 TO N;C(I,J)=A(I)*B(J);END;END;
10024.         RETURN;END OUTPROD;
10025.
10030.       OUTPRODX:PROCEDURE(A,B,N,C);/* :A><B: = C (N BY N ) */
10031.         DCL(A(*),B(*)) COMPLEX FLOAT(12);DCL(I,J,N)REAL FIXED(2);
10032.       DCL C(*,*) COMPLEX FLOAT(12); C=0.;
10033.       DO I=1 TO N;DO J=1 TO N;C(I,J)=A(I)*B(J);END;END;
10034.         RETURN;END OUTPRODX;
10100.       FIXEPS:PROCEDURE(FOBS,S,FCAL,EPSWAY,EPS,RFAC);
10100.1      /*CODED BY MARTIN GOLDBERG ON AUGUST 3,1983*/
10101.       /*FOR VARIOUS REASONS,THE SIGN CONVENTION IN THIS PROGRAM IS
10102.         FOBS-FCAL.THIS RESULTS IN P'=P MINUS DP.  */
10103.       DCL(FOBS(*),S(*),C,FCAL(*),EPS)FLOAT(12);DCL(EPSWAY,K)DECIMAL FIXED(2);
10104.            EPS=0.;
10104.1      J=0;DO K=1 TO DIM(FOBS,1);
10104.11     Q=Q+ABS(FOBS(K));EPS=EPS+ABS(ABS(FOBS(K))-ABS(FCAL(K)));
10104.12     END;RFAC=EPS/C;EPS=0.;
10104.13
10105.       SELECT(EPSWAY);
10106.         WHEN ( 1)
10107.           DO K=1 TO DIM(FOBS,1) WHILE (FOBS(K)>1.E-20);
10108.           EPS=EPS+S(K)*ABS(ABS(FOBS(K))-ABS(FCAL(K)));END;
10109.         WHEN ( 2)
10110.           DO K=1 TO DIM(FOBS,1) WHILE (FOBS(K)>1.E-20);
10111.           EPS=EPS+ABS(ABS(FOBS(K))-ABS(FCAL(K)));
10112.           END;
10113.         WHEN ( 3)
10114.           DO K=1 TO DIM(FOBS,1) WHILE (FOBS(K)>1.E-20);
10115.           Q=ABS(FOBS(K))-ABS(FCAL(K));EPS=EPS+S(K)*Q*Q;END;
10116.         WHEN ( 4)
10117.           DO K=1 TO DIM(FOBS,1) WHILE (FOBS(K)>1.E-20);
10118.           Q=(ABS(FOBS(K))-ABS(FCAL(K)));EPS=EPS+Q*Q;
10119.           END;
10120.         WHEN ( 5)
10121.           DO K=1 TO DIM(FOBS,1) WHILE (FOBS(K)>1.E-20);
10122.           EPS=EPS+S(K)*ABS(FOBS(K)*FOBS(K)-FCAL(K)*FCAL(K));
10123.           END;
10124.         WHEN ( 6)
10125.           DO K=1 TO DIM(FOBS,1) WHILE (FOBS(K)>1.E-20);
10126.           Q=FOBS(K)*FOBS(K);Q=ABS(Q-FCAL(K)*FCAL(K));
10127.           EPS=EPS+Q;END;
10128.         WHEN ( 7)
10129.           DO K=1 TO DIM(FOBS,1) WHILE (FOBS(K)>1.E-20);
10130.           Q=FOBS(K)*FOBS(K)-FCAL(K)*FCAL(K);EPS=EPS+S(K)*Q*Q;
10131.           END;
10132.         WHEN ( 8)
10133.           DO K=1 TO DIM(FOBS,1) WHILE (FOBS(K)>1.E-20);
10134.           Q=FOBS(K)*FOBS(K);Q=(Q-FCAL(K)*FCAL(K));EPS=EPS+Q*Q;
10135.           END;
10136.         WHEN ( 9)
```

```
14170.      DO J = 1 TO 12;
14180.      DO L = 1 TO 3; BX(L) = FLO1(J,L);
14190.      CX(L) = FLO2(J,L); END;
14195.       IF #PIJ > 0.  THEN
14200.      FTABLE(K,1,3) = FTABLE(K,1,3) + FT(CTR,BX,S,S,ZETAS(I,1)
14210.        ,ZETAS(14,1),KVEC)*ZETAS(I,2);
14215.       IF #PIJ = 2 THEN
14220.      FTABLE(K,1,4) = FTABLE(K,1,4) + FT(CTR,CX,S,S,ZETAS(I,1)
14230.        ,ZETAS(15,1),KVEC)*ZETAS(I,2);
14240.      END; END;
14250.      DO I = 16 TO 25; DO J=16 TO 25 ;
14260.      FTABLE(K,2,2) = FTABLE(K,2,2) + FT(CTR,CTR,S,S,ZETAS(I,1),
14270.        ZETAS(J,1),KVEC)*ZETAS(I,2)*ZETAS(J,2);
14280.      END; DO J = 1 TO 12;
14290.      DO L = 1 TO 3; BX(L) = FLO1(J,L); CX(L) = FLO2(J,L); END;
14295.         IF #PIJ > 0 THEN
14300.      FTABLE(K,2,3) = FTABLE(K,2,3) + FT(CTR,BX,S,S,ZETAS(I,1),
14310.         ZETAS(14,1),KVEC)*ZETAS(I,2);
14315.         IF #PIJ = 2 THEN
14320.      FTABLE(K,2,4) = FTABLE(K,2,4) + FT(CTR,CX,S,S,ZETAS(I,1),
14330.         ZETAS(15,1),KVEC)*ZETAS(I,2);
14340.      END; END;
14340.1     DO I=1 TO 12;
14340.2     DO L=1 TO 3;BX(L)=FLO1(I,L);CX(L)=FLO2(I,L); END;
14340.3     DO J=1 TO 12;
14340.4     DO L=1 TO 3;BT(L)=FLO1(J,L);CT(L)=FLO2(J,L);END;
14340.45       IF #PIJ > 0 THEN
14340.5     FTABLE(K,3,3)=FTABLE(K,3,3)+FT(BX,BT,S,S,ZETAS(14,1),
14340.6                    ZETAS(14,1),KVEC);
14340.61       IF #PIJ < 0 THEN
14340.62    FTABLE(K,3,3)=FTABLE(K,3,3)+FT(BX,BX,S,S,ZETAS(14,1),
14340.63                   ZETAS(14,1),KVEC);
14340.65       IF #PIJ = 2 THEN
14340.7     FTABLE(K,3,4)=FTABLE(K,3,4)+FT(BX,CT,S,S,ZETAS(14,1),
14340.8                    ZETAS(15,1),KVEC);
14340.85       IF #PIJ = 2 THEN
14340.9     FTABLE(K,4,4)=FTABLE(K,4,4)+FT(CX,CT,S,S,ZETAS(15,1),
14341.                     ZETAS(15,1),KVEC);
14341.5        IF #PIJ = -2 THEN
14341.51    FTABLE(K,4,4)=FTABLE(K,4,4)+FT(CX,CX,S,S,ZETAS(15,1),
14341.52                   ZETAS(15,1),KVEC);
14342.      END; END;
14343.
14350.      END;
14350.3     DO I = 1 TO 3; DO J = I TO 4;DO K=0 TO 58;
14350.5     FTABLE(K,J,I) = CONJG(FTABLE(K,I,J));
14350.7     END; END; END;
14351.      /*NOW TO RENORM THE ENTIRE FTABLE*/
14351.1     DO I=1 TO (2 + ABS(#PIJ)) ;NORM(I)=SQRT(ABS(FTABLE(0,I,I)));END;
14351.2     DO K=0 TO 58;DO I=1 TO (2+ABS(#PIJ));DO J=1 TO (2+ABS(#PIJ));
14351.3     FTABLE(K,I,J)=FTABLE(K,I,J)/NORM(I)/NORM(J);
14351.4     END;END;END;
14360.      /* NON-ORTHOGONALIZED FTABLE IS NOW COMPLETE. NEXT WE
14370.         (THE COMPUTER AND I) SCHMIDT-ORTHOGONALIZE THE VALENCE
14380.         (2,3,4) TO THE CORE(1) */
14390.      DO I = 2 TO 4; DO J = I TO 4;
14400.      LAPI=FTABLE(0,I,I);
14402.      LAPJ=FTABLE(0,I,J);
14410.      DO K = 0 TO 58;
14420.      FTABLE(K,I,J) = FTABLE(K,I,J) - LAPI*FTABLE(K,1,J) -
14430.         LAPJ*CONJG(FTABLE(K,1,I)) + LAPI*LAPJ*FTABLE(K,1,1);
14435.      FTABLE(K,J,I)=CONJG(FTABLE(K,I,J));
14440.      END; END;END;
14450.      DO I=1 TO 3;DO J=1 TO 3;ESS(I,J)=REAL(FTABLE(0,I+1,J+1));END;END;
14455.      IF ESS(2,1)>.95 THEN DO;TRUBL=2;RETURN;END;
14460.      IF ESS(3,1)>.95 THEN DO;TRUBL=3;RETURN;END;
14465.      IF ESS(3,2)>.95 THEN DO;TRUBL=4;RETURN;END;
14470.
14475.      ESS=ESS*1.E-18;CALL POWER(ESS,-0.5,SINV2,#PIJ,TRUBL);
14480.            SINV2=SINV2*1.E-9;
14490.
14500.      IF TRUBL>0 THEN SINV2=9999;RETURN;END CALCINTS;
17710.      CALCF: PROCEDURE(#PIJ,P,FTABLE,SINV2,VIB,VARY,CENTER,HKLAJ,FCAL);
17720.      /* CODED BY MARTIN GOLDBERG ON JUNE 8 AND DEC 12,1983 */
17730.      DCL(P(*,*),VARY(*),HKLAJ(*,*),FCAL(*),CENTER(*),
17740.      SINV2(*,*),FRINGE, KVEC(3),PI) FLOAT (12);DCL(VIB(*,*),
17750.        FTABLE(*,*,*),EFF(5E),FIJ(3,3),R(3,3),FRINGEX) COMPLEX FLOAT(12);
17760.      DCL(I,J,K,#PIJ) DECIMAL FIXED (2);
17770.      PI = 3.14159265359;
17775.
17780.      DO K = 1 TO 58; DO I = 1 TO 3; KVEC(I) = HKLAJ(K,I); END;
17790.      FRINGE = 2*PI*INPRCO(KVEC,CENTER,3);
17795.
17800.      DO I = 1 TO 3; DO J = 1 TO 3;
17810.      FIJ(I,J) = FTABLE(K,I+1,J+1); END; END;
17813.      CALL MATMULX(FIJ,COMPLEX(SINV2,0.),3,R);
17816.      CALL MATMULX(COMPLEX(SINV2,0.),R,3,FIJ);
17820.      CALL MATMULX(COMPLEX(P,0.),FIJ,3,R);
```

```
10137.          DO ;PUT LIST('JOBLST-RESISTANT NOT IMPLEMENTED');END;
10138.        OTHERWISE PUT LIST('EPSWAY INPUT ERROR');
10139.       END;
10140.       RETURN;END FIXEPS;
10141.
12270.
12280.       INITGUES : PROCEDURE(VARY,P);
12290.       /* CODED BY MARTIN GOLDBERG ON JUNE 3,1983 */
12300.       DCL(I,J) DECIMAL FIXED(2);
12310.       DCL(VARY(*),P(*,*)) FLOAT (12);
12320.
12330.
12340.
12350.
12360.       VARY(2)=0.3744;VARY(3)=0.2629;VARY(4)=3.20;VARY(5)=60.00;
12370.       VARY(6)=100;VARY(7)= .3733;VARY(8)=2.55;
12380.       VARY(9)=5;VARY(10)=5;VARY(11)=0.676;VARY(12)=.0033;
12381.       VARY(13)=.02202;VARY(14)= .01937;VARY(15)=.9955;VARY(16)=1;
12385.       VARY(17)=1;VARY(18),VARY(19),VARY(20)=0;
12390.       RETURN;
12500.          END INITGUES;
12510.       /* CODED BY MARTIN GOLDBERG ON JUNE 3,1983 */
12520.       STARTUP : PROCEDURE(ZETAS,HKLAU,CENTER);
12530.       DCL (ZETAS(*,*),HKLAU(*,*),CENTER(*)) FLOAT (12);
12540.
12570.       DCL (CELCON(6),CELINV(6)) FLOAT(12);DCL HKL(0:58,3) DECIMAL
12575.          FIXED(2) INITIAL    (0,0,0,
12580.       0,0,2,  0,0,4,  0,0,6,  0,0,8,  0,1,0,  0,1,1,  0,1,2,
12585.       0,1,3,  0,1,4,  0,1,5,  0,1,6,  0,1,7,  0,1,8,  0,2,0,
12590.       0,2,1,  0,2,2,  0,2,3,  0,2,4,  0,2,5,  0,2,6,  0,2,7,
12595.       0,3,0,  0,3,2,  0,3,4,  0,3,6,
12600.       0,4,0,  0,4,1,  0,4,2,  0,4,3,  0,4,4,
12605.       1,1,0,  1,1,2,  1,1,4,  1,1,6,  1,1,8,  1,2,0,  1,2,1,
12610.       1,2,2,  1,2,3,  1,2,4,  1,2,5,  1,2,6,  1,2,7,  1,3,0,
12615.       1,3,1,  1,3,2,  1,3,3,  1,3,4,  1,3,5,  1,4,0,  1,4,2,
12620.       2,2,0,  2,2,2,  2,2,4,  2,3,0,  2,3,1,  2,3,2,  2,3,3 );
12625.
12630.       CELCON(1), CELCON(2) = 431861; CELCON(3) = 677327;
12635.       CELCON(4), CELCON(5) = 90.0  ; CELCON(6) = 120.0;
12640.       CELINV(1), CELINV(2) = 0.26737891; CELINV(3) = 0.14764004;
12645.       CELINV(4), CELINV(5) = 90.0  ; CELINV(6) = 60.0;
12675.       DCL TE(0:58,3)FLOAT (12);TE=FLOAT(HKL,12);
12680.       CALL ORTHAU(TE,HKLAL,58,CELINV);
12690.       CENTER(1) = 0.; CENTER(2) = 2.49334C8; CENTER(3) = 1.69329;
12700.
12710.       ZETAS(1,1) = 3.66826;     ZETAS(1,2) = 0.43211;
12720.       ZETAS(2,1) = 32.6562;     ZETAS(2,2) = 0.08689;
12730.       ZETAS(3,1) = 117.799;     ZETAS(3,2) = 0.02239;
12740.       ZETAS(4,1) = 532.280;     ZETAS(4,2) = 0.00422;
12750.       ZETAS(5,  1) =1.35431;    ZETAS(5,2) = 0.33942;
12760.       ZETAS(6,1) = 0.38905;     ZETAS(6,2) = 0.03710;
12770.       ZETAS(7,1) = 0.15023;     ZETAS(7,2) = -0.00791;
12780.       ZETAS(8,1) = 10.4801;     ZETAS(8,2) = 0.24152;
12790.       ZETAS(9,1) = 3630.38;     ZETAS(9,2) = 0.00053;
12800.       ZETAS(10,1) = 0.052406;   ZETAS(10,2) = 0.00183;
12810.       /* ZETAS 1 TO 10 ARE HUZINAGA'S IS CORE FROM JCP(1965)42,
12820.          PAGE 1300.  ZETAS 11 TO 14 ARE POPLE'S STO-3G FROM
12830.          JCP(1969)51,PAGE 2658.*/
12840.       ZETAS(11,1) = -2.012297 ;   ZETAS(11,2) = -.112649;
12850.       ZETAS(12,1) =  .704886;   ZETAS(12,2) = -.229506;
12860.       ZETAS(13,1) =  .207339;   ZETAS(13,2) = 1.18692;
12870.       ZETAS(14,1) = 1.0656169;  ZETAS(15,1) = 1.000;
12871.        DCL Q DECIMAL FIXED(2);DO Q=16 TO 25;ZETAS(Q,1)=ZETAS(Q-15,1);END;
12871.5      ZETAS(16,2)=-.10274;ZETAS(17,2)=-.01628;ZETAS(18,2)=-.00414;
12872.       ZETAS(19,2)=-.00077;ZETAS(20,2)=-.15719;ZETAS(21,2)= .04809;
12872.5      ZETAS(22,2)= .59C95;ZETAS(23,2)=-.04911;ZETAS(24,2)=-.00010;
12873.       ZETAS(25,2)= .47194;
12880.       RETURN; END STARTUP;
12890.
14000.       CALCINTS: PROCEDURE(NPIJ,FTABLE,FLO1,FLO2,HKLAL,ZETAS,SINV2,TRUBL);
14010.       /* CODED BY MARTIN GOLDBERG ON JUNE 4 AND OCT 6,1983 */
14020.       DCL (FTABLE(*,*,*),LAPI,LAPJ) COMPLEX FLOAT (12);
14030.       DCL (CTR(3),FLO1(*,*),FLO2(*,*),HKLAU(*,*),ZETAS(*,*),KVEC(3),
14040.          NORM(4),BX(3),CX(3),ET(3),CT(3),SINV2(*,*),ESS(3,3)) FLOAT (12);
14050.       DCL(NPIJ,S(3),I,J,K,L,TRUBL)DECIMAL FIXED(2);S=0; FTABLE=0.;CTR=0.;
14051.       TRUBL=0;
14060.       DO K = 0 TO 58;
14070.       DO I = 1 TO 3; KVEC(I) = HKLAU(K,I); END;
14080.       DO I = 1 TO 10;
14090.       DO J = 1 TO 10;
14100.       FTABLE(K,1,1) = FTABLE(K,1,1) + FT(CTR,CTR,S,S,
14110.          ZETAS(I,1),ZETAS(J,1),KVEC)*ZETAS(I,2)*ZETAS(J,2);
14120.       END;
14130.       DO J = 16 TO 25; FTABLE(K,1,2) = FTABLE(K,1,2) +
14140.          FT(CTR,CTR,S,S,ZETAS(I,1),ZETAS(J,1),KVEC)*
14150.          ZETAS(I,2)*ZETAS(J,2);
14160.       END;
```

```
17822.      FRINGEX= EXP(1.I * FRINGE );
17824.      EFF ( K ) = (FTABLE(K,1,1)*TRACEX(K))**2;
17826.      EFF(K)=(EFF(K)*VIB(K,1)*VIB(K,2)*FRINGEX *
17828.          CONJG(EFF(K))*CONJG(VIB(K,1))*CONJG(VIB(K,2))*CONJG(FRINGEX));
17831.      DCL (A,ET(3)) FLOAT(12);
17831.2     ET(1)=ET(1)*REAL(R(1,1))
17831.4        ;ET(2)=ET(2)+REAL(R(1,2))**2;
17831.6     ET(3)=ET(3)+REAL(R(2,2));
17835.      /*FTABLE(K,1,1) IS THE CORE SCATTERING */
17840.      F=AL(K) = REAL(EFF(K))*VARY(15); END;

17843.
17850.      RETURN;END CALCF;
17860.
17870.      FIXUP: PROCEDURE(#PIJ,P,A,N,VARY,ZETAS,ZETAL);
17880.      /* CODED BY MARTIN GOLDBERG ON JUNE 10,1983 */
17890.      DCLIP(*,*),VARY(*),ZETAS(*,*),ZETAL(*,*)) FLOAT (12);
17900.      DCL(A,N,I,J,#PIJ) DECIMAL FIXED (2);
17910.      DCL TR FLOAT (12);
17955.      ZETAS(1*,1)=VARY(7);ZETAS(15,1)=VARY(11);
17956.      DO  I=16 TO 25;ZETAS(I,1)=ZETAL(I,1)*VARY(17);
17957.            ZETAS(I-15,1)=ZETAL(I-15,1)*VARY(16); END;
17960.      TR=N-VARY(2)*VARY(2)-VARY(3)*VARY(3);VARY(1)=SQRT(ABS(TR));
17965.       IF #PIJ > -1 THEN
17970.      DO  I=1 TO 3;DO J=I TO 3;P(I,J),P(J,I)=VARY(I)*VARY(J);END;END;
17975.       ELSE
18000.       DO; P=0;DO I=1 TO 3;P(I,I)=VARY(I)**2;END;END;
18056.      RETURN; END FIXUP;
18060.       TRACE :PROCEDURE(X) RETURNS(  FLOAT(12));
18060.1                          /* THE TRACE OF A COMPLEX MATRIX*/
18060.2      DCL X(*,*)  FLOAT(12);
18060.3      RETURN(X(1,1)+X(2,2)+X(3,3));END TRACE ;
18070.
18090.
18100.
18130.
18200.      TRACEX:PROCEDURE(Q) RETURNS(COMPLEX FLOAT(12));
18210.      DCL(Q(*,*),T) COMPLEX FLOAT(12),N DECIMAL FIXED(2);
18220.      T=0.;
18230.      DO N=1 TO DIM(Q,1);T=T+Q(N,N);END;
18240.      RETURN(T);END TRACEX;
18250.
19000.       MATMULX:PROCEDURE(A,B,N,C);
19010.                /* THE COMPLEX MATRIX EQUATION  C=A*B  */
19020.       DCL (D,A(*,*),B(*,*),C(*,*)) COMPLEX FLOAT(12),(I,J,K,N)DECIMAL
19030.           FIXED(2,0);
19040.                          C=0.0 ;
19050.        /*THE CALLING ROUTINE MUST NAME C DIFFERENTLY FROM A AND B*/
19060.       DO I=1 TO N;DO J=1 TO N;DO K=1 TO N;
19070.        ON UNDERFLOW D=0.;D=A(I,K)*B(K,J);
19080.          C(I,J)=C(I,J)+D;END;END;END;RETURN;END MATMULX;
19090.
19100.       MATMULT:PROCEDURE(A,B,N,C);
19110.                          /* THE MATRIX EQUATION  C=A*B  */
19120.       DCL (D,A(*,*),B(*,*),C(*,*))FLOAT(12),(I,J,K,N)DECIMAL FIXED(2,0);
19130.        /*THE CALLING ROUTINE MUST NAME C DIFFERENTLY FROM A AND B*/
19140.                C=0.0;
19150.       DO I=1 TO N;DO J=1 TO N;DO K=1 TO N;
19160.        ON UNDERFLOW D=0.;D=A(I,K)*B(K,J);
19170.            C(I,J)=C(I,J)+D;END;END;END;RETURN;END MATMULT;
19180.
20000.      KET:PROCEDURE(MAT,VEC,DIM,VECTOR);/* :MAT:VEC>=:VECTOR> */
20010.        DCL (MAT(*,*),VEC(*),REG) FLOAT(12);
20020.        DCL(DIM,I,J,K) DECIMAL FIXED(2),VECTOR(*) FLOAT(12);
20030.        VECTOR=0.;
20040.      DO J=1 TO DIM;DO I=1 TO DIM;VECTOR(J)=MAT(I,J)*VEC(I)+VECTOR(J);
20050.       END;END;RETURN;END KET;
21000.      POWER:PROCEDURE(A,N,B,#PIJ,DOOM);
21005.      /*CODED BY MARTIN GOLDBERG ON 18-MAY-1982*/
21010.         /*THIS CALCULATES THE MATRIX B=A**N,WHERE N
21020.         IS EITHER -1.0 OR -0.5                    */
21030.      DCL (A(*,*),B(*,*),D(3,3),CC(3,3),D3(3,3),DIF,DET) FLOAT(12);
21040.       DCL(T(3,3),D4(3,3)) FLOAT(12);
21050.      DCL(N,I,J,K,L,M,H) DECIMAL FIXED(2,1),DOOM DECIMAL FIXED(2);
21055.      DCL #PIJ DECIMAL FIXED(2);IF #PIJ < 1 THEN DO;B=0;
21056.        B(1,1),B(2,2),B(3,3)=1.E9;RETURN;END;
21060.       IF N=-1.0 THEN GO TO INVERT;
21070.       IF N=-1.1 THEN GO TO GENINV;
21080.       IF N=-0.5 THEN GO TO RUSSIA;
21090.       PUT SKIP LIST('NOT IMPLEMENTED YET');B=9999.;RETURN;
21100.      RUSSIA: /* THIS ITERATIVE PROCEDURE TO GENERATE THE INVERSE
21110.                 SQUARE ROOT OF A COMES FROM REFERENCE #9 IN
21120.                 DOKL. AKAD. NAUK SSSR 254(SEPT. '80)P. 370,TC
21130.                 VESTN. LENINGR. UNIV. 4 (1965)  P. 5,BY
21140.                 V.N. GOLKIN AND M.M. MESTECHKIN                */
21150.        D=0.;D(1,1),D(2,2),D(3,3)=1./SQRT(1+#PIJ);
21155.      IF #PIJ=1 THEN D(3,3),A(3,3)=1.;
21157.      IF #PIJ=1 THEN A(1,3),A(2,3),A(3,1),A(3,2)=0.;
21160.      DET=1000 ;
```

```
21170.        DO WHILE (DOOM=0) UNTIL (DET<1.E-24);
21175.        ON OVERFLOW BEGIN;PUT LIST('21175');DOOM=1;B=C;GO TO U;END;
21180.        CALL MATMULT(D,A,1+#PIJ,T);CALL MATMULT(T,C,1+#PIJ,DD);
21190.        CALL MATMULT(DD,J,1+#PIJ,D3);CALL MATMULT(D,DD,1+#PIJ,D4);
                B=1.5*C-(D4+D3)/4.0; /*THE RUSSIAN ITERATIVE FORMULA */
21200.        DO I=1 TO 3;B(I,I)=ABS(B(I,I));END;
21210.        /*THE ABS(DIAGONAL) IS TO GET THE POSITIVE SQRT,NOT THE NEGATIVE */
21220.          DET=0.;
21230.          DO I=1 TO 3;
21240.                    DO J=1 TO 3; DIF=ABS(B(I,J)-C(I,J));
21250.             DIF=MIN(10.,DIF);DET=DET+DIF*DI=;
21260.        END;END;DET=DET*(A(1,1)+A(2,2)+A(3,3));
21270.          /*NOW FOR THE NEXT ITERATION*/  D=B;
21280.        END; /* THE END OF THE DO WHILE LOOP.B=A**(-1/2)  */
21290.        J:RETURN;
21300.       INVERT: /* BY THE METHOD OF THE COFACTORS C(I,J)  */
21310.       D(1,1)=A(2,2)*A(3,3)-A(2,3)*A(3,2);
21320.       D(1,2)=-A(2,1)*A(3,3)+A(3,1)*A(2,3);D(2,1)=D(1,2);
21330.       D(1,3)=A(2,1)*A(3,2)-A(3,1)*A(2,2); D(3,1)=D(1,3);
21340.       D(2,2)=A(1,1)*A(3,3)-A(3,1)*A(1,3);
21350.       D(3,2)=-A(1,1)*A(2,3)+A(2,1)*A(1,3);D(2,3)=D(3,2);
21360.       D(3,3)=A(1,1)*A(2,2)-A(2,1)*A(1,2);
21370.        DET=A(1,1)*D(1,1)+A(1,2)*D(1,2)+A(1,3)*C(1,3);
21380.        B=D/DET;
21390.        RETURN;
21400.
21410.        GENINV:/*THIS DOESN'T REALLY CALCULATE THE -1.1TH POWER OF A MATRIX.
21420.                 RATHER,IT CALCULATES THE GENERALIZED INVERSE A+,IN THE
21430.                 MOORE-PENROSE SENSE,BY THE ITERATIVE PROCEDURE OF
21440.                 GUPTA,AS REPORTED BY A.L.MACKAY, IN ACTA CRYST A33(1977)PAGE 213.
21450.        THIS SUB-SUBROUTINE ISNT CALLED AND STILL HAS BUGS   IN IT    */
21460.        B=A*.05;
21470.       D)=0.;DD(1,1)=2;DD(2,2)=2.;DD(3,3)=2.;
21480.        AGAIN:CALL MATMULT(A,B,3,D);
21490.        CALL MATPULT(B,DD-D,3,D3);
21491.        /*D3 IS THE NEXT ITERATE*/
21500.       DET=D(1,1)+D(2,2)+D(3,3);  B=D3;
21510.       IF(CEIL(DET)-DET )> .00001 THEN GO TO AGAIN;
21520.        /*B HAS CONVERGED BY MACKAY'S SUGGESTED CRITERION*/
21530.       RETURN;          END POWER;
21540.       LPOS:  PROCEDURE(Z,FLOATER);
30000.       /* CODED BY MARTIN GOLDBERG ON 4-AUG-1983 */
30010.       /* GIVEN THE RADIAL AND ANGULAR DISTANCES, WHAT ARE THE
30020.          CARTESIAN COORDS OF THE 12 FSGD? */
30030.       DCL (I,J) DECIMAL FIXED (2);
30040.       DCL(Z(*),FLOATER(*,*),R,TH,PHI,UP) FLOAT(12);
30050.       FLOATER = 0.;
30060.       PHI = Z(3); R = Z(1); TH = Z(2);
30070.
30080.       UP = R*SIND(PHI);
30090.       DO I=1 TO 6;FLOATER(I,3)=UP;FLOATER(I+6,3)=-UP;END;
30100.
30110.
30120.
30130.       UP=R*COSD(PHI);
30190.
30200.       FLOATER(1,1) =UP*COSD(-30+TH);FLOATER(2,1)=-FLOATER(1,1);
30205.       FLOATER(6,1)=UP*COSD(-30-TH);FLOATER(3,1)=-FLOATER(6,1);
30210.       FLOATER(5,1)=UP*COSD(90-TH);FLOATER(4,1)=-FLOATER(5,1);
30220.       FLOATER(1,2),FLOATER(2,2) =UP*SIND(-30.+TH);
30230.       FLOATER(3,2),  FLOATER(6,2) = UP*SIND(-30. -TH);
30240.       FLOATER(4,2),FLOATER(5,2) = UP*SIND(90.  -TH);
30250.
30260.
30270.       DO I=7 TO 12;DO J = 1 TO 2;
30280.       FLOATER(I,J) = FLOATER(I-6,J);
30290.       END;END;
30300.        RETURN; END LPOS;
35000.       RP:/*HOW TO START A 3-BASIN CALC FROM A 1-BASIN*/
35010.        /*CODED BY MARTIN GOLDBERG ON 3-AUGUST-1983*/
35020.       PROCEDURE(SINV2,P,VARY);
35030.       DCL(X,SINV2(*,*),P(*,*),SHALF(3,3),VARY(*)) FLOAT(12);
35040.       DCL(I,J,FAIL)DECIMAL FIXED(2);
35050.       SHALF=SINV2;CALL INVSYM(SHALF,3,FAIL);IF FAIL>0 THEN X=10/0;
35060.       DO I=1 TO 2;DO J=I TO 3;SHALF(J,I)=SHALF(I,J);END;END;
35070.       PUT SKIP DATA(SHALF);
35080.       X=0.;DO I=1 TO 3;X=X+SHALF(I,1)*SHAL=(I,1);END;X=1./X;
35090.       DO I=1 TO 3;DO J=1 TO 3;
35100.       P(I,J)=SHALF(I,1)*X*SHALF(1,J);END;END;
35110.       VARY(2)=SHALF(1,2)*SQRT(X);VARY(3)=SHALF(1,3)*SQRT(X);
35120.       PUT SKIP DATA(VARY,P);RETURN;END RP;
99995.         FIN;END TREFCIL;
99997.      //GO.SYSIN  DD  *
99998.      /*
```

Appendix C

Beryllium Metal Structure Factors from Various Sources

Reference				(172)		(172)		(56)		(29)	(29)	(29)	(93)	(94)
				Silver		Molybdenum		Average		Totally Empirical			Ab Initio	
#	h	k	l	I-obs	Error	I-obs	Error	F-obs	Error	Free Atom F-cal	Quantum F-cal	Multi-pole F-cal	Plane Wave F-cal	LCAO F-cal
1	0	0	2	11.219	.283	11.527	.288	3.348	.029	-3.365	-3.348	-3.349	-3.330	-3.398
2	0	0	4	4.954	.126	5.012	.126	2.216	.019	2.209	2.211	2.209	2.173	2.202
3	0	0	6	1.470	.018	1.495	.009	1.212	.003	-1.213	-1.214	-1.212	-1.184	-1.215
4	0	0	8	.362	.024	.353	.004	.590	.003	.589	.591	.593	*	*
5	0	1	0	3.408	.086	3.452	.087	1.839	.016	-1.761	-1.840	-1.839	-1.829	-1.892
6	0	1	1	7.983	.200	8.096	.203	2.815	.024	2.857	2.814	2.816	-2.816	-2.798
7	0	1	2	2.194	.056	2.209	.056	1.473	.013	1.458	1.469	1.466	1.442	1.434
8	0	1	3	4.651	.117	4.735	.119	2.151	.019	-2.144	-2.149	-2.150	2.105	2.132
9	0	1	4	.999	.026	1.009	.025	.995	.008	-.993	-.993	-.991	-.977	-.990
10	0	1	5	1.728	.015	1.734	.010	1.307	.003	1.307	1.308	1.305	-1.280	-1.307
11	1	1	6	.313	.005	.308	.002	.551	.001	.552	.552	.551	.539	.553
12	0	1	7	.474	.006	.469	.004	.680	.002	-.678	-.679	-.679	*	*

13	0	1	8	.085	.010	.076	.001	.273	.001	-.272	-.273	-.273	*	*
14	0	2	0	1.421	.036	1.447	.036	1.188	.010	-1.192	-1.193	-1.193	-1.168	-1.182
15	0	2	1	4.080	.103	4.093	.102	2.007	.017	-1.999	-1.998	-2.000	1.975	1.998
16	0	2	2	1.092	.028	1.121	.029	1.044	.009	1.050	1.049	1.049	1.036	1.050
17	0	2	3	2.433	.016	2.449	.027	1.550	.004	1.556	1.556	1.553	-1.534	-1.557
18	0	2	4	.532	.008	.539	.004	.727	.002	-.728	-.728	-.726	-.714	-.730
19	0	2	5	.970	.014	.969	.006	.977	.002	-.975	-.975	-.974	.956	.980
20	0	2	6	.169	.007	.178	.002	.418	.001	.419	.420	.420	*	*
21	0	2	7	.272	.009	.280	.002	.524	.001	.526	.527	.528	*	*
22	0	3	0	2.015	.014	2.009	.012	1.408	.003	1.412	1.410	1.407	1.390	1.421
23	0	3	2	1.605	.016	1.583	.010	1.251	.003	-1.257	-1.256	-1.254	-1.238	-1.267
24	0	3	4	.822	.008	.827	.005	.902	.002	.904	.904	.904	*	*
25	0	3	6	.302	.006	.307	.002	.549	.001	-.549	-.551	-.552	*	*
26	0	4	0	.149	.007	.134	.002	.364	.002	-.368	-.368	-.368	*	*
27	0	4	1	.393	.008	.395	.003	.623	.002	.621	.621	.621	*	*
28	0	4	2	.114	.005	.113	.001	.334	.001	.333	.333	.333	*	*
29	0	4	3	.266	.006	.267	.002	.513	.001	-.510	-.510	-.511	*	*
30	0	4	4	.054	.006	.062	.001	.247	.001	-.250	-.250	-.250	*	*
31	1	1	0	7.221	.183	7.220	.183	2.668	.023	2.658	2.665	2.672	2.621	2.632
32	1	1	2	5.507	.138	5.561	.141	2.335	.020	-2.338	-2.338	-2.340	-2.303	-2.330
33	1	1	4	2.609	.018	2.623	.015	1.606	.003	1.611	1.611	1.608	1.582	1.612
34	1	1	6	.866	.007	.853	.057	.919	.002	-.917	-.918	-.918	*	*
35	1	1	8	.220	.006	.218	.022	.463	.002	.464	.466	.467	*	*
36	1	2	0	.755	.006	.756	.050	.863	.002	-.866	-.865	-.863	-.854	-.868
37	1	2	1	2.137	.014	2.127	.115	1.449	.003	1.454	1.453	1.450	-1.434	-1.459

38	1	2	2	.588	.004	.592	.035	.762	.001	.767	.766	.765	.755	.770
39	1	2	3	1.319	.011	1.328	.091	1.142	.002	-1.147	-1.147	-1.144	1.129	1.154
40	1	2	4	.297	.004	.297	.034	.541	.002	-.544	-.544	-.543	-.535	-.548
41	1	2	5	.558	.005	.557	.040	.741	.002	.740	.741	.740	*	*
42	1	2	6	.102	.004	.109	.011	.327	.001	.324	.325	.325	*	*
43	1	2	7	.174	.005	.176	.015	.416	.001	-.413	-.414	-.415	*	*
44	1	3	0	.235	.003	.239	.018	.484	.001	-.481	-.480	-.480	*	*
45	1	3	1	.676	.006	.664	.042	.811	.002	-.811	-.810	-.809	*	*
46	1	3	2	.201	.004	.192	.015	.436	.001	.432	.432	.432	*	*
47	1	3	3	.435	.007	.439	.029	.657	.001	.658	.658	.658	*	*
48	1	3	4	.094	.003	.107	.012	.321	.001	-.319	-.319	-.320	*	*
49	1	3	5	.205	.005	.205	.016	.449	.001	-.446	-.447	-.448	*	*
50	1	4	0	.245	.004	.241	.019	.488	.001	.485	.486	.486	*	*
51	1	4	2	.201	.004	.200	.017	.443	.001	-.442	-.443	-.444	*	*
52	2	2	0	1.141	.010	1.126	.076	1.056	.002	1.055	1.054	1.053	1.041	1.068
53	2	2	2	.927	.012	.909	.058	.948	.002	-.947	-.946	-.945	*	*
54	2	2	4	.502	.008	.494	.044	.699	.002	.695	.695	.695	*	*
55	2	3	0	.080	.004	.083	.012	.286	.001	-.285	-.285	-.286	*	*
56	2	3	1	.235	.004	.236	.018	.481	.001	.482	.483	.483	*	*
57	2	3	2	.072	.004	.068	.008	.260	.001	.259	.260	.260	*	*
58	2	3	3	.162	.004	.164	.016	.402	.001	-.400	-.401	-.402	*	*
Unweighted residual R3								.00578		.01044	.00247	.00242	.01500	.00555
Unweighted residual R1								.00491		.00542	.00249	.00237	.01225	.00827
Number of reflections used to calculate residuals								58		58	58	58	27	27

* denotes reflection not reported

Appendix D

The PL/I Program EXAMPLE

```
10.     //MJGHCKRY JOB MJGHC500,TIME=40
20.     // EXEC PLIXCG ,TIME=40
25.     //*MAIN LINES=10
30.     //PLI.SYSIN DD *
111.     EXAMPLE: PROCEDURE OPTIONS(MAIN) ;
112.       /*THIS PROGRAM DEALS WITH THE X-RAY SCATTERING FROM A LINE
113.         OF EQUIDISTANT H ATOMS,ALL SPIN-UP,OR A ROW OF HE,ASSUMING
114.       THAT THE SPIN-UP AND -DOWN COMPONENTS ARE IDENTICAL */
115.     DCL (SZERO(3,3),SSCRIPT(3,3),DIST,BASIS(3),PEXACT(3,3)) FLOAT(12);
116.    DCL (FOBS(0:30),PISOL(3,3),PXTAL(3,3),FCALI(0:30),FCALX(0:30))
116.1     FLOAT(12);DCL(SSCRIP(3,3),SZER(3,3))FLOAT(12);
117.    DCL (FZERO(3,3,0:30),FSCRIPT(3,3,0:30),FZER(3,3,0:30),
117.1         FSCRIP(3,3,0:30))COMPLEX FLOAT(12);
118.                      /* THE VARIABLES ARE AS FOLLOWS:
119.                       FOBS   THE "OBSERVED" STRUCTURE FACTORS
120.                       SZERO  THE ISOLATED ATOM BASIS OVERLAP MATRIX
121.                FZERO  THE     "        "    "   FOURIER TRANSFORM TENSOR
122.                       SSCRIPT THE CRYSTAL BASIS OVERLAP MATRIX
123.                       FSCRIPT THE     "        "   FOURIER TRANSFORM TENSOR
124.             BASIS   THE EXPONENTS ON THE 3 GAUSSIAN 1S BASIS FUNCTIONS
125.             PEXACT  THE (ASSUMED) EXACT DENSITY MATRIX FOR THE SYSTEM
126.             PISOL   THE LSQR BEST FIT P-MATRIX ASSUMING AN ISOLATED ATOM
127.             PXTAL   THE   "    "   "    "       ASSUMING OUR FORMALISM
128.              FCALI   THE CALCULATED STRUCTURE FACTORS FROM PISOL
129.            FCALX   THE       "          "          "     FROM PXTAL   */
130.
131.
132.      CALL ASSUMED(PEXACT);
133.        CALL SETUP (SZERO,FZERO,SSCRIPT,FSCRIPT,BASIS,DIST);
133.5   CALL INV2(SSCRIPT,SSCRIP);CALL POWER(SZERO,-0.5,SZER);
133.7    CALL SCATTER(FSCRIPT,SSCRIP,FSCRIP);
133.8    CALL SCATTER(FZERO,SZER,FZER);
134.     CALL CALCF (SSCRIP,FSCRIP,PEXACT,FOBS);
134.5   PUT SKIP DATA(FOBS,BASIS,DIST);
135.
136.            /* WE HAVE NOW CALCULATED THE F AND S TENSORS,WHICH HAVE
137.          NO ADJUSTABLE PARAMETERS,AND USED AN ARBITRARY "EXACT"
138.    SOLUTION PEXACT TO CALCULATE 30 OBSERVED REFLECTION AMPLITUDES
139.            FOBS,ASSUMED REAL. NOW WE WILL SHOW THAT THE LEAST-SQUARES
140.       "BEST-FIT" F IS PEXACT USING OUR FORMALISM FOR THE FULL-MATRIX
141.          CASE,  AND NOT PEXACT IF WE ASSUME ISOLATED ATOMS  */
142.
143.           /*TO PLAY , WE  COULD
144.        CALL ANOTHER (BASIS,DIST,SZERO,FZERO,SSCRIPT,FSCRIPT);
145.           WHICH WOULD USE A DIFFERENT BASIS,TO SEE WHAT HAPPENS */
145.5    CALL LSQRFIT(FOBS,SZER,FZER,PISOL);
146.     CALL LSQRFIT(FOBS,SSCRIP,FSCRIP,PXTAL);
149.      CALL CALCF(SZER,FZER,PISOL,FCALI);
150.      CALL CALCF(SSCRIP,FSCRIP,PXTAL,FCALX);
151.     CALL VIEWF(FOBS,FCALI,FCALX);
152.          CALL VIEWP(PEXACT,PISOL,PXTAL);
153.    GO TO THATSALL; /*WHICH IS JUST THE END STATEMENT */
154.
154.01  /*HERE IS A LIST OF SUBROUTINES
154.02  :::::::::::::::::::::::::::::::::::::::::::::::::::::::::::::::::::::::::::::
154.03  NAME              LINE         USE
154.04  -----------------------------------------------------------------------------
154.05  EXAMPLE            111          MAIN PROGRAM
154.06  ASSUMED            156         SETS UP THE "EXACT" P-MATRIX
154.07  BASISFN            167         THE GAUSSIAN BASIS FOR ALL CALCULATIONS
154.08  DISTFIX            172         THE INTERATOMIC DISTANCE
154.09  TRACEX             176         TRACE OF A COMPLEX MATRIX
154.1   TRACE              178         TRACE OF A REAL     MATRIX
154.11   INV2         179.1         CALCULATES THE SQUARE ROOT INVERSES OF
154.14                                THE TWO OVERLAP MATRICES
154.17   SCATTER          500         CHANGES F TO S**-.5*F*S**-.5
154.2   MATMULT            181          A-MATRIX TIMES B-MATRIX =C-MATRIX,REAL
154.23  MATMULX            187.1        A TIMES B = C,COMPLEX MATRICES
154.26  START              188         STARTING GUESS AT P FROM SUBROUTINE ASSUMED
154.29  SETUP              191         CALCULATES S AND F TENSORS FOR THE BASIS FUNCTIONS
154.32  SSOVLP             249         OVERLAP BETWEEN TWO S ORBITALS
154.35  FT                 261         FOURIER TRANSFORM OF AN S-ORBITAL PRODUCT
154.38  CALCF              271         CALCULATES THE STRUCTURE FACTORS FROM S AND F
154.41  VIEWF              284         OUTPUTS F-CALCULATEDS
154.44  VIEWP              305         OUTPUTS CALCULATED P-MATRICES
154.47  POWER             3200         A**N=B,REAL MATRICES.N=-.5,-1.,GENERALIZED INVERSE
154.5   CUBIC             3700         SOLVES CUBIC EQUATIONS.NOT USED.
154.53  PURIFY            4000         MCWEENY-PURIFIES AN IDEMPOTENT MATRIX
154.56  TENSOR            4070         CONTRACTS A RANK-3 TENSOR TO A MATRIX BY SUMMATION
154.59  LSQRFIT          4200           LEAST-SQUARE FITS P TO THE F-OBS
154.62  FIXEPS            4600          CALCULATES THE INDEX OF FIT'EPSILON'
154.65                                 */
155.           /* THE FOLLOWING ARE SMALL FUNCTIONS AND SUBROUTINES */
```

```
ASSUMED:PROCEDURE(PEXACT);
     /*THIS DEFINES THE ASSUMED 'EXACT' DENSITY MATRIX */
DCL (P(3,3),PEXACT(*,*)) FLOAT(12);DCL T FLOAT(12);
    T=.333333333333E+0          ;
 P(1,1)=T;P(1,2)=-T;P(1,3)=-T;
P(2,1)=-T;P(2,2)=T;P(2,3)=T;
P(3,1)=-T;P(3,2)=T;P(3,3)=T;
PEXACT=P; RETURN; END ASSUMED;

BASISFN :PROCEDURE (BASIS);
     /* THIS DEFINES THE EXPONENTS FOR THE AO BASIS OF THREE
          1S-TYPE GAUSSIANS EXP(-BASIS(I)*R**2)   */
   DCL BASIS(*) FLOAT(12);BASIS(1)=19.2406;BASIS(2)=2.89915;
       BASIS(3)=0.65341;
 /*L.C. SNYDER AND H.BASCH,'MOLECULAR WAVE FUNCTIONS AND PROPERTIES' USE THESE
 AS THE 3 EXPONENTS OF THE INNER AO OF H IN A DZ BASIS*/
       RETURN; END BASISFN;

DISTFIX:PROCEDURE(DIST);
  /* THIS IS THE INTERCELL , OR INTERATOMIC, DISTANCE, IN A.U. */
 /*T.C.ACTA41(1976)P 89,M. KERTESZ ET AL FIND THIS H-CHAIN DIST*/
DCL DIST FLOAT(12);DIST=1.88;RETURN;END DISTFIX;
  PUT SKIP LIST(BASIS,DIST);

TRACEX :PROCEDURE(X) RETURNS( COMPLEX FLOAT(12));
                /* THE TRACE OF A MATRIX*/
DCL X(*,*) COMPLEX FLOAT(12);
RETURN(X(1,1)+X(2,2)+X(3,3));END TRACEX ;

TRACE :PROCEDURE(X) RETURNS(  FLOAT(12));
                /* THE TRACE OF A COMPLEX MATRIX*/
DCL X(*,*)  FLOAT(12);
RETURN(X(1,1)+X(2,2)+X(3,3));END TRACE ;

INV2:PROCEDURE(SFULL,SINV2);
/*FOR SOME REASON,IT WORKS BETTER TO TAKE THE INVERSE OF THE INVERSE
SQUARE ROOT OF THE INVERSE,(((M**-1)**-.5)**-1) THAN THE SIMPLE
 M**-.5 ONE-STEP METHOD. I THINK IT DOESNT LIKE EIGENVALS >1*/
DCL (SFULL(*,*),SINV2(*,*))  FLOAT(12);
 DCL(ST(3,3),SH(3,3)) FLOAT(12);
     ST=0.;SH=0.;
 ST=1.E-8*SFULL;CALL POWER(ST,-.5,SH);
  SINV2=1.E-4*SH;
     ST=0.;SH=0.;
RETURN;END INV2;

MATMULT:PROCEDURE(A,B,C);
                /* THE MATRIX EQUATION  C=A*B   */
DCL (D,A(*,*),B(*,*),C(*,*))FLOAT(12),(I,J,K)DECIMAL FIXED(1,0);
 /*THE CALLING ROUTINE MUST NAME C DIFFERENTLY FROM A AND B*/
          C=C-C;
DO I=1 TO 3;DO J=1 TO 3;DO K=1 TO 3;
 ON UNDERFLOW D=0.;C=A(I,K)*B(K,J);
     C(I,J)=C(I,J)+D;END;END;END;RETURN;END MATMULT;

MATMULX:PROCEDURE(A,B,C);
          /* THE COMPLEX MATRIX EQUATION  C=A*B   */
DCL (D,A(*,*),B(*,*),C(*,*)) COMPLEX FLOAT(12),(I,J,K)DECIMAL
    FIXED(1,0);
          C=0.0 ;
 /*THE CALLING ROUTINE MUST NAME C DIFFERENTLY FROM A AND B*/
DO I=1 TO 3;DO J=1 TO 3;DO K=1 TO 3;
 ON UNDERFLOW D=0.;D=A(I,K)*B(K,J);
   C(I,J)=C(I,J)+D;END;END;END;RETURN;END MATMULX;

  START: PROCEDURE(P); /* STARTING GUESS FOR P-CALCULATED */
DCL P(*,*) FLOAT (12);P=0.;P(1,1)=1;

RETURN;END START;
/*NOW THE IMPORTANT PARTS  */
  SETUP: PROCEDURE(SZERO,FZERO,SSCRIPT,FSCRIPT,BASIS,DIST);
     /* THIS CALCULATES THE OVERLAP AND FOURIER TRANSFORMS OF THE
    PAIRS OF BASIS FUNCTIONS,FOR THE ISOLATED ATOM APPROXIMATION
     ("ZERO" DIFFERENTIAL OVERLAP BETWEEN CELLS) AND FOR THE
     REALISTIC CRYSTAL ("SCRIPT" ARRAYS) WITH INTERATOMIC SPACING
"DIST" A.U.                 */
   DCL(BASIS(*),SZERO(*,*),SSCRIPT(*,*),PI,DIST,WAY)FLOAT(12);
DCL ESERR FLOAT(12);DCL EFERR COMPLEX FLOAT(12);
DCL(FZERO(*,*,*),FSCRIPT(*,*,*)) COMPLEX FLOAT(12);
 DCL(I,J, K ) DECIMAL FIXED(2,0);PI=3.14159265359;
DCL STEN(3,3,-10:10)FLOAT(12),FTEN(3,3,C:3C,-10:10)COMPLEX FLOAT(12);
   CALL BASISFN(BASIS);
  CALL DISTFIX(DIST);
 ISOLAT: /*  ISOLATED ATOM APPROX */
  DO I=1 TO 3;DO J=1 TO 3;
    SZERO(I,J)=SSOVLP(BASIS(I),0.,BASIS(J),0.);
     DO K= 0 TO 30;
```

```
207.          FZERO(I,J,K)=FT(BASIS(I),0.,BASIS(J),0.,K);
208.
209.
210.           FZERO(J,I,K)=CONJG(FZERO(I,J,K));     END;
211.          SZERO(J,I)=SZERO(I,J);     END; END;
212.          FULL:  /* FULL CRYSTAL,INCLUDING TENTH-NEIGHBOR  OVERLAPS */   ;
213.        DCL(L,M,N)DECIMAL FIXED(6,0),(WL,WM)FLOAT(12);
214.          /*SET UP THE M-TH NEIGHBOR SUBMATRICES OF F AND S  */
215.        DO I=1 TO 3;DO J=1 TO 3;STEN(I,J,0)=SZERO(I,J);
216.         STEN(J,I,0)=SZERO(J,I);DO M=1 TO 10;WAY=M*DIST;
217.         STEN(I,J,M)=SSOVLP(BASIS(I),0.,BASIS(J),WAY);
218.         STEN(J,I,M)=STEN(I,J,M);STEN(I,J,-M)=STEN(I,J,M);
219.          STEN(J,I,-M)=STEN(I,J,M);
220.            DO K=0 TO 30;
221.           FTEN(I,J,K,M)=FT(BASIS(I),0.,BASIS(J),WAY,K);
222.          FTEN(J,I,K,M)=CONJG(FTEN(I,J,K,M));
223.         FTEN(I,J,K,-M)=FTEN(J,I,K,M);
224.           FTEN(J,I,K,-M)= FTEN(I,J,K,M);
225.        END;END;DO K=0 TO 30;FTEN(I,J,K,0)=FZERO(I,J,K);
226.                FTEN(J,I,K,0)=FZERO(J,I,K);END;END;END;
227.          SSCRIPT=0.;FSCRIPT=0.;
228.        DCL(SERY(-10:10),C(-10:10),V)  FLOAT(12);C=0.;SERY=0.;
229.         DCL(Z,Q)DECIMAL FIXED(7,0);V=2.*PI*PI*DIST;
230.         DO L=-10 TO 10; C(L)= COS(V*L);END;
231.           DO M=-59999 TO 59999;IF M=0. THEN GO TO JUMP1;
232.         DO L=-10 TO 0;Z=M+L;Q=Z+M;IF Z=0. THEN GO TO JUMP2;
233.          SERY(L)=SERY(L)+(C(L)-COS(V*Q))/(M*Z);  GO TO LINSET;
234.          JUMP2:SERY(L)=SERY(L)+V*SIN(V*M)/M;
235.         LINSET:  END;  /* LOOP OVER L  */   GO TO MINSET;
236.        JUMP1:SERY(0)=SERY(0)+4*PI*PI*(PI*DIST)*(PI*DIST);
237.          DO L=-10 TO -1;SERY(L)=SERY(L)+V*SIN(V*L)/L;END;
238.          MINSET: END;V=V*DIST;SERY=SERY/V;
239.           DO N=1 TO 10;SERY(N)=SERY(-N);END;
239.5          DO L=-10 TO 10;DO I=1 TO 3;DO J=1 TO 3;
240.        IF(STEN(I,J,L)<1.E-15) THEN ESERR=0.;
240.3       ELSE    ESERR=SERY(L)*STEN(I,J,L);
240.5         SSCRIPT(I,J)=SSCRIPT(I,J)+ESERR;
241.          DO K=0 TO 30; IF ABS(FTEN(I,J,K,L))<1.E-20 THEN EFERR=0.;
242.        ELSE EFERR=SERY(L)*FTEN(I,J,K,L);
242.5        FSCRIPT(I,J,K)=FSCRIPT(I,J,K)+EFERR;  END; END ;   END;END;
243.          PUT SKIP(2) LIST('F AND S TENSORS ALL DONE');
243.5          RETURN;END SETUP;
244.
248.
249.           SSOVLP:PROCEDURE(A,RA,B,RB) RETURNS(FLOAT(12));
250.          /* THIS CALCULATES THE OVERLAP BETWEEN TWO NORMALIZED 1S-TYPE
251.            GAUSSIANS CENTERED AT RA AND RB WITH EXPONENTS A AND   B
252.            RESPECTIVELY. THIS FORMULA CAN BE DERIVED FROM THE FORMULA OF
253.           CHANDLER AND SPACKMAN,ON PAGE 342 OF ACTA CRYST.,VOL.A34(1978),
254.            BY SETTING K=0.          */
255.            DCL(A,B,RA,RB,PI,P,EXPO) FLOAT(12);PI=3.14159265359;
255.5        ON UNDERFLOW GO TO   SZIP;
256.          P=A+B;EXPO=EXP(-(A*B)/P*(RA-RB)*(RA-RB));
257.         P=PI/P;P=P*SQRT(P)*EXPO; P=P*(4*A*B/PI/PI)**.75;
258.           RETURN(P); SZIP:RETURN(0);END SSOVLP;
259.
261.           FT:PROCEDURE(A,RA,B,RB,K)RETURNS(COMPLEX FLOAT(12));
262.          /* THIS CALCULATES THE FOURIER TRANSFORM OF THE PRODUCT OF TWO
263.           NORMALIZED 1S GAUSSIANS LOCATED A DISTANCE(RA-RB) APART.
264.           THE FORMULA IS FROM ACTA CRYST. A34(1978)P.342     */
264.5        ON UNDERFLOW GO TO  FZIP;
265.            DCL(A,B,RA,RB,PI,P,R,KF)FLOAT(12), K  DECIMAL FIXED(2,0);
266.            DCL  INTER COMPLEX FLOAT(12);
267.         PI=3.14159265359;P=A+B;KF=K*2.*PI;R=RA-RB;R=R*R;
268.         INTER=EXP(-A*B*R-KF*KF*.25+1.I*KF*(A*RA+B*RB))/P);
269.         P=PI/P;P=P*SQRT(P);INTER=P*INTER;
269.5        INTER=INTER*(4*A*B/PI/PI)**.75;
270.           RETURN(INTER);FZIP:RETURN(0); END FT;
270.5
271.          CALCF:PROCEDURE(S,F,P,FCAL);
272.             /*FCAL(I)=TRACE(P*F(I)   )  */
273.           DCL(S(*,*),P(*,*),FCAL(*)) FLOAT(12);
273.5          DCL (TEMP(3,3), TMP(3,3)) COMPLEX  FLOAT(12);
274.            DCL( I,J,K,L) DECIMAL FIXED(2,0);
275.           DCL(F(*,*,*),SMINUS2(3,3)) COMPLEX FLOAT(12);
276.         SMINUS2=COMPLEX(S,0.);
277.        DO K=0 TO 30;DO I=1 TO 3;DO J=1 TO 3;
278.         TMP(I,J)=F(I,J,K);  END;END;
279.        CALL MATMULX(COMPLEX(P,0.),TMP,TEMP);
280.        FCAL(K)=REAL(TRACEX(TEMP));
281.           END  /* K LOOP */   ;
283.           RETURN;END CALCF;
284.          VIEWF: PROCEDURE(FOBS,FCAL,FCALX);
285.                /* THIS PROCEDURE PRINTS,IN TABULAR FORM,THE
286.              EXACT SCATTERING AMPLITUDES,AND THOSE CALCULATED
287.              IN EACH OF TWO METHODS: ISOLATED ATOMS (I) AND
288.               FULL CRYSTAL (X), AND GIVES THE R-FACTOR
289.                 SUM(|FCALJ-|FOBSJ|)/SUM(|FOBSJ|)          */
290.          PUT PAGE;
```

```
            PUT SKIP LIST('F-OBSERVED','F-ISOLATED','F-CRYSTAL'
           ,'ERROR-ISOL','ERROR-XTAL');
         DCL (FOBS(*),FCALI(*),FCALX(*),ERRI,ERRX,RISOL,RXTAL,SUM)FLOAT(12);
            DCL I FIXED(2,0);
              RISOL=0.;RXTAL=0.;SUM=0.;
               DO I=1 TO 30;
                 SUM=SUM+ABS(FOBS(I));
                 ERRX=ABS(ABS(FOBS(I))-ABS(FCALX(I)));RXTAL=RXTAL+ERRX;
              ERRI=ABS(ABS(FOBS(I))-ABS(FCALI(I)));RISOL=RISOL+ERRI;
               PUT SKIP LIST(FOBS(I),FCALI(I),FCALX(I),ERRI,ERRX);END;
              RISOL=RISOL/SUM;RXTAL=RXTAL/SUM;
              PUT SKIP LIST('R-FACTOR =  ',RISOL,RXTAL);
                 RETURN;END VIEWF;

              VIEWP:PROCEDURE(PEXACT,PISOL,PXTAL);
             /*  THIS PRINTS OUT THE 3 P-MATRICES AND AN ERROR MEASURE
               SUM(I,J)(PEXACT(I,J)**2-PCALC(I,J)**2)  */
               DCL(PEXACT(*,*),PISOL(*,*),PXTAL(*,*)) FLOAT(12);
               DCL(ERRI,ERRX) FLOAT(12),(I,J) DECIMAL FIXED(1,0);
               PUT PAGE;ERRI=0.;ERRX=0.;
               PUT SKIP LIST(' "EXACT" DENSITY MATRIX ');
             DO I=1 TO 3;
              PUT SKIP LIST(PEXACT(I,1),PEXACT(I,2),PEXACT(I,3)); END;
               PUT SKIP;
            PUT SKIP LIST ('DENSITY MATRIX CALCULATED FOR AN ISOLATED ATOM');
              DO I=1 TO 3;
               PUT SKIP LIST(PISOL(I,1),PISOL(I,2),PISOL(I,3));
            DO J=1 TO 3;ERRI=ERRI+(PEXACT(I,J)*PEXACT(I,J)-PISOL(I,J)*PISOL(I,J));
              END;END;
             PUT SKIP LIST('THE ERROR IS',ERRI); PUT SKIP;
           PUT SKIP LIST ('THE DENSITY MATRIX CALCULATED FOR THE WHOLE CRYSTAL');
              DO I=1 TO 3;
               PUT SKIP LIST(PXTAL(I,1),PXTAL(I,2),PXTAL(I,3));
            DO J=1 TO 3;ERRX=ERRX+(PEXACT(I,J)*PEXACT(I,J)-PXTAL(I,J)*PXTAL(I,J));
              END;END;
               PUT SKIP LIST ('THE ERROR IS',ERRX);PUT SKIP;
                ERRI=ERRI/ERRX;
             PUT SKIP LIST('THE ISOLATED ATOM APPROXIMATION IS',ERRI);
            PUT LIST('TIMES AS BAD AS OUR TREATMENT COMPARED TO THE EXACT P');
                    RETURN; END VIEWP;
           SCATTER:PROCEDURE(F,S,FADJ);/*THIS CHANGES F IN A BASIS WITH
                 OVERLAP MATRIX S**-2 TO AN ORTHONORMAL BASIS */
            DCL(F(*,*,*),FADJ(*,*,*),SMINUS2(3,3),FNEW(3,3,0:30),NO)
            COMPLEX FLOAT(12);DCL S(*,*) FLOAT(12),(I,J,K,L) REAL FIXED(2);
             SMINUS2=COMPLEX(S,0);
             FNEW=0.;FADJ=0.;
            DO I=1 TO 3;DO J=1 TO 3;DO L=1 TO 3;DO K=0 TO 30;
               IF ABS( F(L,J,K))<1.E-25 THEN NO=0;ELSE
                     NO=SMINUS2(I,L)*F(L,J,K);
              FNEW(I,J,K)=FNEW(I,J,K)+NO;
           END;END;END;END;
            DO I=1 TO 3;DO J=1 TO 3;DO L=1 TO 3;DO K=0 TO 30;
               IF ABS( FNEW(I,L,K))<1.E-25 THEN NO=0.;ELSE
                     NO=FNEW(I,L,K)*SMINUS2(L,J);
             FADJ(I,J,K)=FADJ(I,J,K)+NO;
           END;END;END;END;
                     RETURN;END SCATTER;

          POWER:PROCEDURE(A,N,B);
             /*THIS CALCULATES THE MATRIX B=A**N,WHERE N
             IS EITHER -1.0 OR -0.5                    */
          DCL (A(*,*),B(*,*),C(3,3),CC(3,3),D3(3,3),DIF,DET) FLOAT(12);
           DCL(T(3,3),D4(3,3)) FLOAT(12);
          DCL(N,I,J,K,L,M,H) DECIMAL FIXED(2,1);
           IF N=-1.0 THEN GO TO INVERT;
           IF N=-1.1 THEN GO TO GENINV;
           IF N=-0.5 THEN GO TO RUSSIA;
           PUT SKIP LIST('NOT IMPLEMENTED YET');B=9999.;RETURN;
          RUSSIA: /* THIS ITERATIVE PROCEDURE TO GENERATE THE INVERSE
                     SQUARE ROOT OF A COMES FROM REFERENCE #9 IN
                     DOKL. AKAD. NAUK SSSR 254(SEPT. '80)P. 370,TO
                     VESTN. LENINGR. UNIV. 4 (1965)  P. 5,BY
                     V.N. GOLKIN AND M.M. MESTECHKIN                */
            D=0.;D(1,1)=1./SQRT(3.);D(2,2)=D(1,1);D(3,3)=D(1,1);
          DET=1000.;
           DO WHILE( DET > 1.E-8);
             CALL MATMULT(D,A,T);CALL MATMULT(T,D,DD);
             CALL MATMULT(CC,C,D3);CALL MATMULT(D,DD,D4);
             B=1.5*D-(D4*D3)/4.0; /*THE RUSSIAN ITERATIVE FORMULA */
           DO I=1 TO 3;B(I,I)=ABS(B(I,I));END;
           /*THE ABS(DIAGONAL) IS TO GET THE POSITIVE SQRT,NOT THE NEGATIVE */
             DET=0.;
             DO I=1 TO 3;
                          DO J=1 TO 3; DIF=ABS(B(I,J)-D(I,J));
               DIF=MIN(10.,DIF);DET=DET+DIF*DIF;
           END;END;DET=DET*(A(1,1)+A(2,2)+A(3,3));
            /*NOW FOR THE NEXT ITERATION*/  D=B;
          END; /* THE END OF THE DO WHILE LOOP.B=A**(-1/2)  */
          RETURN;
```

```
3231.       INVERT: /* BY THE METHOD OF THE COFACTORS D(I,J)  */
3232.       D(1,1)=A(2,2)*A(3,3)-A(2,3)*A(3,2);
3233.       D(1,2)=-A(2,1)*A(3,3)+A(3,1)*A(2,3);D(2,1)=D(1,2);
3234.       D(1,3)=A(2,1)*A(3,2)-A(3,1)*A(2,2); D(3,1)=D(1,3);
3235.       D(2,2)=A(1,1)*A(3,3)-A(3,1)*A(1,3);
3236.       D(3,2)=-A(1,1)*A(2,3)+A(2,1)*A(1,3);D(2,3)=D(3,2);
3237.       D(3,3)=A(1,1)*A(2,2)-A(2,1)*A(1,2);
3238.        DET=A(1,1)*D(1,1)+A(1,2)*D(1,2)+A(1,3)*D(1,3);
3239.        B=D/DET;
3240.        RETURN;
3241.
3242.        GENINV:/*THIS DOESN'T REALLY CALCULATE THE -1.ITH POWER OF A MATRIX.
3243.                 RATHER,IT CALCULATES THE GENERALIZED INVERSE A*,IN THE
3244.                 MOORE-PENROSE SENSE,BY THE ITERATIVE PROCEDURE OF
3245.                 GUPTA,AS REPORTED BY A.L.MACKAY, IN ACTA CRYST A33(1977)PAGE 213.
3246.        THIS SUB-SUBROUTINE ISAT CALLED AND STILL HAS BUGS   IN IT    */
3247.        B=A*.05;
3248.       DD=0.;DD(1,1)=2;DD(2,2)=2.;DD(3,3)=2.;
3249.        AGAIN:CALL MATMULT(A,B,C);CALL MATMULT(B,DD-D,D3);
3250.        /*D3 IS THE NEXT ITERATE*/
3251.       DET=D(1,1)*D(2,2)*D(3,3);  B=D3;
3252.       IF(CEIL(DET)-DET )> .00001 THEN GO TO AGAIN;
3253.        /*B HAS CONVERGED BY MACKAY'S SUGGESTED CRITERION*/
3254.       RETURN;       END POWER;
3590.
3700.       CUBIC:PROCEDURE(C,R);
3710.        /*  Q IS THE COEFFICIENT VECTOR OF THE CUBIC EQUATION WITH ROOTS
3720.             R, WHICH ARE HOPEFULLY REAL                    */
3730.       DCL Q(*) FLOAT(12), (A,B,C,D,R(*)) COMPLEX FLOAT(12);
3740.       A=(3*Q(3)-Q(2)*Q(2))/9.;
3750.       B=(9.*Q(2)*Q(3)-27.*Q(4)-2.0*Q(2)*Q(2))/54.;
3760.       C=SQRT(A*A*A+B*B);
3770.       IF REAL(C)>0. THEN PUT SKIP LIST(' COMPLEX ROOTS OF OVERLAP MATRIX');
3780.        D=(B-C)**.333333333333;
3790.        C=(B+C)**.333333333333;
3800.        R(1)=C+D-Q(2)/3.;
3810.        R(2)=(C+D)/(-2.)-Q(2)/3.;
3820.        R(3)=R(2)-.5I*SQRT(3.)*(C-D);
3830.        R(2)=R(2)+.5I*SQRT(3.)*(C-D);
3840.          RETURN;  END CUBIC;
3890.
4000.       PURIFY:PROCEDURE(A);
4010.        /* THIS PROCEDURE PURIFIES,BY THE MCWEENY PROCESS,A MATRIX.
4020.             THE ITERATIVE EQUATION IS A(NEW)=3*A**2-2*A**3       */
4030.       DCL (A(*,*),A2(3,3),A3(3,3) ) FLOAT(12);
4040.        CALL MATMULT(A,A,A2);CALL MATMULT(A,A2,A3);
4050.        A=3.*A2-2.*A3;A(2,1)=A(1,2);A(3,1)=A(1,3);A(3,2)=A(2,3);
4055.              RETURN;END PURIFY;
4060.
4070.        TENSOR:PROCEDURE(F2,F3,WEIGHT);/*F2=SUM(K)F3(K)*WEIGHT(K)  */
4080.        DCL(F2(*,*),F3(*,*,*))COMPLEX FLOAT(12); DCL WEIGHT(*)FLOAT(12);
4090.        DCL(I,J,K) DECIMAL FIXED(2,0);   F2=0.;
4100.        DO I=1 TO 3;DO J=1 TO 3;DO K=1 TO 30;
4110.          F2(I,J)=F2(I,J)+F3(I,J,K)*WEIGHT(K);
4120.        END;END;END;
4130.       RETURN;END TENSOR;
4190.
4200.       LSQRFIT:PROCEDURE(FOBS,S,F,P);
4210.        /*  THIS GENERATES THE "BEST-FIT" P MATRIX TO THE OBSERVED
4220.          SCATTERING FACTORS FOBS,IN THE ORTHONORMAL BASIS WITH FOURIER
4230.          TRANSFORM F.  NOTE THAT THE TWO FORMALISMS ISOL AND XTAL ARE
4240.          TREATED ON AN ENTIRELY EQUIVALENT FOOTING                */
4250.       DCL(I,J,K,L,SIGNUM(30))FIXED(2,0);DCL ITER FIXED(5);
4255.       DCL (F(*,*,*),GEE(3,3),
4260.                 GTWICE(3,3))COMPLEX FLOAT(12);
4265.       DCL ( S(*,*),ONE(3,3),WEIGHT(30),
4270.             TEMP(3,3),PINITL(3,3),P(*,*),NOR,FCAL(0:30),
4275.            OHAT(2,2),OSHOE(2,2),EPS,EPSINIT,EPSLOW,DOF,DET,
4280.       PTEXT(3,3),LAMBDA(2),   B(2),FOBS(*)   ) FLOAT(12);
4285.       ITER=1;ONE=0;DO I=1 TO 3;ONE(I,I)=1.00;END;
4300.       CALL START(PINITL);P=PINITL;
4305.       CALL CALCF(S,F,P,FCAL);CALL FIXEPS(FOBS,FCAL,EPSINIT);
4310.       EPS=.75*EPSINIT;EPSLOW=EPSINIT;
4320.       LOOPUP: /*THIS THE ITERATIVE PROCEDURE  */
4335.         CALL CALCF(S,F,P,FCAL);
4340.       DO K=1 TO 30;SIGNUM(K)=SIGN(FCAL(K)-FOBS(K)); END;    WEIGHT=SIGNUM;
4345.       GEE=0.;  CALL TENSOR(GEE,F,WEIGHT);
4350.          CALL MATMULX(GEE,GEE,GTWICE);
4355.          OSHOE(1,1)=3;
4360.          OSHOE(1,2)=REAL(TRACEX(GEE));OSHOE(2,1)=OSHOE(1,2);
4365.          OSHOE(2,2)=REAL(TRACEX(GTWICE));
4370.        DET=OSHOE(1,1)*OSHOE(2,2)-OSHOE(1,2)*OSHOE(2,1);
4375.        OHAT(1,1)=OSHOE(2,2)/DET;
4380.        OHAT(1,2)=-OSHOE(2,1)/DET;
4385.        OHAT(2,1)=-OSHOE(1,2)/DET;
4390.        OHAT(2,2)=OSHOE(1,1)/DET;
4395.        B(1)=1.-TRACE(P);
4400.        B(2)=EPS;
4405
```

```
4410.        DO K=1 TO 30;
4415.        B(2)=B(2)+FOBS(K)*SIGNUM(K)-FCAL(K)*SIGNUM(K);  END;
4420.          LAMBDA(1)=CHAT(1,1)*B(1)+CHAT(1,2)*B(2);
4425.          LAMBDA(2)=CHAT(2,1)*B(1)+CHAT(2,2)*B(2);
4430.       /*************************************************/
4435.        PNEXT=P+LAMBDA(1)*ONE+LAMBDA(2)*REAL(GEE);
4440.       /*************************************************/
4443.          DO I=1 TO 3;IF PNEXT(I,I)>0. THEN GO TO OKAY;
4444.       ELSE PNEXT(I,I)=ABS(PNEXT(I,I)); OKAY:END;
4444.1       DO I=1 TO 3;IF(P(I,I))>1. THEN P(I,I)=2-P(I,I);END;
4450.        DO I=1 TO 5;CALL PUTIFY(PNEXT);END;
4455.        GOF=0.;
4460.        DO I=1 TO 3;DO J=1 TO 3;GOF=GOF+ABS(P(I,J)-PNEXT(I,J));END;END;
4465.        P=PNEXT;IF ABS(LAMBDA(1))+ABS(LAMBDA(2))<1.E-10 THEN GOTO FINISH;
4467.       IF EPS<1.E-8 THEN GO TO BACK;
4470.          ITER=ITER+1;
4475.       IF ITER=3000 THEN GO TO NOCONVG;ELSE GO TO LOOPUP;
4480.
4485.        NOCONVG: IF(ABS((EPSLOW-EPS)/EPS))<1.E-2 THEN GO TO BACK;
4490.            ELSE EPS=SQRT(EPS*EPSLOW);
4495.               ITER=1;PUT LIST('TOO FAST',EPS);  GO TO LOOPLP;
4500.
4505.        FINISH: PUT SKIP DATA(EPS,ITER,P,GOF,LAMBDA);
4507.       PUT SKIP LIST('EPS GOING DOWN');  CALL FIXEPS(FOBS,FCAL,EPSINIT);
4508.        PUT DATA (EPSINIT);IF EPSINIT/EPS>1.2 THEN PUT SKIP LIST('UH OH');
4508.5       PUT SKIP;EPS=SQRT(EPS*EPSINIT);
4510.            EPSLOW=MIN(ESLOW,EPSINIT);EPS=.66*EPS;ITER=1;
4515.           GO TO LOOPUP;
4520.
4525.        BACK:PUT SKIP;PUT SKIP DATA(LAMBDA,EPS,P);
4530.        PUT SKIP LIST('MINIMUM EPSILON FOR CONVERGENCE IN 3000 ITERATIONS');
4535.        RETURN;END LSQFIT;
4540.
4545.
4550.
4600.        FIXEPS:PROCEDURE(FOBS,FCAL,EPS);
4510.         DCL(FOBS(*),FCAL(*),EPS) FLOAT(12);DCL K DECIMAL FIXED(2);
4520.              EPS=0.;
4630.        DO K=1 TO 30;EPS=EPS+ABS(FCAL(K)-FOBS(K));END;
4650.        RETURN;END FIXEPS;
4650.
10000.      THATSALL:     END EXAMPLE;
99998.     //GO.SYSIN  DD  *
99999.     /*
```

Appendix E

Subroutines to Explicitly Impose the Idempotency Constraint

```
ROSEN: PROCEDURE(P,DIM,NOR,BEND);/*THIS SUBROUTINE CALCULATES BEND;
        AN IDEMPOTENT PRO-JECTOR ONTO THE SUBSPACE OF IDEMPOTENT
        AND N-ORMALIZED P-MATRICES FROM THE FULL SPACE OF MATRICES
        IN THE SMALL-CORRECTION TANGENT LIMIT. SEE ROSEN,SIAM J.
        APPL. MATH.,9(1961) PP. 514-553                    */

 DCL(P(*,*),BEND(*,*),NOR,PROD(2,2),PRODINV(2,2) ) FLOAT(12);
 DCL (DIM,LENG,I,J) DECIMAL FIXED(2);LENG=DIM*(DIM + 1)/2;
 DCL(M(2,LENG),MADJ(LENG,2),ALMOST(2,LENG),DELP(DIM,DIM),
      DELPVEC(LENG) )   FLOAT(12);

 M,MADJ,ALMOST,BEND,PROD=0.;
 CALL DELIDEM(P,DIM,DELP);CALL PACK(DELP,DIM,DELPVEC);
 DO I=1 TO LENG;M(1,I),MADJ(I,1)=DELPVEC(I);END;
 DELP=0.;DO I=1 TO DIM;DELP(I,I)=1.00000;END;
 CALL PACK(DELP,DIM,DELPVEC);
 DO I=1 TO LENG;M(2,I),MADJ(I,2)=DELPVEC(I);END;
 CALL RECTANG(M,MADJ,2,LENG,2,PROD);
 /*THE FIRST ROW OF M IS THE IDEMPOTENCY,THE SECOND ROW IS
    THE NORMALIZATION                                  */
 PRODINV(1,1)=PROD(2,2);PRODINV(2,2)=PROD(1,1);
 PRODINV(1,2)=-PROD(2,1);PRODINV(2,1)=-PROD(1,2);
 PRODINV=PRODINV/(PROD(2,2)*PROD(1,1)-PROD(2,1)*PROD(1,2));
 CALL RECTANG(PRODINV,M,2,2,LENG,ALMOST);
 CALL RECTANG(MADJ,ALMOST,LENG,2,LENG,BEND);BEND=DELP-BEND;
   RETURN;END ROSEN;


DELIDEM:PROCEDURE(P,DIM,DELP);/*THE DERIVATIVE OF THE
                                IDEMPOTENCY CONSTRAINT */
  DCL(P(*,*),DELP(*,*),P2P(99,99) CONTROLLED) FLOAT (12);
  DCL(I,J,K,L,DIM) DECIMAL FIXED(2);
 ALLOCATE P2P(DIM,DIM);P2P=0.;DELP=0.;
 CALL MATMULT(P,P,DIM,P2P);P2P=P2P-P; /* P2P=P SQUARED MINUS P */
 DO I=1 TO DIM;    /*THE DIAGONAL ELEMENTS OF DELP FIRST */
  DELP(I,I)=2*P2P(I,I)*(2*P(I,I)-1.00);
  DO J=1 TO DIM;
    IF I=J THEN GO TO NEXTDIAG;
    DELP(I,I)=DELP(I,I)+4*P(I,J)*P2P(I,J);
NEXTDIAG:END;END;
   /*  NOW THE OFF-DIAGONAL ELEMENTS  */
DO I=1 TO DIM;DO J=I+1 TO DIM;
DELP(I,J)=4*((P(I,J)*(P2P(I,I)+P2P(J,J))+P2P(I,J)*(P(I,I)+P(J,J)));
DO K=1 TO DIM;IF K=I THEN GO TO NEXTK;IF K=J THEN GO TO NEXTK;
  DELP(I,J)=DELP(I,J)+4*(P(I,K)*P2P(K,J)+P(J,K)*P2P(K,I));
NEXTK:END;
NEXTIJ:DELP(J,I)=DELP(I,J); END;END;
FREE P2P;RETURN;END DELIDEM;/*I DERIVEC THIS MYSELF */
```

Appendix F

Subroutines to Go To and From a Local Coordinate Frame

```
TOPAS:PROCEDURE(OLDXYZ,NEWXYZ,ROT,TRANS);
      /* THIS MOVES ALL COORDINATES TO A PRINCIPAL AXIS SYSTEM
      DEFINED BY THE THREE ANGLES ROT AND THE THREE TRANSLATIONS
      TRANS, USING THE SET OF MATRICES GIVEN IN
      BIANCHI,GREMASCHI,MOROSI,AND SIMONETTA
      CHEM. PHYS. 22 (1977 ) P. 268                    */

DCL (OLDXYZ(*,*),OLD(3),NEWXYZ(*,*),NEW(3),
     ROT(3),TRANS(3),  MATX(3,3),MAT(3,3),
     MAT1(3,3),MAT2(3,3),MAT3(3,3),  C(3),S(3) )  FLOAT(12);
DCL (I,J,NATOMS) DECIMAL FIXED(2);
NATOMS=DIM(OLDXYZ,1);
NEWXYZ=0.00;
LINEAR:  /* TRANSLATORY PART */
DO I=1 TO NATOMS; DO J=1 TO 3;
 NEWXYZ(I,J)=OLDXYZ(I,J) + TRANS(J);
END;END;
TWIST: /* FIRST CONSTRUCT A ROTATION MATRIX,THEN ROTATE THE
          COORDINATES WITH THIS UNITARY LEFT-MULTIPLICATION */
DO I=1 TO 3;C(I)=COS(ROT(I));S(I)=SIN(ROT(I));END;
MAT1,MAT2,MAT3=0.00;
MAT1(1,1),MAT2(2,2),MAT3(3,3)=1.00;
MAT1(2,2),MAT1(3,3)=C(1);
MAT1(2,3)=S(1);MAT1(3,2)=-S(1);
MAT2(3,3),MAT2(1,1)=C(2);
MAT2(1,3)=S(2);MAT2(3,1)=-S(2);
MAT3(1,1),MAT3(2,2)=C(3);
MAT3(1,2)=S(3);MAT3(2,1)=-S(3);

CALL MATMULT(MAT2,MAT1,3,MATX);
CALL MATMULT(MAT3,MATX,3,MAT );
DO I= 1 TO NATOMS;DO J=1 TO 3;
 OLD(J)=NEWXYZ(I,J);END;
 CALL MET(MAT,OLD,3,NEW);
 DO J=1 TO 3;NEWXYZ(I,J)=NEW(J);END;
END;
RETURN;END TOPAS;


FROMPAS:PROCEDURE(OLDXYZ,NEWXYZ,ROT , TRANS);
      /* THIS MOVES ALL COORDINATES FROM A PRINCIPAL AXIS SYSTEM
      DEFINED BY THE THREE ANGLES ROT AND THE THREE TRANSLATIONS
      TRANS, USING THE SET OF MATRICES GIVEN IN
      BIANCHI,GREMASCHI,MOROSI,AND SIMONETTA
      CHEM. PHYS. 22 (1977 ) P. 268                    */

DCL (OLDXYZ(*,*),OLD(3),NEWXYZ(*,*),NEW(3),
     ROT(3),TRANS(3),  MATX(3,3),MAT(3,3),
     MAT1(3,3),MAT2(3,3),MAT3(3,3),  C(3),S(3) )  FLOAT(12);
DCL (I,J,NATOMS) DECIMAL FIXED(2);
NATOMS=DIM(OLDXYZ,1);
OLDXYZ=0.00;
TWIST: /* FIRST CONSTRUCT A ROTATION MATRIX,THEN ROTATE THE
          COORDINATES WITH THIS UNITARY LEFT-MULTIPLICATION */
DO I=1 TO 3;C(I)=COS(ROT(I));S(I)=SIN(ROT(I));END;
MAT1,MAT2,MAT3=0.00;
MAT1(1,1),MAT2(2,2),MAT3(3,3)=1.00;
MAT1(2,2),MAT1(3,3)=C(1);
MAT1(2,3)=-S(1);MAT1(3,2)=S(1);
MAT2(3,3),MAT2(1,1)=C(2);
MAT2(1,3)=-S(2);MAT2(3,1)=S(2);
MAT3(1,1),MAT3(2,2)=C(3);
MAT3(1,2)=-S(3);MAT3(2,1)=S(3);

CALL MATMULT(MAT2,MAT3,3,MATX);
CALL MATMULT(MAT1,MATX,3,MAT );
DO I= 1 TO NATOMS;DO J=1 TO 3;
 NEW(J)=NEWXYZ(I,J);END;
 CALL MET(MAT,NEW,3,OLD);
 DO J=1 TO 3;OLDXYZ(I,J)=OLD(J);END;
END;
LINEAR:  /* TRANSLATORY PART */
DO I=1 TO NATOMS; DO J=1 TO 3;
 OLDXYZ(I,J)=OLDXYZ(I,J) - TRANS(J);
END;END;
RETURN;END FROMPAS;
```

References

(1) Stout, G.H.; Jensen, L.H. "X-Ray Structure Determination: A Practical Guide"; MacMillan: New York, 1968; page 222

(2) Lonsdale, K. Revs. Mod. Phys. 1958, 30, 168

(3) Frishberg, C.A.; Massa, L.J. Int. J. Quantum Chem. 1978, 13, 801

(4) Chelikowsky, J.R. Phys. Rev. Lett. 1981, 47, 387

(5) Coppens, P.; Boehme, R.; Price, P.F.; Stevens, E.D. Acta Crystallogr. Sect. A 1981, 37, 857

(6) Schwartzenbach, D.; Thong, N. Acta Crystallogr. Sect. A 1979, 35, 652

(7) Thong, N.; Schwartzenbach, D. Acta Crystallogr. Sect. A 1979, 35, 658

(8) Lewis, J.; Schwartzenbach, D. Acta Crystallogr. Sect. A 1981, 37, 507

(9) Schulke, W.; Kramer, B. Acta Crystallogr. Sect. A 1979, 35, 953

(10) Hohenberg, H.; Kohn, W. Phys. Rev. 1964, 136, B864

(11) Gilbert, T.L. Phys. Rev. B 1975, 12, 2111

(12) Harriman, J.E. Phys. Rev. A 1981, 24, 680

(13) Clinton, W.L.; Galli, A.J.; Massa, L.J. Phys. Rev. 1969, 177, 7

(14) Stewart, R.F. J. Chem. Phys. 1972, 57, 1664

(15) Stewart, R.F. Chem. Phys. Lett. 1979, 65, 335

(16) Stewart, R.F. Chem. Phys. Lett. 1974, 26, 121

(17) Pecora,L.M. Bull. Amer. Phys. Soc. March 28,1983, 307 (Abstract BQ3)

(18) Mukherji, A.; Karplus, M. J. Chem. Phys. 1963, 38, 44

(19) Chandra, P.; Buenker, R.J. J. Chem. Phys. 1983, 79, 358

(20) Stewart, R.F. Isr. J. Chem. 1977, 16, 112 (equation 12)

(21) Chandra, P.; Buenker, R.J. J. Chem. Phys. 1983, 79, 365

(22) Tsirel'son, V.G.; Zavodnik, V.E.; Fomicheva, E.B.; Ozerov, R.P.; Kuznetsova, L.I.; Rez, I.S. Kristallografiya 1980, 25,735

(23) Tsirel'son, V.G.; Parini, E.V.; Ozereov, R.P. Dokl. Akad. Nauk. SSSR 1980, 254, 370

(24) Ozerov, R.P.; Tsirel'son, V.G.; Korkin, A.A.; Ionov, S.P.; Zavodnik, V.E.; Fomicheva, E.B. Kristallografiya 1981, 26, 42

(25) Frishberg, C.A.; Massa, L.J. Phys. Rev. B 1981, 24, 7018

(26) Clinton, W.L.; Massa, L.J. Phys. Rev. Lett. 1972, 29, 1363

(27) Frishberg, C.A.: Massa, L.J. Acta Crystallogr. Sect. A 1982, 38, 93

(28) Goldberg, M.J.; Massa, L.J. Int. J. Quantum Chem. 1983, 24, 113

(29) Goldberg, M.J.; Massa, L.J.; Frishberg, C.A.; Boehme, R.; LaPlaca, S.J. (Unpublished)

(30) Stanley, E. Acta Crystallogr. Sect. A 1979, 35, 966

(31) Grant, D.F.; Killean, R.C.G. Acta Crystallogr. Sect. A 1981, 37, C-330

(32) Hansen, N.K.; Coppens, P. Acta Crystallogr. Sect. A 1978, 34, 909

(33) McWeeny, R. Acta Crystallogr. 1951, 4, 513

(34) Rae, I.M.; Maslen, E.N. Acta Crystallogr. 1965, 19, 1061

(35) Kitajgordskij, A.I. Nature 1957, 179, 410

(36) Lonsdale, K.; Mason, R.; Grenville-Wells, J. Nature 1957, 179, 856

(37) Cox, E.G.; Cruikshank, D.W.J. Nature 1957, 179, 858

(38) Price, P.F.; Maslen, E.N.; Delaney, W.T. Acta Crystallogr. Sect. A 1978, 34, 194

(39) Coppens, P.; Pautler, D.; Griffin, J.F. J. Am. Chem. Soc. 1971, 93, 1051

(40) Coppens, P.; Csonka, L.; Willoughby, T.V. Science 1970, 167, 1126

(41) Clinton, W.L.; Frishberg, C.A.; Goldberg, M.J.; Massa, L.J.; Oldfield, P.A. Int. J. Quantum Chem. Symposia 1983, 17, 517

(42) Hirshfeld, F.L. Isr. J. Chem. 1977, 16, 226

(43) Coppens, P. Isr. J. Chem. 1977, 16, 159

(44) Kurki-Suonio, K. Isr. J. Chem. 1977, 16, 119

(45) Kurki-Suonio, K. Isr. J. Chem. 1977, 16, 132

(46) Stewart, R.F. Isr. J. Chem. 1977, 16, 124

(47) Kurki-Suonio, K. Isr. J. Chem. 1977, 16, 136

(48) Benesch, R.; Singh, S.R.; Smith, V.H., Jr. Chem. Phys. Lett. 1971, 10, 151

(49) Iwata, S. Chem. Phys. Lett. 1980, 69, 305

(50) Hirshfeld, F.L. Theor. Chim. Acta 1977, 44, 129

(51) Pant, L.M. Acta Crystallogr. Sect. A 1978, 34, 1021

(52) Coppens, P.; Hansen, N.K. Isr. J. Chem. 1977, 16, 163

(53) Ibers, J.A. Acta Crystallogr. 1961, 14, 853

(54) Coppens, P. Acta Crystallogr. Sect. A 1975, 31, S218

(55) Varghese,J.N.; Mason, R. Proc. R. Soc. London Ser. A 1980, A372, 1

(56) Larsen, F.K.; Hansen, N.K. (Unpublished)

(57) Present, R.D. Contemp. Phys. 1971, 12, 595

(58) Thakkar, A.J.; Smith, V.H. Chem. Phys. Lett. 1976, 42, 476

(59) Lauer, G.; Meyer, H.; Schulte, K.-W.; Schweig, A.; Hase, H.-L. Chem. Phys. Lett. 1979, 67, 503

(60) Kurki-Suonio, K. Isr. J. Chem. 1977, 16, 117

(61) Steiner, E. J. Chem. Phys. 1961, 39, 2365

(62) McWeeny, R. Phys. Rev. 1959, 114, 1528

(63) Mestechkin, M.M. "The Density Matrix Method in the Theory of Molecules"; Naukova Dumka: Kiev, 1977

(64) Henderson, G.A.; Zimmerman, R.K., Jr. J. Chem. Phys. 1976, 65, 619

(65) Nicholson, J.; Prince, E.; Buchanan, J.; Tucker, A. Acta Crystallogr. Sect. A 1981, 37, C-330

(66) Frishberg, C.A. private communication, July 1983

(67) Derewenda, Z.S.; Brzozowski, A.M.; Stepien, A.; Grabowski, M.J. Acta Crystallogr. Sect. A 1982, 38, 432

(68) Hamilton, W. Acta Crystallogr. 1965, 18, 502

(69) Wilson, A.J.C. Acta Crystallogr. Sect. A 1978, 34, S23

(70) Zangwill, W.I. "Nonlinear Programming: A Unified Approach"; Prentice-Hall: Englewood Cliffs, 1969; page 381

(71) Rosen, J.B. SIAM J. Applied Math 1969, 9, 514

(72) Bentley, J.; Stewart, R.F. Acta Crystallogr. Sect. A 1974, 30, 60

(73) Avery, J.; Watson, K.J. Acta Crystallogr. Sect. A 1977, 33, 679

(74) Avery, J. Acta Crystallogr. Sect. A 1978, 34, 582

(75) Avery, J.; Ormen, P.-J. Acta Crystallogr. Sect. A 1979, 35, 849

(76) Rae, A.D.; Wood, R.A. Acta Crystallogr. Sect. A 1978, 34, 724

(77) Taketa, H.; Huzinaga, S.; O-ohata, K. J. Phys. Soc. Jpn. 1966, 21, 2313

(78) Chandler, G.S.; Spackman, M.A. Acta Crystallogr. Sect. A 1978, 34, 341

(79) O-ohata, K.; Taketa, H.; Huzinaga, S. J. Phys. Soc. Jpn. 1966, 21, 2306

(80) Huzinaga, S. J. Chem. Phys. 1965, 42, 1293

(81) Almlof, J.; Otterson, T. Acta Crystallogr. Sect. A 1979, 35, 137

(82) Hase, H.L.; Schweig, A. Angew. Ch. Int. Ed. Engl. 1977, 16, 258

(83) Rothenberg, S.; Schaefer, H.F., III J. Chem. Phys. 1971, 54, 2764

(84) Andre, J.M.; Bredas, J.L. Chem. Phys. 1977, 20, 367

(85) Wright, J.S.; Williams, R.J. J. Chem. Phys. 1983, 78, 5264

(86) Simons, G.; Talaty, E. Chem. Phys. Lett. 1976, 38, 422

(87) Quinn, C.M. "An Introduction to the Quantum Chemistry of Solids"; Clarendon Press: Oxford, 1973

(88) Euwema, R.N. Int. J. Quantum Chem. 1971, 5, 471

(89) Louie, S.G.;Ho, K.-M.; Cohen, M.L. Phys. Rev. B 1979, 19, 1774

(90) Brown, P.J. Philos. Mag. 1972, 26, 1377

(91) Cook, D.B. Theor. Chim. Acta 1972, 27, 161

(92) Basch, H.; Topiol, S. J. Chem. Phys. 1979, 71, 802

(93) Chou, M.Y.; Lam, P.K.; Cohen, M.L. (Unpublished)

(94) Dovesi, R.; Pisani, C.; Ricca, F.; Roetti, C. Phys. Rev. B 1982, 25, 3731

(95) Stevens, E.D.; Coppens, P. Acta Crystallogr. Sect. A 1976, 32, 915

(96) Hirshfeld, F.L.; Rabinovich, D. Acta Crystallogr. Sect. A 1973, 29, 510

(97) Arnberg, L.; Hovmoller, S.; Westman, S. Acta Crystallogr. Sect. A 1979, 35, 497

(98) Killean, R.C.G.; Lawrence, J.L. Acta Crystallogr. Sect. B 1979, 25, 1750

(99) Hansen, N.K.; Pattison, P.; Schneider, J.R. Acta Crystallogr. Sect. A 1981, 37, C-132

(100) Chen, R.; Trucano, P.; Stewart, R.F. Acta Crystallogr. Sect. A 1977, 33, 823

(101) Stewart, R.F. private communication, July 1983

(102) Karplus, M.; Porter, R.N. "Atoms and Molecules"; W.A. Benjamin: Menlo Park, 1970; page 368

(103) Frishberg, C.A. Ph.D. dissertation, City University of New York, 1975

(104) Oldfield, P.A. Ph.D. dissertation, City University of New York, 1975

(105) Goddard, W.A., III; Dunning, T.H.; Hunt, W.J.; Hay, P.J. Accts. Chem. Res. 1973, 6, 368

(106) Matthai, C.C.; Grout, P.J.; March, N.H. Phys. Lett. A 1978, 68, 351

(107) Matthai, C.C.; Grout, P.J.; March, N.H. J. Phys. F 1980, 10, 1621

(108) Kertesz, M.; Koller, J.; Azman, A. Theor. Chim. Acta 1976, 41, 89

(109) Snyder, L.C.; Basch, H. "Molecular Wavefunctions and Properties"; Wiley: New York, 1972; page 22

(110) Henry, B.R. Accts. Chem. Res. 1977, 10, 207

(111) Heller, E. Chem. Phys. Lett. 1979, 61, 583

(112) Ishii, P.; Scheringer, C. Acta Crystallogr. Sect. A 1979, 35, 618

(113) Swaminathan S.; Craven, B.M.; McMullan, R.K. Amer. Crystallographic Assn. Winter Meeting Program and Abstracts March 1983, Ser. 2, Vol 11, No. 1, 35 (Abstract PC12)

(114) Eriksson, A.; Hermansson, K.; Lindgren, J.; Thomas, O. Acta Crystallogr. Sect. A 1982, 38, 138

(115) Cruikshank, D.W.J. Revs. Mod. Phys. 1958, 30, 163

(116) Halford, R.S. J. Chem. Phys. 1946, 14, 8

(117) Scheringer, C. Acta Crystallogr. Sect. A 1973, 29, 70

(118) Dawson, B.; Hurley, A.C.; Maslen, V.W. Proc. R. Soc. London Ser. A 1967, A298, 289

(119) Johnson, C.K. Acta Crystallogr. Sect. A 1969, 25, 187

(120) Zucker, U.H.; Schulz, H. Acta Crystallogr. Sect. A 1982, 38, 568

(121) Burns, D.M.; Ferrier, W.G.; McMullan, J.T. Acta Crystallogr. 1967, 23, 1098

(122) Pawley, G.S. Adv. Struct. Res. Diffr. Meth. 1972, 4, 1

(123) Scheringer, C. Acta Crystallogr. Sect. A 1978, 34, 905

(124) Lonsdale, K.; Milledge, H.J.; Rao, C. Proc. R. Soc. London Ser. A 1960, A255, 82

(125) Cruikshank, D.W.J. Acta Crystallogr. 1960, 13, 1103

(126) Scheringer, C. Acta Crystallogr. Sect. A 1978, 34, 702

(127) Koetzle, T. private communication, August 1981

(128) Schomaker, V.; Trueblood, K. Acta Crystallogr. Sect. B 1968, 24, 63

(129) Petricek, V. Acta Crystallogr. Sect. A 1975, 31, 694

(130) Hoy, H.R.; Mills, I.M.; Strey, G. Mol. Phys. 1972, 24, 1265

(131) Scheringer, C. Acta Crystallogr. Sect. A 1979, 35, 838

(132) Simons, G.; Choc, P. Chem. Phys. Lett. 1974, 25, 413

(133) Hirshfeld, F.L. Acta Crystallogr. Sect. A 1976, 32, 239

(134) Simons, G. J. Chem. Phys. 1974, 61, 369

(135) Kafri, O. Chem. Phys. Lett. 1979, 65, 538

(136) Kratzer, A. Ann. Phys. (Leipzig) 1922, 67, 127

(137) Busing, W.R.; Levy, H.A. Acta Crystallogr. 1964, 17, 142

(138) Stevens, E.D.; Rys, J.; Coppens, P. Acta Crystallogr. Sect. A 1977, 33, 335

(139) Epstein, J.; Stewart, R.F. Acta Crystallogr. Sect. A 1979, 35, 476

(140) Pines, D. "Elementary Excitations in Solids"; W.A. Benjamin: New York, 1964; page 91

(141) Lonsdale, K.; Milledge, H.J. Acta Crystallogr. 1960, 13, 499

(142) Bloch, F. Z. Phys. 1932, 74, 309

(143) Clinton, W.L.; Henderson, G.A.; Prestia, J.V. Phys. Rev. 1969, 177, 13

(144) Coulson, C.; Thomas, O. Acta Crystallogr. Sect. B 1971, 27, 1354

(145) Bonham, R.A. In "Electron and Magnetization Densities in Molecules and Crystals"; Becker, P., Ed.; Plenum: New York, 1980; page 153

(146) Epstein, J.; Stewart, R.F. In "Electron and Magnetization Densities in Molecules and Crystals"; Becker, P., Ed.; Plenum: New York, 1980; page 549

(147) Epstein, J.; Stewart, R.F. In "Electron and Magnetization Densities in Molecules and Crystals"; Becker, P., Ed.; Plenum: New York, 1980; page 560

(148) Mills, I.M. Specialist Periodical Reports - Theoretical Chemistry 1972, 1, 110

(149) Morrison, N. "Introduction to Sequential Smoothing and Prediction"; McGraw-Hill: New York, 1969; page 200

(150) Turrell, G. "Infrared and Raman Spectra of Crystals"; Academic Press: New York, 1972

(151) Scheringer, C. Acta Crystallogr. Sect. A 1980, 36, 814

(152) Rae, A.D. Acta Crystallogr. Sect. A 1973, 29, 74

(153) Ruysink, A.F.J.; Vos, A. Acta Crystallogr. Sect. A 1974, 30, 497

(154) Lowdin, P.-O. J. Chem. Phys. 1950, 18, 365

(155) Igolkin, V.N.; Mestechkin, M.M. Vestn. Leningr. Univ. 1965, 4, 5

(156) Goldstein, H. "Classical Mechanics"; Addison-Wesley: Reading, 1959

(157) Scheringer, C. Acta Crystallogr. 1963, 16, 546

(158) Powell, M.J.D. SIAM Rev. 1970, 12, 79

(159) Bazaraa, M.S.; Shetty, C.M. "Nonlinear Programming: Theory and Algorithms"; Wiley: New York, 1979; page 126

(160) Bazaraa, M.S.; Shetty, C.M. "Nonlinear Programming: Theory and Algorithms"; Wiley: New York, 1979; page 274

(161) Rosenbrock, H.H. Comp. J. 1960, 3, 175

(162) Luksan, L. Computing 1982, 28, 155

(163) Shanno, D.F. SIAM J. Numer. Anal. 1970, 7, 366

(164) Fletcher, R.; Powell, M.J.D. Comp. J. 1963, 6, 168

(165) Fletcher, R. Comp. J. 1965, 8, 33

(166) Gabay, D.; Luenberger, D.G. SIAM J. Control Opt. 1976, 14, 42

(167) Scheringer, C. Acta Crystallogr. Sect. A 1982, 38, 618

(168) Thomas, J.O. Acta Crystallogr. Sect. A 1978, 34, 819

(169) Wilson, A.J.C. Acta Crystallogr. Sect. A 1978,34, 474

(170) Southwell, W.H. Comp. J. 1974, 19, 69

(171) Lonsdale, K. Nature 1959, 184, 1545